de Oliveira-Pierce, A.N. The Role of Loops C and F in Interspecies Differential Pharmacology of the 5-HT_{3A} Receptor. Doctor of Philosophy (Graduate School of Biomedical Sciences), May 2009, pp., 10 tables, 18 illustrations, 98 references.

Mouse and human 5-Hydroxytryptamine$_{3A}$ receptors (5-HT_{3A}R's) share 84% amino acid identity. Nevertheless, different compounds have different functions at mouse and human wild-type receptors. The antagonist *d*-tubocurarine (curare) has much greater potency at mouse wild-type (MWT) than human wild-type (HWT) receptors, and 3-(2-hydroxy,4-methoxybenzylidene)-anabaseine (2-OHMBA) functions as a partial agonist at MWT and as an antagonist at HWT 5-HT_{3A}R's. In the present study, specific residues in Loop C and F of the 5-HT_{3A}R have been identified as critical for interspecies differences in function and sensitivities of both these compounds. Residues in or near Loop C were probed by substituting the human receptor with mouse receptor orthologs and then assessing the mutants with two-electrode voltage clamp electrophysiological and radioligand binding assays. The chimera H-Y217Q/M223I/E224D/Y228S (IC_{50} = 35 nM) was the smallest chimera with the same curare potency as H-Loop C+1. In radioligand binding assays, curare displaced the competitive antagonist [^{3}H]-BRL-43694 with rank order affinities (K_i) of MWT (9.59 nM) = H-Y217Q/M223I/E224D/Y228S Y217Q/M223I/E224D/Y228S (10.9 nM) > HWT (3.6 μM) > H-E224D (318 μM). As for studies using 2-OHMBA, two residues (I207 and I228) in the ligand binding domain of the mouse receptor were identified as critical for partial agonist activity of this compound. Receptors in which mutations to the corresponding human orthologs were inserted lost partial agonism of 2-OHMBA and gained competitive antagonism.

Furthermore, Ile and Leu appear to possess specific physicochemical properties required at residues 207 and 228 for agonist function of 2-OHMBA and 5-HT. Another finding of the present studies was that the 2'–OH group of 2-OHMBA interacts directly with I228, a residue in Loop C of the LBD of the MWT receptor, to form a hydrogen bond. Findings of this study have contributed to a more refined model of ligand binding to 5-HT_{3A}R's and an improved understanding of the molecular interactions governing function of this receptor.

THE ROLE OF LOOPS C AND F IN INTERSPECIES DIFFERENTIAL PHARMACOLOGY OF THE 5-HT_{3A} RECEPTOR

DISSERTATION

Presented to the Graduate Council of the

Graduate School of Biomedical Sciences

University of North Texas

Health Science Center at Fort Worth

In Partial Fulfillment of the Requirements

For the Degree of

DOCTOR OF PHILOSOPHY

By

Andreia Naomi de Oliveira-Pierce, B.S.

Fort Worth, Texas

July 2009

ACKNOWLEDGMENTS

First and foremost, I want to thank my mentor, Dr. Tina K. Machu, for her unparalleled guidance, patience and support during the three years I spent working in her laboratory.

I would like to extend my gratitude to all the members of my PhD dissertation committee: Drs. Glenn Dillon, Harold Sheedlo, John Schetz and Michael Forster. Thank you for all you assistance and invaluable contribution.

I also wish to acknowledge Dr. Michael White for his contribution with the molecular modeling work presented in this dissertation.

This dissertation work is dedicated to my mother, *Solange de Oliveira Guimarães*, whose life example inspired me in the pursuit of excellence; to *David Bell*, who showed endless confidence in my abilities; and to *John Bell*, who sadly died in the course of my studies. The memory of *John's* insurmountable support remained a source of motivation for me throughout this journey.

TABLE OF CONTENTS

LIST OF TABLES

CHAPTER 1

CHAPTER 2

CHAPTER 3

APPENDIX

LIST OF ILLUSTRATIONS

CHAPTER 1

CHAPTER 2

CHAPTER 3

CHAPTER I

INTRODUCTION

A. Significance

The 5-HT_3 receptor is a ligand-gated ion channel (LGIC) found in the central nervous system (the area postrema, the hippocampus, the limbic system and the cerebral cortex), peripheral nervous system, gut, lymphocytes, monocytes, and fetal tissues (Fiebich et al., 2004). Pharmacological uses for drugs targeting the 5-HT_3 receptor include treatment of chemotherapy induced nausea and vomiting (Leibundgut et al., 1987; Forni et al., 2003), post-operative nausea and vomiting (Ang et al., 1998; White et al., 2006), alcohol consumption (Hodge et al., 1993; Johnson 2004; Lê et al., 2006) and irritable bowel syndrome (IBS) (Camilleri et al., 1999; Jones et al., 1999; Spiller 2006). Additionally, studies examining the effects of 5-HT_3 receptor antagonists show that these drugs have positive effects on conditions such as migraines and chronic neuropathic pain (Dahlof et al., 1998; McCleane et al., 2003; Faerber et al., 2007). A clinical study using a single dose of odansetron (a 5-HT_3 receptor antagonist) on patients suffering chronic neuropathic pain resulted in significant decreases of 1.17 in pain scores just two hours following drug injection. Pain was measured on an 11-point Likert scale (0 for no pain and 10 for most amount of pain imaginable in accordance with the Visual Analog Scale) (McCleane et al., 2003). Acquiring a better understanding of the role of specific amino acids in structure-function relationships underlying the mechanisms of action of the 5-HT_3 receptor is of interest to the scientific community in general but more specifically, to

the pharmaceutical industry as this knowledge may contribute to the design and development of better suited, more specifically targeted pharmaceutical compounds.

B. The 5-HT_3 Receptor: A Ligand-Gated Ion Channel

The current classification of receptors set by the International Union of Pharmacology Committee (IUPHAR) for Receptor Nomenclature and Drug Classification is based on criteria such as amino acid sequence, pharmacology of the receptor and signal transduction mechanisms. Following the criteria set by the IUPHAR, these are the classes of receptors: ligand-gated ion channels (LGIC's), G protein-coupled receptors (GPCR's), enzyme-linked receptors, and transcription factor receptors (Humphrey, 1997). Each of these classes is composed of a number of super families grouped according to structural features. One example is the cys-loop superfamily, which includes the 5-HT_3 receptor, the only 5-HT receptor not classified as a GPCR. All cys-loop receptors are pentameric LGIC's possessing a characteristic bond between two cysteines located in the N-terminal domain (Schofield et al., 1987; Brejc et al., 2001). Other members of the cys-loop superfamily of LGIC's include the nicotinic acetylcholine receptor (nAChR), the glycine receptor (GlyR), and the γ-aminobutyric acid type A ($GABA_A$) and type C ($GABA_C$) receptors.

Phylogenetic studies have identified two groups within the cys-loop family of receptors; the first forming anionic channels, and the second forming cationic channels (Ortells and Lunt, 1995; Le Novère and Changeux, 1995; van Nierop et al., 2005). Activation of the 5-HT_3 receptor by agonist binding induces conformational changes that

result in conductance of cations (Na^+, K^+, and Ca^{2+}). Similar to the 5-HT_3 receptor, nACh receptors also conduct cations, while $GABA_A$, $GABA_C$, and Glycine receptors mediate synaptic transmission by conducting primarily Cl- and bicarbonate (Bormann et al., 1987; review by Enz, 2001; Menzikov and Menzikova, 2005). It has been reported that electrostatic interactions and pore diameter play an important role in determining ion selectivity. One of the important components in establishing favorable electrostatic interactions is the presence of polar or charged residues lining the channel pore. While there is a great deal of sequence homology lining the pore of all members of the cys-loop family of receptors (Brejc et al., 2001), a net positive charge is found lining the channel pore of anionic LGIC's with the presence of conserved arginine residues in Glycine, $GABA_A$, and $GABA_C$ receptors; conversely, negatively charged residues can be found lining the channel pore in 5-HT_3 and nACh receptors (Keramidas et al., 2004). A number of mutagenesis studies have been used to investigate the effect of amino acid mutations on conductance ratios as well as charge selectivity (see review by Karlin, 2002). As little as three residue substitutions in transmembrane (TM)1 and TM2 resulted in a change from cationic to anionic influx for both homomeric α7 nACh receptors (Galzi et al., 1992; Corringer et al., 1999) and 5-HT_{3A} receptors (Gunthorpe and Lummis, 2001). Additionally, mutation of three equivalent residues in the α1 homomeric glycine receptor converted this otherwise anionic channel into a cationic channel (Keramidas et al., 2000).

Excitation of a number of cells is dependent on regulation of ion flux, a process in which LGIC's play a very important role. Ion selectivity mediates the nature of synaptic potentials. In the brain, synaptic potentials classified as excitatory or inhibitory, regulate

firing of neurons and message transmission. Recent studies have reported that the rate of firing of nACh receptors is involved in post-synaptic deficiencies such as congenital myasthenic syndromes and Congenital Lambert-Eaton Syndrome (Sine and Engel, 2006). Also important for regulation of synaptic transmission is the 5-HT_3 receptor. This member of the cys-loop family of receptors mediates fast synaptic transmission in the central nervous system (CNS), peripheral nervous system and the gut (Tyers 1991). Clinical studies have reported a role for 5-HT_3 receptors in regulation of drug-related pathways (Alex and Pehek, 2007; Englemann et al., 2008), in addition to the previously established role of this receptor in regulation of initiation and coordination of emesis (reviewed in Barnes et al., 2009). Understanding the role of cys-loop receptors in regulation of brain function can thus have a significant impact in design and production of pharmaceutical compounds.

C. Receptor Structure

The 5-HT_3 receptor is formed by five homo-/hetero-pentameric subunits (A, B, C, D, and E), all of which have been cloned. Hydropathy plots of deduced amino acid sequences of 5-HT_{3A} receptor suggest all subunits are composed of a long extracellular N-terminus (which contains a short disulfide bonded cys-cys Loop), four transmembrane spanning domains (TM1-TM4), and a short extracellular C-terminus. Two intracellular loops connect TM1-TM2 and TM3-TM4, while an extracellular loop connects TM2-TM3. The N-terminus contains the ligand recognition site for 5-HT (Eisele et al., 1993), and TM_2 lines the channel pore. In humans, the 5-HT_{3A} gene has 9 exons and 8 introns

(Weiss et al., 1995). In other species such as mouse, rat, and guinea pig, the 5-HT_{3A} gene can exist in two known splice variants, a short truncated splice variant, 5-HT_{3A}(b), and a long splice variant, 5-HT_{3A}(a) (review by Barnes et al., 2009). The long splice variant is homologous to the human 5-HT_{3A} isoform and is also expressed in a long (5-HT_{3A}L) and a truncated (5-HT_{3A}T) form. Both the 5-HT_{3A}L and the 5-HT_{3A}T isoforms are expressed in the brain, and studies have suggested these variants may be linked to pathogenesis of genetic diseases such as schizophrenia and depression (Miquel et al., 2002; Kurzwelly et al., 2004; Krzywkowski et al., 2007). The 5-HT_{3B} gene, while sharing 41% homology with 5-HT_{3A}, is differentially expressed in brain and intestinal tissue as a result of the existence of tissue specific promoters (Barnes et al., 2009). The A subunit is required for the formation of functional 5-HT_3 receptors and for assistance of trafficking of B subunits to the membrane surface (Barnes et al., 2009). Receptors composed of A-homomers and A/B-heteromers have been reported to have functional significance in the central and peripheral nervous systems (Reeves and Lummis, 2002).

Studies investigating expression and function of human A/C-, A/D- and A/E-heteromers have reported that C subunits have an almost ubiquitous distribution, whereas D and E subunits are largely expressed peripherally. Especially in the gastro-intestinal tract. The C, D, and E subunits do not appear to be natively expressed in rodents, but are present in other species, such as chimpanzee and dog (Niesler et al., 2007; Holbrook et al., 2009). Subunits C and E possess similar structural features to those of subunits A and B. However, subunit D was reported to lack the N-terminus, the signal sequence, and the putative binding domain (Niesler et al., 2007). Subunits C, D, and E do not form

homomeric receptors. In two studies, the functional properties of A/C, A/D, and A/E receptor have been investigated. The heteromeric receptors had similar 5-HT concentration response curves, current-voltage relationships, and picrotoxin sensitivities as the A homomer. In the absence of any electrophysiology measurements that delineate a difference in biophysical properties of the A homomer and A heteromeric receptor containing an A subunit and A, C, D or E subunit, the functional significance of C, D and E subunits remains to be established.

Figure 1 Loops composing the principal and the complementary components of the ligand binding domain of the 5-HT3 receptor.

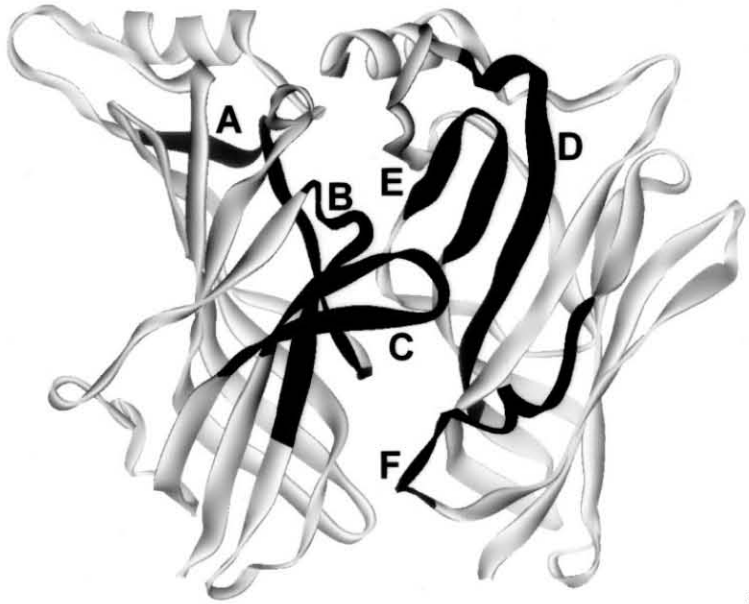

Thompson et al., 2005

The ligand binding domain (LBD) of the 5-HT_3 receptor is located in the N-terminus at the interface between subunits and consists of six loops: A, B, C, D, E, and F (Fig 1). Loops A-C join to form the principal component of the LBD, and Loops D-F

form the complementary component of the LBD (Fig 2), and the mechanism of activation of LGIC's is highly conserved among all members of this family. Crystallization of the Acetylcholine Binding Protein (AChBP), a structural homolog of the N-terminus of the nACh receptor (Brejc 2001) used as a prototype for LGICs, has enabled researchers to elucidate the role of individual residues in orthosteric ligand recognition.

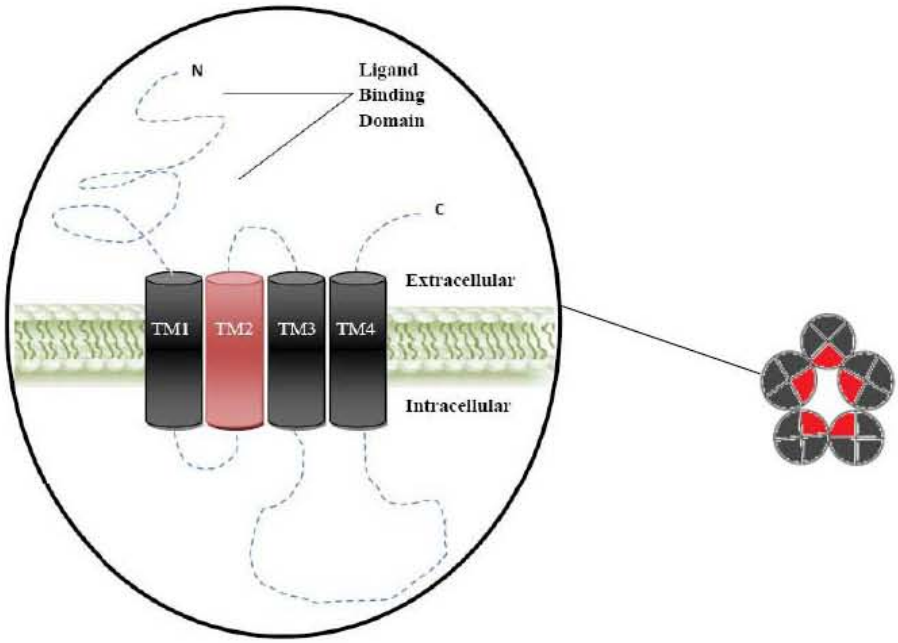

Figure 2 Schematic representation of a 5-HT_3 receptor subunit

The 5-HT_3 receptor has an oligopentameric structure, similar to that of the structure of nACh receptor. Electron microscopy of the affinity purified 5-HT_3 receptor shows that the five subunits are arranged around a long cylindrical axis of 11 nM and the external diameter of the ion channel is 8 nM. The ion channel opens at the external side of the cell wall and the diameter of the open channel is 2-3 nM (Boess et al., 1992; Boess

et al 1995). The intracellular loop connecting TM3-TM4 contains an amphipathic α helix, named as the MA stretch or HA stretch, and presents multiple consensus sequences for phosphorylation by various kinases (Unwin, 2005; reviewed in Peters et al., 2005).

Alignment of TM2 domain from the A subunit with that of the other members of the ligand-gated ion channel superfamily reveals many similarities (Karlin and Akabas 1995), particularly with regard to the rings of negative charges that are localized at the extracellular and intracellular borders of TM2 and the hydrophobic residue located at position two of the channel (Thompson and Lummis, 2003). Furthermore studies using substituted cysteine accessibility method (SCAM) have demonstrated the largely helical structures of TM2 (Reeves et al., 2001), which is similar to the other members of the superfamily.

D. Receptor Assembly and Trafficking

As with a number of proteins, the assembly of the 5-HT_3 receptor takes place in the endoplasmic reticulum (ER), where it is thought to interact with a molecular chaperone immunoglobulin heavy chain binding protein and with calnexin (Boyd et al., 2002). Once assembled, A-homomers and A/B-heteromers are then transported to the membrane surface where they are expressed. Studies looking at assembly and trafficking of 5-HT_3 A and B subunits in COS 7 and ts201 cells suggest that the level of expression of the 5-HT_3 receptor is highly regulated by subunit retention in the ER and by assembly (Boyd et al., 2002; Boyd et al., 2003).

Assembly affects trafficking, in that only receptors containing A subunits, whether A-homomers or A/B heteromers, were successfully translocated and expressed onto the cell membrane. Interestingly, the presence of A subunits was important for expression even when constructed as a non-functional A subunit (Boyd et al., 2002), further building a case of the critical role subunit A plays in receptor transport and expression. One of the important features in 5-HT_3 receptor stability is the presence of N-glycosylation sites. Independent studies attempting to identify N-glycosylation sites in both human and mouse homomeric receptors (5-HT_{3A}) have reported three potential N-linked glycosylation sites at human positions N-104, 170 and 186, and mouse positions N-209, 174, 190 (Boyd et al., 2002; Quirk et al., 2004). As for the human heteromeric receptor (5-$HT_{3A/B}$), Boyd et al. (2002) reported this receptor has five potential glycosylation sites at positions N-47, 91, 133, 163 and 198. Another study suggested four potential N-glycosylation sites for the 5- HT_{3A} homomer at N-5, 81, 147 and 163. These residues appeared to play a very important role in membrane expression. When individually mutated the ability of the receptor to translocate to the cell surface appeared seriously impaired and mutated receptors were predominantly found in the intracellular compartment. Furthermore, mutant receptors able to express on the cell surface had a signicantly lower binding affinity for 5-HT and odansetron (Monk et al., 2004). While N-glycosylation is critical for 5-HT_3 receptor trafficking, other residues plan an important role in translocation and expression on the cell surface. Studies investigating assembly and trafficking of the mouse 5-HT_3 receptor reported Y50, Y91 and E235 play an important role in receptor assembly (Schreiter et al., 2003; Price and Lummis, 2004).

Another player in the translocation of 5-HT_3 receptors to the membrane is tubulin. A study by Ilegems et al. (2004) reported that in HEK295 cells treated with colchicine, a microtubule depolymerizing agent, translocation of 5-HT_3 receptors to the membrane was significantly impaired. Another accessory protein reported to mediate 5-HT_3 receptor translocation is the Resistance to Inhibitors of Cholinesterase-3 (RIC-3) protein. This protein is thought to have differential effects on transport of varying ligand-gated ion channels, i.e. while enhancing transport of certain subtypes of nACh receptors, the RIC-3 protein appeared to block trafficking of 5-HT_3 receptors to the membrane (Castillo et al., 2006; review by Millar, 2007). A separate study, reported RIC-3 mediated enhancement of 5-HT_{3A} homomeric receptor translocation to the membrane while the same protein seemed to downregulate translocation of 5-$HT_{3A/B}$ heteromers (Cheng et al., 2007).

E. Molecular Dynamics of the Cys-loop Superfamily

The ligand-binding pocket, located on the interface of two adjacent subunits of all cys-loop receptors, undergoes a conformational change upon orthosteric binding. This conformational change induces channel opening and permeation of cations, in the case of 5-HT_3 and nACh receptors, and anions, in the case of Glycine, $GABA_A$ and $GABA_C$ receptors (Absalom et al., 2004). Studies using molecular dynamic stimulation, disulfide bond trapping, SCAM, and electron microscopy revealed the Cys-loop and the β1-β2 loop straddle opposite sides of the TM2-TM3 linker from the channel pore region with ligand-binding inducing lateral rotation of this region resulting in a twisting motion at TM2 allowing ion flow (Horenstein et al., 2001; Miyazawa et al., 2003; Absalom et al.,

2004). The pre-M1 region is also thought to be involved in agonist-binding coupling to channel gating, as it contacts the Cys-loop (Bouzat et al., 2004). Sequence conservation is high among different receptors with key differences thought to account for differential ligand recognition and ionic flow. Electron microscopy of the Torpedo nACh receptor shows rotational movement at the extracellular domain and channel pore as a result of ligand-binding (Unwin 1998) and a study investigating the role Loop F in orthosteric binding, suggests ligand-dependent movement of W195, and D204 residues of the 5-HT_{3A} receptor.

Members of the cys-loop family of LGICs are so named because of the presence of a conserved signature disulfide loop in the extracellular region of the receptor. This loop is of a hydrophobic nature enabling it to interact with the transmembrane domains of the receptor (Schofield et al., 2003). Studies in the $GABA_AR$ using SCAM in conjunction with assessment of the crystallized AChBP and refined electron micrograph of the nACh receptor revealed that rotational rearrangements in TM2 induce channel opening (Horenstein et al., 2001; Absalom et al., 2004). Molecular interactions involving the TM2-TM3 loop have also been proposed to participate in a 'pin and socket' interaction inducing a 15° clockwise rotation near TM2 followed by destabilization of the hydrophobic girdle that composes the channel gate. Destabilization is thought to induce opening of the channel and subsequent ion permeation (Miyazawa et al., 2003). In the Glycine receptor, TM2-TM3 seems to perform different functions in different subunits and mutations in this region of the receptor do not block channel gating (Shan et al., 2003). A recent breakthrough in the study of LGIC's was the crystallization of the

extracellular domain of the mouse nACh receptor α1 subunit revealing for the first time the cys-loop with the disulfide between Cys128 and Cys142 at the atomic level. This crystal structure has also revealed the role of Lys145 and Asp200 in direct electrostatic interaction with each other and the role of Thr202 in forming hydrogen bonds when the nACh receptor is bound to an antagonist, in this case the α-bungarotoxin (Dellisanti et al., 2007). A study using SCAM to probe the 5-HT_3 receptor pore identified water-accessible residues in the TM2 region (Asp274, Gly276, Glu277, Ser280, Thr284, Leu285, Leu287, Val291, Leu293, Ile294 and Ile295) in the presence of 5-HT, supporting the idea that these amino acid residues participate in lining of the channel pore (Reeves et al., 2001).

F. The Use of Interspecies Studies

The ionotropic 5-HT_3 receptor shares a high degree of homology among its six cloned species (80-95%). Nevertheless, this receptor is known to exibit significant interspecies differential pharmacology. The use of interspecies studies is a powerful tool in understanding the underlying mechanisms that govern distribution and function of the 5-HT_3 receptor. A study using human brain membranes confirmed that interspecies differences in 5-HT_3 receptor expression include levels of expression in different regions of the brain with the area postrema being the most abundant in 5-HT_3 receptors (Marazziti et al., 2001), not unlike animal brains (Kilpatrick et al., 1987; Kilpatrick et al., 1989; Jones et al., 1992). However high levels of expression found in the striatum seem to be unique to human brains (Abi-Dargham et al., 1993; Marazziti et al., 2001).

Another interesting difference in 5-HT_3 expression is the presence of 5-HT_{3C}, 5-HT_{3D}, and 5-HT_{3E} subunits in a number of mammalian species such as humans, dogs and monkeys, and absence in rodents (Niesler et al., 2007; Holbrook et al., 2009). Isoform expression differences aside, actual pharmacological sensitivities such as differences in potency of curare (Hope et al., 1999; Zhang et al., 2007), differential actions of 2-OHMBA (Zhang et al., 2006), differential modulation by colchicine (de Oliveira-Pierce et al., 2009), and different single channel conductance properties (Barnes, 2005) strengthen the case of the use of interspecies studies to further scientific knowledge of the structure-function relationships-of the 5-HT_3 receptor.

It is important to point out that while A homomeric and A/B heteromeric receptors are different in their biophysical properties, such as ratio of response (Dubin et al., 1999), and kinetics of channel activation and desensitization (Hapfelmeir et al., 2003), they have strikingly similar pharmacology within species. In a side by side comparison of human 5-HT_{3A} homomers and 5-$HT_{3A/B}$ heteromers, it was reported that these receptors have curare IC_{50}'s of 3 μM and 14 μM, respectively (Davies et al., 1999). Both the rat 5-HT_{3A} and the 5-$HT_{3A/B}$ receptors have comparable curare potencies of 14 and 28 nM (Hanna et al., 2000). Additionally, 2-OHMBA is an antagonist at both human 5-HT_{3A} and 5-$HT_{3A/B}$ receptors, and a partial-agonist at both mouse 5-HT_{3A} and 5-$HT_{3A/B}$ receptors. Unpublished data from studies conducted at this laboratory reveal that sensitivities of curare and 2-OHMBA at both mouse and human 5-$HT_{3A/B}$ receptors are close in sensitivity to their respective species A homomers.

G. The 5-HT_3 Binding Site and the Role of Loop C

Residues in both the principal (Loops A-C) and the complementary (Loops D-F) interfaces of the binding site are important for ligand binding. Electrophysiology studies show that Loop C residues play a critical role in determining 5-HT and curare potencies, with a 2,200-fold decreased curare IC_{50} in mouse223human chimeras when compared to mouse wild-type (Hope et al., 1999). In rats, affinity of m-chlorophenylbiguanide (*m*CPBG) at 5-HT_3 receptors is ~13-fold higher than in humans. Human/rat interspecies chimeras revealed specific residues in Loop C contribute to differential potency of this agonist at the 5-HT_{3A} receptor (Mochizuki et al., 1999). Another study investigating specific regions affecting differential sensitivities to *m*CPBG between human and guinea pig, narrowed the region to 28 amino acids, including Loop C (Lankiewicz et al., 1998). In line with previous studies, preliminary results for the present project identified specific residues in Loop C as being important for interspecies differential pharmacology of both 2-OHMBA and curare.

In addition creation of interspecies chimeras, alanine scanning mutagenesis has been widely used to identify the role of specific residues in the function of 5-HT_{3A} receptors. Suryanarayanan et al., (2005) and Thompson et al. (2005) investigated the role of residues Phe226, Ile228, Asp229, Ile230, and Tyr234 within Loop C using alanaine cycling and reported that point mutant receptors had reduced affinities of [^{3}H]-BRL-43694 compared to MWT, and in some cases did not bind the antagonist. Furthermore, residues Phe226, Ile228, and Tyr234 were reported to contribute to efficacy of 5-HT and *m*CPBG in mouse receptors. Joshi et al., (2006) identified a region composed of Loops B,

C and E of the 5-HT_3 receptor as critical for binding of BRL-43694, with ablation of binding at the point mutant receptor containing the S223A substitution. In a study using unnatural amino acid mutagenesis, changes to the Tyr234 residue affected binding of BRL-43694, and 5-HT induced activation of the 5-HT_3 receptor (Beene et al., 2004). Homology models indicate that there is direct ligand-receptor interaction at a number of residues within Loop C (Suryanarayanan et al., 2005). Collectively, these data support an important role for Loop C in binding and function of the 5-HT_3 receptor.

H. The 5-HT_3 Binding Site and the Role of Loop F

Homology models using the AChBP, along with biochemical studies, have identified important residues for ligand-binding on both the primary (Loops A-C) and the complementary (Loops D-F) interfaces of the binding site (Fig 1 and Fig 2). Loop F has, however, remained a challenge due to weak resolution of this loop in the crystallized AChBP structure (Brejc et al., 2001). Studies using isothermal titration calorimetry found that Loops A-E alone cannot account for differences in affinity, suggesting a critical role for Loop F in ligand-binding (Celie et al., 2005). Espinoza-Fonseca et al. (2006) reported direct contact between residues of Loops C and F in binding of β-amyloid peptide and heptapeptide IQTTWSR to the α7 nACh receptor. Mutagenesis and molecular modeling were used to assess specific residues at the 5-HT_{3A} receptor, with twenty-one substitutions at or near Loop F. The results revealed significant ligand-dependent differences in the orientation of Trp195 and Asp204 (Thompson et al., 2006). A previous study investigating amino acids in both Loop F and Loop C identified residues

responsible for differential pharmacology in mouse and human 5-HT_{3A} receptors with Loop F playing a significant role (Zhang et al., 2007).

I. Loops A, B, D, and E of the 5-HT3 receptor

In addition to Loops C and F, a number of studies have been conducted investigating the role of residues located in the remaining four loops that play a role in binding and function of LGIC's. Photoaffinity labeling has enabled researchers to identify Tryptophan residues in Loops A, B and D in the nACh receptor as putative ligand binding residues (see review by Galzi and Changeux, 1995). More specific to the 5-HT_3 receptor, studies in which W90 (Loop D), W183 and W185 (Loop B) were mutated to tyrosine or serine residues revealed that these substitutions had a marked effect on ligand binding and function (Spier and Lummis, 2000). A separate study by Beene et al., (2002) reported that W183 is the cation-π binding site that interacts with the quaternary ammonium moiety of serotonin. Yan et al., (1999) identified two other amino acid residues that are important for binding and function of the 5-HT_{3A} receptor, R92 and Y94, both located in Loop D. These residues had differential effects on affinity of 5-HT and other 5-HT_{3A} receptor ligands, suggesting different ligands have different points of interaction with the receptor. Mutation of Loop A residue E129 to the negatively charged Asp or to the polar, but uncharged Asn, reportedly decreased affinity of selective 5-HT_{3A} receptor antagonists and agonists (Boess et al., 1997), while mutation of the adjacent residue, F130, caused a reduction in affinity of 5-HT and a slowing of activation kinetics of maximal inward currents (Stweard et al., 2000). In summary, while this study focuses

on Loops C and F of the 5-HT_{3A} receptor, it is important to keep in mind that Loops A, B, D, and E are also important for binding affinity and ligand recognition.

J. Double-mutant Thermodynamic Cycle Analysis

Double-mutant thermodynamic cycle analysis involves a wild-type and two point mutant proteins, as well as two drugs that vary in a functional group or domain. This technique is useful in isolating energetic contributions between a functional group and an amino acid residue of interest, allowing for pair-wise comparisons (Horovitz, 1996). The use of double-mutants in ligand-gated ion channel studies has provided critical insight into the orientation of specific ligands at their respective binding sites (Malany et al., 2000; Yan et al, 2005; Yan et al, 2006; Zhang et al., 2007). In the present study double-mutant cycles were used to evaluate the pairwise affinity interactions between residues in Loops C and F of the 5-HT_{3A} receptor and benzylidene-anabaseine analogs. This approach has been successfully used to investigate specific interactions between the Asn128 in the mouse receptor and the 2'N curare, providing data that led to the creation of molecular models for the docking of curare at the mouse 5-HT_3 receptor (Yan et al., 2006). Calculation of direct interaction between an amino acid residue and a functional group uses the K_d or K_i values obtained in binding assays and the following formula: $(K_{W,L1}/K_{W,L2})/(K_{M,L1}/K_{M,L2})$, where M is the wild-type protein, W is the mutant protein and L1 and L2 correspond to the mutant ligands. The result is an interaction coefficient (Ω); a Ω value significantly different than 1 indicates a direct interaction between the

amino acid residue of the receptor and the functional group of the ligand (Malany et al, 2000; Yan et al, 2005; Yan et al, 2006).

K. Preliminary Data

In addition to studies described in appendix A investigating the role of Loops C and F in interspecies differential pharmacology of colchicine at the 5-HT_{3A} receptor, (de Oliveira-Pierce et al., 2009), the following preliminary studies provided a wealth of data confirming the importance of these loops in conferring differential pharmacological sensitivities to two additional chemical compounds: curare and benzylidene analogs of anabaseine. Compounds that bind at the ligand binding domain, 3-(2-hydroxy, 4-methoxybenzylidene)-anabaseine (2-OHMBA), Curare, and Serotonin (5-HT) were used. Wild-type (WT) and mutant receptors were expressed in *Xenopus laevis* oocytes. As described in more detail in the upcoming chapters, receptor response was recorded from days 2-7 following injection of WT or mutant cRNA in a 100 µl recording chamber. Clamping currents were measured with a Warner Instruments Model OC-725B or C two-electrode voltage clamp.

Response to curare was used due to 140-fold increased potency of this drug in the MWT receptor when compared to the HWT receptor regardless of receptors sharing 86% amino acid identity (Zhang et al., 2007). Response to 2-OHMBA was used due to its differential pharmacological effects on the human and mouse receptors to identify residues critical for agonist-induced channel opening in the 5-HT_3 receptor. In the mouse

receptor, 2-OHMBA functions as a partial-agonist and in the human receptor it functions as an antagonist (Machu et al., 2001; Zhang et al., 2006).

a) Characterization of the Differential Actions of Curare at the Mouse and the Human 5-HT_{3A} Receptors:

Curare has differential potencies at mouse and human 5-HT_{3A} receptors (Hope et al., 1999; Zhang et al., 2007). Experiments focusing on the distal 1/3 of the N-terminus of the receptor were conducted to further identify the region where critical residues for 140-fold increased potency of curare in MWT (IC_{50} of 13 nM) when compared to HWT (IC_{50} of 1800 nM) receptors are located. The region that the chimera H176M244H (IC_{50} of 8 nM) has in common with MWT is the distal 1/3 of the N-terminus, and in this chimeric receptor, curare potency increases significantly. Results revealed that reciprocal substitutions of the distal 1/3 of the N-terminus were sufficient to confer mouse-like curare potency at human chimeric receptors and vice-versa with the M181H239M having an IC_{50} of 1.7 μM and H176M244H having an IC_{50} of 8 nM (Zhang et al., 2007). Individual point-mutations at the human receptor with mouse orthologs result in enhanced curare potency at the mutant receptor, with each additional substitution yielding further increases in potency. This stepwise effect was not observed with systematic introduction of human residues in the mouse background. Rather, individual substitutions appear to significantly contribute to curare potency at the mouse receptor (Hope et al., 1999). Therefore, the human 5-HT_{3A} receptor background was chosen for these studies.

To further investigate the location of critical residues for curare potency, chimeras in which Loop C and the non-conserved residue between Loop C and TM1 were changed (Loop C+1) or in which Loop F and the non-conserved residue immediately N-terminal to Loop F and the two non-conserved residues between Loop F and C have been changed (Loop F+3) in the human receptor were tested. Both chimeras had greater curare potencies than HWT, with a 22-fold increase for Loop F+3 and a 45-fold increase for Loop C+1 (Zhang et al., 2007).

Point Mutant	**Curare IC_{50} (nM)**
Loop F+3 [a]	
H-S188T	**2010**
H-L192S	**1600**
***H-K195E**	**546**
H-K197R	**1700**
H-R200K	**2200**
***H-V202I**	**255.7**
H-M204I	**2140**
H-G213E	**1670**
H-L215F	**1300**
***H-K195E, V202I**	**133**

Loop C+1	
H-Y217Q	**1100**
***H-R219K**	**660**
***H-M223I**	**930.2**
H-E224D	**8917**
H-S225I	**2100**
H-Y228S	**920**
***H-217, 219, 223, 228**	**100**
***H-217, 223, 224, 228**	**34**

Table 1 Testing of the 16 residues that differ between mouse and human in the distal 1/3 of the N-terminus shows that K195, V202 in Loop F and R219 in Loop C contribute to a significant increases in curare potencies; [a] indicates data taken from Zhang et al., (2007). Increased potency nears that of MWT receptor when Loop C mutants Y217Q, R219K, M223I or E224D, and Y228S are combined.

b) Characterization of the Differential Actions of 2-OHMBA at Mouse and Human 5-HT_{3A} Receptors:

The anabaseine analog, 2-OHMBA, functions as a partial agonist at the mouse 5-HT_{3A} receptor and as an antagonist at the human 5-HT_{3A} receptor. Substitutions of the entire N-terminus of mouse and human 5-HT_{3A} receptors with species reciprocal residues were sufficient to confer partial agonist or antagonist activity of this compound. In order to further identify the region in which critical residues for pharmacological differentiation are located, experiments focusing on the distal 1/3 of the N-terminus of the receptor were conducted (Zhang et al., 2006). Partial agonist activity of 2-OHMBA was maintained in the chimeric receptor containing substitutions of human residues in the distal 1/3 of the N-terminus with mouse ortologs, H176M244H, with an EC_{50} of 5.0 μM. A loss of partial agonist activity of 2-OHMBA was observed in chimeras containing the reciprocal substitutions in the human distal 1/3 of the N-terminus, M181H239M, with an IC_{50} of 3.0 μM.

Given that our studies revealed the importance of the distal 1/3 of the N-terminus, our next set of experiments were designed to identify critical residues for 2-OHMBA function in Loops C and F of the 5-HT_3 receptor. Preliminary studies reveal that substitution of either Loop C or Loop F in the mouse receptor result in loss of partial agonist activity and gain of antagonist activity of 2-OHMBA (Fig. 2). In human receptors, both loops must be substituted with mouse residues in order for partial agonist activity of 2-OHMBA to be observed (data not shown). Therefore, the mouse receptor was chosen as the background for the point-mutant studies.

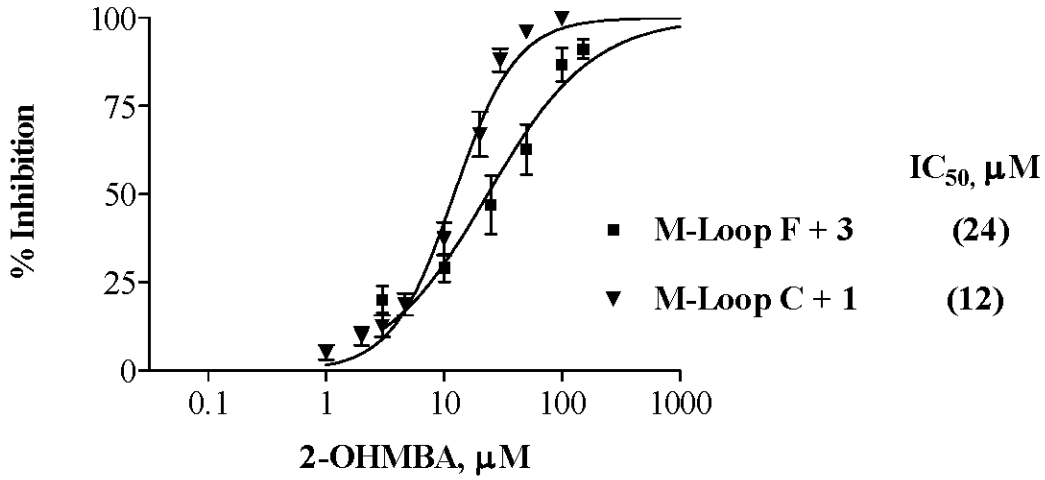

Fig. 2 To further investigate the location of critical residues conferring agonist or antagonist activity chimeras where Loop C and the non conserved residue between Loop C and TM1 were changed (Loop C+1) or where Loop F and the non-conserved residue immediately N-terminal to Loop F and the two non-conserved residues between Loop F and C have been changed (Loop F+3) in the mouse receptor were created. In both cases there is a loss of agonist activity and a gain in antagonist activity.

Having demonstrated that critical residues that confer differential sensitivities between human and mouse 5-HT_3 receptors are located within Loop C and Loop F regions, point-mutants corresponding to each of the differing residues in this region were created (Table 1).

Point Mutant	% Efficacy	Point Mutant	% Efficacy
Loop F+3		**Loop C+1**	
M-T193S	38.59±8.41	M-Q222Y	41.93±5.01
M-S197L	39.42±6.27	M-K224R	51.26±3.50
M-E200K	57.89±4.82	*M-I228M	—
M-R202K	58.18±5.22	M-D229E	43.70±6.08
M-K205R	62.70±6.74	M-I230S	51.27± 3.05
*M-I207V	—	M-S233Y	35.80±6.94
*M-I209M	10.37±2.62	M-I242V	56.40±3.97
M-E218G-F220L	29.37±7.04		

Table 2 Testing of each of the Loops C and F residues that differ between mouse and human in the distal 1/3 of the N-terminus shows that M-I207V, M-I209M, and M-I228M play a critical role in coffering partial-agonist activity to 2-OHMBA.

L. Hypothesis and Specific Aims

This project was based on the aforementioned preliminary studies and literature review. Both sets of data identify specific amino acid residues within Loops C and F as playing an important role in the interspecies differential pharmacology of at the 5-HT_{3A} receptor. In the present study, the contribution of individual amino acid residues to binding affinity was assessed, thus further defining the ligand-binding domain for each specific compound. In addition, the present study identified physicochemical properties of residues required for gating of the 5-HT_{3A} receptor by 2-OHMBA. Additionally, this study has identified amino acids required for binding. It is hypothesized that residues in

Loops C and F play a critical role in direct ligand-5-HT_{3A} receptor interaction accounting for differences in pharmacological sensitivities to 2-OHMBA and curare between mouse and human receptors. In order to test this hypothesis a combination of site-directed mutagenesis, two-electrode voltage clamp electrophysiology and radioligand binding studies were implemented to address the following specific aims:

Specific Aim 1: Identify residues within Loops C and F of the 5-HT_{3A} receptor that are directly involved in binding of curare.

The ligand binding domain of the 5-HT_3 receptor is located in the N-terminus (extracellular) region of the receptor. Substitution of the human distal N-terminus with residues from the mouse receptor and vice-versa result in a complete shift in potency of curare mimicking that of the other species. Loops C and F are the only regions within the one-third distal N-terminus. Other loops are in the first two-thirds, and while there are three differences between species in Loop E, they do not appear to play a role in the differential pharmacology of curare at mouse and human 5-HT_{3A} receptors (Zhang et al., 2007). Electrophysiology experiments have revealed specific residues in interspecies differential pharmacology, however binding studies are needed to further determine if these differences are due to changes in binding, gating or both. In this specific aim, residues previously identified as being critical for 140-fold increase in curare potency in the MWT receptor, when compared to the HWT receptor, were probed using competition radioligand binding assays.

Specific Aim 2: Characterize physico-chemical properties of residues within Loops C and F of the 5-HT_{3A} receptor critical for 2-OHMBA function and interspecies differential pharmacology.

Loss of agonist activity and gain in antagonist activity for 2-OHMBA was observed in mouse chimeric and point mutant receptors in which Loop C and the non conserved residue between Loop C and TM1 (Loop C+1) were changed. The same was observed in chimeric receptors in which Loop F and the non-conserved residue immediately N-terminal to Loop F and the two non-conserved residues between Loop F and C were changed (Loop F+3). Additionally, studies using reciprocal point-mutations in mouse and human 5-HT_{3A} receptors revealed mouse I207, I209 and I228 (human orthologs V202, M205 and M223) are responsible for differential pharmacology of 2-OHMBA. Based on these preliminary results, it is proposed that these residues not only play a role in interspecies differences, but also that specific physico-chemical properties of amino acids at these positions are required for maintenance of 2-OHMBA function. Therefore, in this specific aim, representatives of varying classes of amino acids, i.e.: hydrophobic, hydrophilic, charged etc were systematically introduced into positions 207, 209 and 228 of the mouse receptor. This was followed by assessment of functional expression using electrophysiology.

Specific Aim 3: Establish whether Loops C and F residues of the 5-HT_{3A} receptor critical for interspecies differential pharmacology play a direct role in binding, gating, or both.

Activation of LGIC's is regulated by ligand binding, however actual molecular mechanisms underlying coupling of the two events remain unclear. Residues within Loop C have to be mouse-like for 2-OHMBA to function as a partial agonist, thus supporting homology models in which the -OH group in the agonist ligand directly interacts with Loop C residues in the ligand binding pocket (Suryanarayanan et al., 2005). 3-[2, 4-dimethoxybenzylidene] anabaseine (DMXBA) is a selective α7nAch receptor partial-agonist that differs from 2-OHMBA only in that it has a –OCH3 group instead of a –OH group in the 2' position. Nevertheless, DMXBA functions as an antagonist at both, mouse and human 5-HT_3 receptors (Machu et al., 2001). In this specific aim, point-mutants previously shown to play a role in function of the receptor were further investigated to determine whether they directly interact with the 2'-OH group of 2-OHMBA. This assessment was done with radioligand binding assays where 2-OHMBA and DMXBA displaced [^{3}H]-BRL-43694. Furthermore, 2-OHMBA and DMXBA were assessed for reactivity with MWTA, M-I207V, M-I228M and M-D229E/A by means of double-mutant cycle analysis.

REFERENCES

Abi-Dargham, A., Laruelle, M., Wong, D. T., Robertson, D. W., Weinberger, D. R., and Kleinman, J. E. (1989) Pharmacological and regional characterization of [^{3}H]LY278584 binding sites in human brain. *J. Neurochem.* **60:** 730-737.

Absalom, N. L., Lewis, T. M., Schofield, P. R. (2004) Mechanisms of channel gating of the ligand-gated ion channel superfamily inferred from protein structure. *Exp. Physiol.* **89:** 145-153.

Alex, K. D., and Pehek, E. A. (2007) Pharmacological mechanisms of sertonergic regulation of dopamine neurotransmission. *Pharmacol. Ther.* **113:** 296-320.

Ang, C., Habre, W., Sims, C. (1998) Tropisetron reduces vomiting after tonsillectomy in children. *Br. J. Anaesth.* **80:** 761-763.

Barnes, N. M. (2005) 5-HT_3 receptor antagonists ameliorate fatigue: so much potential, so little knowledge! *Gut* **54:** 1056-1057.

Barnes, N. M., Hales, T. G., Lummis, S. C. R., and Peters, J. A. (2009) The 5-HT3 receptor – the relationship between structure and function. *Neuropharmacol.* **56:** 273-284.

Beene, D. L., Price, K. L., Lester, H. A., Dougherty, D. A., and Lummis, S. C. R. (2004) Tyrosine Residues That Control Binding and Gating in the 5-Hydroxytryptamine$_3$ Receptor Revealed by Unnatural Amino Acid Mutagenesis. *J. Neurosci.* **24:** 9097-9204.

Beene, D. L., Brandt, G. S., Lester, H. A., and Dougherty, D. A. (2002) Comparison of the cationic-π interaction at the agonist binding-sites of the nicotinic acetylcholine receptor and the 5-Hydroxytryptamine3 receptor. *Biophys. J.* **82:** 257a.

Belelli, D., Balcarek, J. M., Hope, A. G., Peters, J. A., Lambert, J. J., and Blackburn, T. P. (1995) Cloning and functional expression of a human 5-Hydroxytryptamine type $_{3A}$ receptor subunit. *Mol. Pharmacol.* **48**: 1054-1062.

Betz, H. (1990) Ligand-gated ion channels in the brain: The amino acid receptor superfamily. *Neuron* **5:** 383-392.

Boess, F. G., Steward, L. J., Steele, J. A., Liu, D., Reid, J., Glencorse, T. A., and Martin, I. L. (1997) Analysis of the ligand binding site of the 5-HT3 receptor using site directed mutagenesis: importance of glutamate 106. *Neuropharmacol.* **36:** 637-647.

Boess, F. G., Beroukhim, R., and Martin, I. L. (1995) Ultrastructure of the 5-hydroxytryptamine3 receptor. *J. Neurochem.* **64:** 1401-1405.

Boess, F. G., Lummis, S. C., and Martin, I. L. (1992) Molecular properties of 5-hydroxytryptamine3 receptor-type binding sites purified from NG108-15 cells. *J. Neurochem.* **59:** 1692-1701.

Bormann, J., Hamill, O. P., and Sakmann, B. (1987) Mechanism of anion permeation through channels gated by glycine and γ-aminobutyric acid in mouse cultured spinal neurons. *J. Physiol.* **385:** 243-286.

Bouzat, C., Gumilar, F., Spitzmaul, G., Wang, H. L., Rayes, D., Hansen, S. B., Taylor, P., Sine, S. M. (2004) Coupling of agonist binding to channel gating in an ACh-binding protein linked to an ion channel. *Nature* **19:** 896-900.

Boyd, G. W., Doward, A. I., Kirkness, E. F., Millar, N. S., and Connolly, C. N. (2003) Cell Surface Expression of 5-Hydroxytryptamine Type 3 Receptors Is Controlled by an Endoplasmic Reticulum Retention Signal. *J. Biol. Chem.* **30**: 27681-27687.

Boyd, G. W., Low, P., Dunlop, J. I., Robertson, L. A., Vardy, A., Lambert, J. J., Peters, J. A., and Connolly, C. N. (2002) Assembly and Cell Surface Expression of Homomeric and Heteromeric 5-HT_3 Receptors: The Role of Oligomerization and Chaperone Proteins. *Mol. Cell. Neurosci.* **21:** 38-50.

Brejc, K., van Dijk, W. J., Klaassen, R. V., Schuurmans, M., van Der Oost, J., Smit, A. B., and Sixma, T. K. (2001) Crystal structure of an ACh-binding protein reveals the ligand-binding domain of nicotinic receptors. *Nature* **411**: 269-276.

Camilleri, M., Mayer, E. A., Drossman, D. A., Heath, A., Dukes, G. E., McSorley, D., Kong, S., Mangel, A. W., Northcutt, A. R. (1999) Improvement in pain and bowel function in female irritable bowel patients with alosetron, a 5-HT_3 receptor antagonist. *Aliment. Pharmacol.Ther.* **13:** 1149–59.

Castillo, M., Mulet, J., Gutierrez, L. M., Ortiz, J. A., Castelan, F., Gerber, S., Sala, S., Sala, F., and Criado, M. (2006) Role of RIC-3 Protein in Trafficking of Serotonin and Nicotinic Acetylcholine Receptors. *J. Mol. Neurosci.* **30:** 153-156.

Celie, P. H., Klaassen, R. V., van Rossum-Fikkert, S. E., van Elk, R., van Nierop, P., Smit, A. B., Sixma, T. K. (2005) Crystal structure of acetylcholine-binding

protein from Bulinus truncatus reveals the conserved structural scaffold and sites of variation in nicotinic acetylcholine receptors. *J. Biol. Chem.* **280:** 26457-26466.

Cheng, A., Bollan, K. A., Greewood, S. M., Irving, A. J., and Connolly, C. N. (2007) Differential Subcellular Localization of RIC-3 Isoforms and Their Role in Determining 5-HT_3 Receptor Composition. *J. Biol. Chem.* **36:** 26158-26166.

Corringer, P. J., Bertrand, S., Galzi, J. L., Devillers-Thiery, A., Changeux, J.-P., and Bertrand, D. (1999) Mutational Analysis of the charge selectivity filter of the alpha7 nicotinic acetylcholine receptor. *Neuron* **22:** 831-843.

Dahlof, C. G. H., Hargreaves, R. J. (1998) Pathophysiology and pharmacology of migraine. Is there a place for antiemetics in future treatment strategies? *Chephalalgia* **18:** 593-604.

Davies, P. A., Pistis, M., Hanna, M. C., Peters, J. A., Lambert, J. J., Hales, T. G., and Kirkness, E. F. (1999) The 5-HT3B subunit is a major determinant of serotonin-receptor function. *Nature* **397:** 359-363.

de Oliveira, A. N., Zhang, R., and Machu, T. K (2009) Colchicine: A Novel Positive Allosteric Modulator of the Human 5-Hydroxytryptamine3A Receptor. *J. Pharmacol. Exp. Ther.* **329:** 838-847.

Dellisanti, C. D., Yao, Y., Stroud, J. C., Wang, Z. Z., and Chen, L. (2007) Crystal structure of the extracellular domain of nAChR α-1bound to α-bungarotoxin at 1.94Å resolution. *Nat. Neurosci.* **10:** 953-962.

Dubin, A. E., Huvar, R., D'Andreas, M. R., Pyati, J., Zhu, J. Y., Joy, K. C., Wilson, S. J., Galindo, J. E., Glass, C. A., Luo, L., Jackson, M. R., Lovenberg, R. W., and Erlander, M. G. (1999) The Pharmacological and Functional Characteristics of the Serotonin 5-HT3A Receptor Are Specifically Modified by a 5-HT3B Receptor Subunit. *J. Biol. Chem.* **43:** 30799-30810.

Eisele′, J. L., Bertrand, S., Galzi, J. L., Deillers-Thiery, A., Changeux, J. P., and Bertrand, D. (1993) Chimaeric nicotinic-serotonergic receptor combines distinct ligand binding and channel specificities. *Nature* **336:** 479-483.

Engleman, E. A., Rodd, Z. A., Bell, R. L., and Murphy, J. M. (2008) The role of 5-HT3 receptors in drug abuse and as a target for pharmacotherapy. *CNS Neurol Disord Drug Targets* **7:** 454-467.

Enz, R. (2001) GABA(C) receptors: a molecular view. *Biol. Chem.* **382**: 1111-1122.

Espinoza-Fonseca, L. M., Trujillo-Ferrara, J. G. (2006) Fully flexible docking models of the complex between α7 nicotinic receptor and a potent heptapeptide inhibitor of the β-amyloid peptide binding. *Bioorg. Med. Chem. Lett.* **16:** 3519-3523.

Faerber, L., Drechsler, S., Ladenburger, S., Gschaidmeier, H., and Fischer, W. (2007) The neuronal 5-HT_3 receptor network after 20 years of research-Evolving concepts in management of pain and inflammation. *Eur. J. Pharmacol.* **560:** 1-8.

Fiebich, B. L., Akindi, R. S., Seidel, M., Geyer, V., Haus, U., MÜller, W., Stratz, T., and Candelario-Jalil, E. (2004) Expression of 5-HT_{3A} receptors in cells of the immune system. *Scand. J. Rheumatol. Suppl.* **119:** 9-11.

Forni, C., Loro, L., Mazzei, T., Beghelli, C., Biolchini, A., Tremosini, M., Triggiani, A., and Bacci, G. (2003) Tropisetron and dexamethasone administered twice daily for the prevention of acute emesis in patients treated with continuous infusion of Cisplatin-Doxorubicin and high-dose fosfamide over 48, 24, and 120 hours. *Cancer Nurs.* **26:** 331-334.

Galzi., J.-L., and Changeux, J.-P. (1995) Neuronal nicotinic receptors: molecular organization and regulations. *Neuropharmacol.* **34:** 563-582.

Galzi, J. L., Deviller-Thiery, A., Hussy, N., Bertrand, S., Changeux, J. P., and Bertrand, D. (1992) Mutations in the channel domain of a neuronal nicotinic receptor convert ion selectivity from cationic to anionic. *Nature* **359:** 500-505.

Galzi, J. L., Revah, F., Black, D., Goeldner, M., Hirth, C., and Changeus, J. P. (1990) Identification of a novel amino acid alpha-tyrosine 93 within the cholinergic ligands-binding sites of the acetylcholine receptor by photoaffinity labeling. Additional evidence for a three-loop model of the cholinergic ligands-binding sites. *J. Biol. Chem.* **265:** 10430-10437.

Grenningloh, G., Gundelfinger, E., Schmitt, B., Betz, H., Darlison, M. G., Barnard, E. A., Schofield, P. R., and Seeburg, P. H. (1987) Glycine vs GABA receptors. *Nature* **330**: 25-26.

Gunthorpe, M. J., and Lummis, S. C. (2001) Conversion of the ion selectivity of the 5-HT3A receptor from cationic to anionic reveals a conserved feature of the ligand-gated ion channel superfamily. *J. Biol. Chem.* **276:** 10977–10983.

Hanna, M. C., Davies, P. A., Hales, T. G., and Kirkness, E. F. (2000) Evidence for expression of heteromeric serotonin 5-HT(3) receptors in rodents. *J. Neurochem.* **75:** 240-247.

Hapfelmeir, G., Tredt, C., Haseneder, R., Zieglgänsberger, W., Eisensamer, B., Rupprecht, R., and Rammes, G. (2003) Co-expression of the 5-HT3B Serotonin Receptor Subunit Alters the Biophysics of the 5-HT3 Receptor. *Biophys. J.* **84:** 1720-1733.

Hodge, C. W., Samson, H. H., Lewis, R. S., Erickson, H. L. (1993) Specific decreases in ethanol- but no water-reinforced responding produced by the 5-HT_3 antagonist ICS 205-930. *Alcohol* **10:** 191-196.

Holbrook, J. D., Gill, C. H., Zebda, N., Spencer, J. P., Leyland, R., Rance, K. H., Trinh, H., Balmer, G., Kelly, F. M., Yusaf, S. P., Coutenay, N., Luck, J., Rhodes, A., Modha, S., Moore, S. E., Sanger, G. J., and Gunthorpe, M. J. (2009) Characterization of 5-HT_{3C}, 5-HT_{3D} and 5-HT_{3E} receptor subunits: evolution, distribution and function. *J. Neurochem.* **108**: 384-396.

Hope, A. G., Belelli, D., Mair, I. D., Lambert, J. J., and Peters, J. A. (1999) Molecular Determinants of (+)-Tubocurarine Binding at Recombinant 5-Hydroxytryptamine$_{3A}$ Receptor Subunits. *Mol Pharmacol* **55**: 1037-1043.

Horenstein, Wagner, D. A., Czajkowski, C., and Akabas, M. H. (2001) Protein mobility and GABA-induced conformational changes in GABAA receptor pore-lining M2 segment. *Nat. Neurosci.* **4:** 477-485.

Horovitz, A. (1996) Double-mutant cycles: a powerful tool for analyzing protein structure and function. *Curr. Biol.* **12:** R121-R126.

Humphrey, P. P. A (1997) The characterization and classification of neurotransmitter receptors. *Ann. N. Y. Acad. Sci.* **812:** 1-13.

Ilegems, E., Pick, H. M., Deluz, C., Kellenberger, S., and Vogel, H. (2004) Noninvasive Imaging of 5-HT_3 Receptor Trafficking in Live Cells. *J. Biol. Chem.* **279:** 53346-53352.

Johnson, B. A. (2004) Role of the serotonergic system in the neurobiology of alcoholism: Implications for treatment. *CNS Drugs* **18:** 1105-1118.

Jones, D. N. C., Barnes, N. M., Costall, B., Domeney, A. M., Kilpatrick, G. J., Naylor, R. J., and Tyers, M. B. (1992) The distribution of 5-HT_3 receptor recognition sites in the marmoset brain. *Eur. J. Pharmacol.* **215:** 63-68.

Jones, R. H., Holtmann, G., Rodrigo, L., Ehsanullah, R. S., Crompton, P. M., Jacques, L. A., and Mills, J. G. (1999) Alosentron relieves pain and improves bowel function compared with mebeverine in female nonconstipated irritable bowel syndrome patients. *Aliment. Pharmacol. Ther.* **13:** 1419-1427.

Joshi, P. R., Suryanarayanan, A., Hazai, E., Schulte, M. K., Maksay, G., and Zsolt, B. (2006) Interactions of Granisetron with an Angonist-Free 5-HT Receptor Model. *Biochem.* **45:** 1099-1105.

Karlin, A. (2002) Emerging Structure of the Nicotinic Acetylcholine Receptors. *Nature* **3:** 102-114.

Karlin, A., Akabas, M. H. (1998) Substituted-cysteine accessibility method. *Methods Enzymol.* **293:** 123-145.

Karlin, A., and Akabas, M. H. (1995) Toward a structural basis for the function of nicotinic acetylcholine receptors and their cousins. *Neuron* **15:** 1231-1244.

Keramidas, A., Moorehouse, A. J., French, C. R., Schofield, P. R., and Barry, P. H. (2000) M2 pore mutations convert the glycine receptor channel from being anion- to cation-selective. *Biophys. J.* **79:** 247-259.

Keramidas, A., Moorhouse, A. J., Schofield, P. R., and Barry, P. H. (2004) Ligand-gated ion channels: mechanisms underlying ion selectivity. *Prog. Biophys. Molec. Biol.* **86:** 161-204.

Kilpatrick, G. J., Jones, B. J., and Tyers, M. B. (1987) Identification and distribution of 5-HT_3 receptors in rat brain using radioligand binding. *Nature* **330:** 746-748.

Kilpatrick, G. J., Jones, B. J., and Tyers, M. B. (1989) Binding of the 5-HT_3 ligand [3H]GR65630, to rat area postrema, vagus nerver, and the brains of several species. *Eur. J. Pharmacol.* **159:** 157-164.

Krzywkowski, K., Jensen, A. A., Connolly, C. N., and Brauner-Osborne, H. (2007) Naturally occurring variations in the human 5-HT_{3A} gene profoundly impact 5-HT_3 receptor function and expression. *Pharmacogenet. Genom.* **17:** 255-266.

Kurzwelly, D., Barann, M., Kostanian, A., Combrink, S., Bonisch, H., Gothert, M., and Bruss, M. (2004) Pharmacological and electrophysiological properties of the naturally occurring Pro391Arg variant of the human 5-HT_{3A} receptor. *Pharmacogenetics* **14:** 165-172.

Lankiewicz, S., Huser, M. B., Heumann, R., Hatt, H., and Gisselmann, G. (2000) Phosphorylation of the 5-hydroxytryptamine$_3$ (5-HT$_3$) receptor expressed in HEK293 cells. *Rec. Chan.* **7:** 9-15.

Lankiewicz, S., Lobitz, N., Wetzel, C. H., Rupprecht, R., Gisselmann, G., and Hatt, H. (1998) Molecular cloning, functional expression, and pharmacological characterization of 5-hydroxytryptamine receptor cDNA and its splice variants from guinea pig. *Mol. Pharmacol.* **53:** 202-212.

Le Novère, N., and Changeux, J.-P. (1995) Molecular evolution of the nicotinic acetylcholine receptor: an example of multigene family in excitable cells. *J. Mol. Evol.* **40:** 155-172.

Lê, A. D., Funk, D., Harding, S., Juzytsch, W., Fletcher, P. J., and Shaham, Y. (2006) Effects of dexfenfluramine and 5-HT$_3$ receptor antagonists on stress-induced reinstatement of alcohol seeking in rats. *Psychopharmacol.* **186:** 82–92.

Leibundgut, U., and Lancrajan, I. (1987) First results with ICS 205-930 (5-HT$_3$ receptor antagonist) in prevention of chemotherapy induced emesis. *Lancet* **23:** 1198.

Machu, T. K., Hamilton, M. E., Frye, T. F., Shanklin, C. L., Harris, M. C., Sun, H., Tenner, Jr., T. E., Soti, F. S., Kem, W. R. (2001) Benzylidene analogs of anabaseine display partial-agonist and antagonist properties at the mouse 5-hydroxytryptamine (3A) receptor. *J. Pharmacol. Exp. Ther.* **299:** 1112-9.

Malany, S., Osaka, H., Sine, S. M., and Taylor, P. (2000) Orientation of α-Neurotoxin at the Subunit Interfaces of the Nicotinic Acetylcholine Receptor. *Biochem.* **39:** 15388-15398.

Marazziti, D., Betti, L., Giannaccini, G., Rossi, A., Masala, I., Baroni, S., Cassano, G. B., and Lucacchini, A. (2001) Distribution of [3H]GR65630 Binding in Human Brain Postmorten. *Neurochem. Res.* **26:** 187-190.

McCleane, G. J., Suzuki, R., Dickenson, A. H. (2003) Does a single intravenous injection of the 5-HT_3 receptor antagonist odansentron have an analgesic effect in neuropathic pain? A double-blinded, placebo-controlled cross-over study. *Anesth. Analg.* **7:** 1474-1478.

Menzikov, S. A., and Menzikova, O. V. (2005) The Molecular Weight of Cl^-, HCO_3^--Activated Mg^{2+}-ATPase of Rat Brain Plasma Membranes That Is Sensitive to $GABA_A$-ergic Ligands. Dokl. *Biochem. Biophys.* **401:** 170-172.

Millar, N. A. (2007) RIC-3: a nicotinic acetylcholine receptor chaperone. *Br. J. Pharmacol.* **153:** Suppl 1 S:177-183.

Miquel, M.-C., Emerit, M. B., Nosjean, A., Simon, A., Tumajogee, P., Brisorgueil, M.-J., Doucet, E., Hamon, M., and Verge, D. (2002) Differential subcellular localization of the 5-$HT_{3\text{-}A}$s receptor subunit in the rat central nervous system. *Eur. J. Neurosci.* **15**: 449-457.

Miyazawa, A., Fujiyoshi, Y., Unwin, N. (2003) Structure and gating mechanisms of the acetylcholine receptor pore. *Nature* **423:** 949-955.

Mochizuki, S., Miyake, A., and Furuichi, K. (1999) Identification of a domain affecting agonist potency of *meta*-chlorophenylbiguanide in 5-HT_3 receptors. *Eur J Pharmacol* **369**: 125-132.

Monk, S. A,, Williams, J. M., Hope, A. G., and Barnes, N. M. (2004) Identification and importance of N-glycosylation of the human 5-hydroxytryptamine3A receptor subunit. *Biochem. Pharmacol.* **68:** 1787-1796.

Niesler, B., Walstab, J., Combrink, **S.,** Möller, D., Kapeller, J., Rietdorf, J., Bönisch, H., Göthert, M., Rappold, G., and Brüss, M. (2007) Characterization of the Novel Human Serotonin Subunits 5-HT_{3C}, 5-HT_{3D}, and 5-HT_{3E}. *Mol. Pharmacol.* **72:** 8-17.

Ortells, M. O., and Lunt, G. G. (1995) Evolutionary History of the Ligand-gated Ion-channel Superfamily of Receptors. *Trends Neurosci.* **18:** 121-126.

Peters, J. A., Malone, H. M., and Lambert, J. J. (1991) Ketamine potentiates 5-HT_3 receptor-mediated currents in rabbit nodose ganglion neurones. *Br. J. Pharmacol.* **103:** 1623-1625.

Price, K. L., and Lummis, S. C. (2004) The role of tyrosine residues in the extracellylar domain of the 5-hydroxytryptamine3 receptor. *J. Biol. Chem.* **279:** 23294-23301.

Quirk, P. L., Rao, S., Roth, B. L., and Siegel, R. E. (2004) Three Putative N-Glycosylation Sites Within The Murine 5-HT_{3A} Receptor Sequence Affect Plasma Membrane Targeting, Ligand Binding, and Calcium Influx in Heterologous Mammalian Cells. *J. Neurosci. Res.* **77:** 498-506.

Reeves, D. C., Goren, E. N., Akabas, M. H., Lummis, S. C. R. (2001) Structural and Electrostatic Properties of the 5-HT_3 Receptor Pore Revealed by Substituted Cysteine Accessibility Mutagenesis. *J. Biol. Chem.* **276:** 42035–42042.

Reeves, D.C., and Lummis, S. C. (2002). The molecular basis of the structure and function of the 5-HT_3 receptor: a model ligand-gated ion channel. *Mol. Membr. Biol.* **19:** 11-26.

Schofield, C. M., Jenkins, A., Harrison, N. L. (2003) A highly conserved aspartic acid residue in the signature disulfide loop of the alpha 1 subunit is a determinant of gating in the glycine receptor. *J. Biol. Chem.* **278:** 34078-34083.

Schreiter, C., Hovius, R., Costioli, M., Pick, H., Kallenberger, S., Schild, L., and Vogel, H. (2003) Characterization of the Ligand-binding Site of the Serotonin 5-HT_3 Receptor. *J. Biol. Chem.* **278:** 22709-22716.

Sine, M. S., and Engel, A. G. (2006) Recent advance in Cys-loop receptor structure function. *Nature* **440:** 448-455.

Spier, A. D., and Lummis, S. C. (2000) The role of tryptophan residues in the 5-Hydroxytryptamine$_3$ receptor ligand binding domain. *J. Biol. Chem.* **275:** 5620-5625.

Spiller, R. (2006) Role of motility in chronic diarrhea. *Neurograstroenterol. Motil.* **18:** 1045-1055.

Stweard, L. J., Boess, F. G., Steele, J. A., Liu, D., Wong, N., and Martin, I. L. (200) Importance of phenylalanine 107 in agonist recognition by the 5-Hydroxytryptamine(3A) receptor. *Mol. Pharmacol.* **57:** 1249-1255.

Suryanarayanan, A., Joshi, P. R., Bikadi, Z., Mani, M., Kulkarni, T. R., Gaines, C., and Schulte, M. K. (2005) The Loop C Region of the Murine 5-HT_{3A} Receptor

Contributes to the Differential Actions of 5-Hydroxytryptamine and m-Chlorophenylbiguanide. *Biochem.* **44:** 9140-9149.

Thompson, A. J., and Lummis, S. C. (2003) A single ring of charged amino acids at one end of the pore can control ion selectivity in the 5-HT_3 receptor. *Br. J. Pharmacol.* **140:** 359-365.

Thompson, A. J., Padgett, C. L., Lummis, S. C. R. (2006) Mutagenesis and Molecular Modeling Reveal the Importance of the 5-HT_3 Receptor F-loop. *J. Biol. Chem.* **281:** 16576-16582.

Thompson, A. J., Price, K. L, Reeves, D., Chan, S. L., Chau, P. L., and Lummis, S. C. (2005) Locating an antagonist in the 5-HT_3 receptor binding site using modeling and radioligand binding. *J. Biol. Chem.* **280:** 20476-20482.

Tyers, M. B. (1991) 5-HT_3 receptors and the therapeutic potential of 5-HT_3 receptor antagonists. *Therapie* **46:** 431-435.

Unwin, N. (1998) The nicotinic acetylcholine receptor of the Torpedo electric ray. *J. Struct. Biol.* **121:** 181-190.

van Nierop, P., Keramidas, A., Bertrand, S., van Minnen, J., Gouwenberg, Y., Bertrand, D., and Smit, A. B. (2005) Identification of Molluscan Nicotinic Acetylcholine Receptor (nAChR) Subunits Involved in Formation of Catio- and Anion-Selective nAChRs. *J. Mol. Neurosci.* **25:** 10617-10626.

Weiss, B., Mertz, A., Schrock, E., Koenen, M., and Rappold, G. (1995) Assignment of a human homolog of the mouse Htr3 receptor gene to chromosome 11q23.1-q23.2. *Genomics* **29:** 304-305.

White, P. F., Tang, J., Hamza, M. A., Ogunnaike, B., Lo, M., Wender, R. H., Naruse, R., Sloninsky, A., Kariger, R., Cunneen, S., Khalili, T. (2006)The use of oral granisetron versus intravenous odansentron for antiemetic prophylaxis in patients undergoing laparoscopic surgery: the effect on emetic symptoms and quality of recovery. *Anesth. Analg.* **102:** 1387-93.

Yan, D., Schulte, M. K., Bloom, K. E., and White, M. M. (1999) Structural features of the ligand-binding domain of the serotonin 5-HT3 receptor. *J. Biol. Chem.* **274:** 5537-5541.

Yan, D., and White, M. M (2005) Spatial Orientation of the Antagonist Granisetron in the Ligand-Binding Site of the 5-HT_3 Receptor. *Mol. Pharmacol.* **68:** 365-371.

Yan, D., Meyer, J. K., and White, M. M. (2006) Mapping Residues in the Ligand-Binding Domain of the 5-HT_3 Receptor onto d-Tubocurarine Structure. *Mol. Pharmacol.* **70**: 571-578.

Zhang, R., Wen, X., Militante, J., Hester, B., Rhubottom, H. E., Sun H, Leidenheimer NJ, Yan D, White MM, Machu TK. (2007) The role of loop F residues in determining differential d-tubocurarine potencies in mouse and human 5-hydroxytryptamine$_{3A}$ receptors. *Biochem.* **46**: 1194-1204.

Zhang, R., White, N. A., Soti, F. S., Kem, W. R., Machu, T. K. (2006). N-Terminal Domains in Mouse and Human 5-Hydroxytryptamine$_{3A}$ Receptors Confer Partial Agonist and Antagonist Properties to Benzylidene Analogs of Anabaseine. *J Pharmacol Exp Ther* **317:** 1276-1284.

CHAPTER II

LOOP C IS THE MAJOR DETERMINANT OF DIFFERENTIAL *d*-TUBOCURARINE AFFINITY IN HUMAN 5-HYDROXYTRYPTAMINE$_{3A}$ RECEPTORS

PREFACE

Structure-activity-relationships of drug-receptor interactions are commonly used, in conjuction with interspecies studies, to identify amino acid residues responsible for key pharmacological differences in drug response. Using electrophysiology, individual residues in Loops C and F of the 5-HT$_{3A}$ receptor have been identified as critical for conferring curare potency in mouse and human receptors. Functional data is not, however, sufficient to determine whether residues play a role in binding, gating or both. This chapter describes both, the electrophysiological studies, as well as the radioligand binding experiments designed to further assess the role of Loop C residues in binding and function of curare at the 5-HT$_{3A}$ receptor, thus addressing the first specific aim of this dissertation project.

CHAPTER II

LOOP C IS THE MAJOR DETERMINANT OF DIFFERENTIAL *d*-TUBOCURARINE AFFINITY IN HUMAN 5-HYDROXYTRYPTAMINE$_{3A}$ RECEPTORS

A.N. de Oliveira-Pierce*[1], Rashmi Lote*[1,] Ran Zhang[1, 2], Michael M. White[3], and Tina K. Machu[1]

1. Department of Pharmacology and Neuroscience, University of North Texas Health Science Center, 3500 Camp Bowie Blvd., Fort Worth, TX 76107

2. Department of Immunology, The University of Texas, M. D. Anderson Cancer Center, 7455 Fannin St., Houston, TX 77054

3. Department of Biochemistry and Molecular Biology, Drexel University College of Medicine, 245 N 15th St., MS 497, Philadelphia, PA 19102

*Equal contribution

Running head: Differential Actions of Curare at Human and Mouse 5-HT$_{3A}$Rs

Address correspondence to: A.N. de Oliveira-Pierce, Department of Pharmacology and Neuroscience, University of North Texas Health Science Center, 3500 Camp Bowie Blvd., Fort Worth, TX 76107. Tel: 817-735-2190; Fax: 817-735-0408; E-mail: aoliveir@hsc.unt.edu

Abbreviation List: 5-Hydroxytryptamine (5-HT); 5-hydroxytryptamine$_{3A}$ receptor (5-HT$_{3A}$); modified Barth's solution (MBS); vesicle dialysis buffer (VDB); nicotinic acetylcholine receptor (nAChR); *d*-Tubocurarine (curare); acetylcholine binding protein

(AChBP); ligand-gated ion channels (LGICs); ligand binding domain (LBD); mouse wild-type 5-hydroxytryptamine$_{3A}$ receptor (MWT); human wild-type 5-hydroxytryptamine$_{3A}$ receptor (HWT); 1-Methyl-N-[(3-endo)-9-methyl-9-azabicyclo[3.3.1]non-3- yl]-1H-indazole-3-carboxamide hydrochloride (BRL-43694).

ABSTRACT

Mouse and human 5-Hydroxytryptamine$_{3A}$ receptors (5-HT$_{3A}$R's) share 84% amino acid identity. Nevertheless, the competitive antagonist, *d*-tubocurarine (curare), has 100-fold greater potency at mouse (MWT) than human (HWT) wild-type 5-HT$_{3A}$ receptors.. Previously, we reported that Loops C and F of the ligand binding domain play a role in conferring differential curare sensitivities of MWT (IC_{50} = 13 nM) and HWT (IC_{50} = 1,817 nM). The human receptor containing six mouse substitutions in, and one near, Loop C (H-Loop C+1), had a curare potency of 40 nM, similar to the MWT receptor. In the present study, we probed residues in or near Loop C by substituting the human receptor residues with mouse receptor orthologs and then assessing the mutants with two-electrode voltage clamp electrophysiological recordings and radioligand binding assays. None of the seven single point-mutant receptors conferred mouse-like curare potency, with IC_{50}'s ranging from 30-fold to 700-fold higher than MWT. A series of chimeras were constructed, and the chimera H-Y217Q/M223I/E224D/Y228S (IC_{50} = 35 nM) had the same curare potency as H-Loop C+1. In radioligand binding assays curare displaced the competitive antagonist [^{3}H]-BRL-43694 with rank order affinities (K_i) of MWT (8.3 nM) = H-Y217Q/M223I/E224D/Y228S (6.4 nM) > HWT (2600 nM) > H-E224D (432,000 nM). These results suggest that the functional effects of curare at 5-HT$_{3A}$R's are due to ligand-binding and gating and that the role of H-E224 is significantly altered by other Loop C residues.

INTRODUCTION

The ionotropic serotonin type 3 receptor (5-HT_3R) is a member of the cys-loop superfamily of ligand-gated ion channels (LGIC's) which contains muscle and neuronal nicotinic acetylcholine receptors (nAChR's), γ-aminobutyric A receptors ($GABA_A$R's), glycine receptors (GlyR's) and 5-HT_3R's. In recent years, this receptor has emerged as a potential target for a number of therapeutic agents (Thompson and Lummis, 2006; Akhondzadeh et al., 2008). The 5-HT_3 receptor is found in the central nervous system, peripheral nervous system, gut, lymphocytes, monocytes, and fetal tissue (Fiebich et al., 2004). Of the five 5-HT_3 subunits (A-E) cloned to date, A and B subunits have been shown to have functional significance in the central or peripheral nervous systems (Hope et al., 1999; Davies et al., 1999).

Subunits are composed of a long extracellular N-terminus, four transmembrane domains (TM1-TM4) and an extracellular C-terminus. The ligand binding domain (LBD) is located in the N-terminus at the interface between subunits and consists of six loops: A, B, C, D, E, and F. Loops A-C are located in the principal component of the LBD, and Loops D-F are located in the complementary component of the LBD (Reeves and Lummis, 2002). The 5-HT_{3A}R and the nAChR share a great deal of homology, and their mechanism of activation is highly conserved (Reeves and Lummis, 2002). Subsequently, much of the research done on LGIC's has been based on structural details obtained from crystallization of the acetylcholine binding protein (AChBP), a homolog of the N-terminus of the nAChR (Brejc et al., 2001), electron microscopy of the *Torpedo* nAChR

(Unwin, 1998), and crystallization of the extracellular domain of the mouse nAChR α1 subunit (Dellisanti et al., 2007).

D-Tubocurarine (curare), a toxic alkaloid best known for its neuromuscular blocking actions at the nAChR, acts as a competitive antagonist at both mouse and human 5-HT_{3A} receptors. However, potency of curare is markedly greater at the mouse wild-type receptor than at the human wild-type receptor (Hope et al., 1999). Studies investigating differential pharmacology of curare (Hope et al., 1999; Zhang et al., 2007) and other compounds such as 3-(2-hydroxy, 4-methoxybenzylidene)-anabaseine (2-OHMBA) (Zhang et al., 2006), colchicine (de Oliveira-Pierce et al., 2009) and *m*-clorophenylbiguanidine (Mochizuki et al., 1999; Yan et al., 1999), indicate that relatively small differences in amino acid sequence play a critical role in determining differential actions of these compounds at the 5-HT_{3A} receptor.

Previously, we reported that Loops C and F of the human and mouse 5-HT_{3A} receptors play a role in conferring curare potency. We identified two residues in Loop F of the human receptor (K195 and V202) which when mutated to their respective mouse orthologs, were sufficient to confer curare potency attributable to the mouse Loop F (Zhang et al., 2007). A previous study reported that single substitutions of Loop C of the mouse receptor with human receptor orthologs resulted in modest changes in curare potency (Hope et al., 1999). The failure to produce a substantial shift in curare potency in the mouse point mutant receptors in this study may be due the participation of multiple Loop C residues in curare binding as well as a contribution of Loop F (Zhang et al., 2007). In the present study, we examined the role of residues in Loop C and the non-

conserved residue between Loop C and the first transmembrane domain in determining curare potency and affinity in the human 5-HT_{3A} receptor. Using site directed mutagenesis, two electrode voltage-clamp electrophysiology, and radioligand binding, we identified four critical residues in Loop C of the human receptor (Y217, M223, E224, and Y228), which when simultaneously mutated to mouse orthologs, resulted in a receptor with mouse-like curare potency. Furthermore, the point-mutation, H-E224D had a lower potency and affinity than HWT, suggesting a unique interaction of E224 with other Loop C residues. Identification of Loop C residues that contribute to binding of competitive antagonists at the ligand recognition site may promote further developments in therapeutics targeting the 5-HT_3 receptor.

EXPERIMENTAL PROCEDURES

Construction of Chimeric and Point Mutant Receptor cDNA's and cRNA's. Mouse and human 5-HT_{3A} receptor cDNA's, provided by Drs. D. Julius and A. Miyake, respectively, were subcloned into pBluescript KS^- and pCR-Script Amp $SK(+)^-$ (Stratagene, La Jolla, CA). Two unique restriction enzyme cleavage sites, Spe I, and Nar I, were introduced in both mouse and human 5-HT_{3A}R cDNAs by site-directed mutagenesis (U.S.E. mutagenesis kit, Pharmacia Biotech Inc., Piscataway, N.J.) of the nucleotides encoding the conserved residues: Thr 181 and Arg 244 in the mouse receptor cDNA and Thr 176 and Arg 239 in the human receptor cDNA, respectively (Fig. 1). Numbering of the amino acids in the two receptors began with the initiating methionine. Both receptor cDNA's were digested with the restriction enzymes, and the appropriate fragments were ligated to generate chimeric receptors in which the distal one-third of the N-termini containing Loops C and F were swapped. Chimeras containing Loop C, Y217Q/M223I/E224D/Y228S, or Y217Q/M223I/E224D/Y228S+V202I substitutions were generated with multiple rounds of mutagenesis, in which one to three substitutions were made simultaneously. Chimeric and point mutant receptor cDNA's were confirmed by dideoxynucleotide sequencing at the Biotechnology Core Facility at Texas Tech University, Lubbock, TX. The cDNAs were transcribed with the T3 mMESSAGE mMACHINE (Ambion, Austin, TX), and oocytes were microinjected with cRNA's.

Receptor Expression and Electrophysiological Recordings. Xenopus oocytes were subjected to chemical separation and defolliculation as previously described (Machu et

al., 2001). Oocytes were incubated at room temperature in ND96 media, containing (in mM) NaCl 96, KCl 2, $CaCl_2$ 1.8, $MgCl_2$ 1, and HEPES 5 (pH 7.5), plus 10 mg/l streptomycin, 50 mg/l gentamicin, 10,000 units/l penicillin, 96 mg/l sulfamethoxazole, 19 mg/l trimethoprim, 0.5 mM theophylline, and 2 mM sodium pyruvate.

5-HT-elicited currents were recorded in the two-electrode voltage clamp configuration in oocytes 2-7 days following injection (Machu et al., 2001). Serotonin and curare were obtained from Sigma (St. Louis, MO) and were dissolved in modified Barth's Solution (MBS) containing (in mM) NaCl 88, KCl 1, $NaHCO_3$ 2.4, HEPES 10, $MgSO_4$ 0.82, $Ca(NO_3)_2$ 0.33, and $CaCl_2$ 0.91 (pH 7.5). Serotonin was applied in the absence or presence of curare at 2 ml/min for 30-60 s.

Membrane Purification. Oocytes were injected with 100 ng HWT or MWT cRNA and tested for expression using two-voltage clamp electrophysiology on day three. Oocytes were homogenized with a hand-held glass Potter-Elvehjem homogenizer (~50 *Xenopus laevis* oocytes per preparation) in ice-cold vesicle dialysis buffer (VDB) containing (in mM) NaCl 96, MOPS 10, EDTA 0.1, and 0.02% NaN3 (pH 7.5), 0.1 ml per oocyte + 10 ul of protease inhibitor cocktail set III (Calbiochem, La Jolla, CA). The homogenate was centrifuged for 10 min at 800 g. The supernatant was collected, the pellet was resuspended in VDB (0.1 ml/oocyte) and re-centrifuged at 800 g for 10 min. Supernatants were then combined and centrifuged for 1 hour at 38,800 g. The membrane pellet was re-suspended in VDB (2-16 ml depending on expression) and divided into several batches for storage at -80 °C. Protein content was measured with the Lowry assay (Lowry et al., 1951).

Radioligand Binding Assays. For K_d determinations, membrane homogenate was incubated at 37 °C for 2 hours with [^{3}H]-BRL-43694 (0.1 nM – 23 μM). For K_i determinations, aliquots of membrane were incubated at 37 °C for 2 hours with curare (0.1 nM – 10 mM) and [^{3}H]-BRL-43694 at its K_d. [Q: do you h Non-specific binding was measured with MDL-72222 (3-tropanyl-3, 5-dichlorobenzoate), a 5-HT_{3A}R competitive antagonist. Following incubation with the radioligand, membranes were harvested by washing with VDB (pH 7.5). Bound radioligand was transferred to Whatman GF/B filters (Whatman, Clifton, NJ) by rapid vacuum filtration. Filters were individually incubated in 3 ml of Econo-Safe™ scintillation cocktail (Research International Products, Mt Prospect, IL) and quantified for radioactivity via scintillation spectrometry.

Data Analysis. In all electrophysiology experiments, the control values were obtained by averaging the 5-HT mediated response before and after the response to 5-HT or 5-HT plus curare. For generation of 5-HT concentration response curves, currents were expressed as a percentage of the maximal 5-HT (25 μM) responses. For antagonism by curare, percent inhibition was calculated by subtracting the current obtained from 5-HT plus curare from the average current obtained with 5-HT alone; the difference was divided by the average 5-HT mediated current, and the quotient was multiplied by 100.

Graphpad Prism (San Diego, CA) was used to calculate EC_{50}'s, IC_{50}'s, K_d's, K_i's and Hill coefficients. The equation used to calculate EC_{50}'s and IC_{50}'s was $I/I_{control} = 1/[1+[D/E(I)C_{50}]^{n}]$, where I is current, $I_{control}$ is the control current, D is the drug concentration, EC_{50} is the concentration of drug that produces 50% of the maximal response, IC_{50} is the concentration of drug that produces 50% inhibition of the response,

and *n* is the Hill coefficient. Specific binding was calculated as $X*B_{max}/(K_d+X)$, where X is the radioligand concentration, B_{max} is the maximum specific binding/mg protein, and K_d is the dissociation constant of the radioligand. Values for the equilibrium dissociation constants (K_i's) were calculated from the IC_{50}'s using the Cheng-Prusoff relationship (here's the reference:)) $K_i = (IC_{50})/(1+([ligand]/K_d))$, where IC_{50} is the concentration of unlabeled drug needed to block 50% of the specific binding, K_d is the affinity of the radioligand for the receptor, and [ligand] is the concentration of the unlabeled drug, One-way analysis of variance (ANOVA) and Tukey-Kramer post-hoc analyses were performed by Instat (San Diego, CA).

In the double mutant thermodynamic cycle analysis, the change in Gibbs free energy (ΔG) was calculated using $\Delta G = -RT \ln (IC_{50}$ receptor), where R is the gas constant and T is the temperature in Kelvin degrees (Ackers and Smith, 1985). It should be noted that the IC_{50} value determined in functional experiments is not a pure measure of antagonist affinity (Colquhoun, 1998), so that changes in IC_{50} may not have a 1:1 correspondence to changes in affinity.

Molecular Modeling and Ligand Docking. A structural model of the extracellular domain of the mouse 5-HT_{3A}R was generated using version 9v6 of the program MODELLER (Sali and Blundell, 1993), using the X-ray structure of the antagonist methllycaconitine-bound form of the *Aplysia* AChBP (Protein Data Bank ID: 2BYR, (Hansen et al., 2005) as the template as described previously (Yan and White, 2005; Yan et al., 2006).

Curare was docked to each binding site in the model using Autodock Vina (http://vina.scripps.edu). AutoDock Vina is significantly faster than AutoDock 4.0

(http://autodock.scripps.edu), and returns essentially similar docked conformations (data not shown). Protein and ligand coordinate pdb files were converted to pdbqt format files using AutoDock 4.0. The docking was performed on a 30x30x40 Å grid that covered the entire ligand-binding site. The size of the grid gives sufficient freedom for the ligands to be docked in all possible orientations while not permitting them move outside of the binding site. Images were produced using PyMOL (http://www.pymol.org).

RESULTS

The majority of the amino acid differences between human and mouse 5-HT_{3A} receptors are located in Loops C and F in the distal one-third of the N-terminal domain (Fig. 1A). We reported that in electrophysiological studies both Loops C and F account for the differential sensitivity of curare at human and mouse 5-HT_{3A} receptors (Zhang et al., 2007). In the present study, we further investigated the role of Loop C in conferring curare potency and affinity of the 5-HT_{3A} receptor. There are six differences between Loop C and one difference in the distal segment between Loop C and TM1 in the mouse and human 5-HT_{3A} receptors. A series of human receptor chimeras were constructed in which single or multiple residues were replaced with the corresponding mouse amino acids (Fig 1A). All receptor constructs were expressed in *Xenopus* oocytes, and two-electrode voltage clamp electrophysiological recordings were performed. Mutant receptor EC_{50} values ranged from 820 nM to 6,320 nM (Table I). Although some of the EC_{50} values for point-mutant and chimeric receptors were significantly different than that of the HWT, the largest fold change was 4.3. These results suggest that these substitutions do not greatly alter the mechanisms underlying coupling of ligand binding to channel gating at the 5-HT_{3A} receptor.

Previously we reported that the chimera in which all seven residues in this region were changed to the corresponding mouse ortholog (H-Loop C+1) had a curare IC_{50} of 41 nM (Zhang et al., 2007). Our first approach in identifying specific residues in H-Loop C+1 that contribute to curare potency was to assess the contribution of all seven amino

acids individually as single point mutations (Fig. 1B). None of the seven point mutants had curare potency equal to that of the H-Loop C+1 chimera. The highest potency (380 nM) was observed with a substitution at H-V237I, the amino acid between Loop C and TM1. The H-E224D receptor had an IC_{50} of 8,900 nM, corresponding to a five-fold decrease in curare potency compared to the HWT receptor (IC_{50} = 1,817 nM). The mouse point mutant receptor containing the reciprocal substitution, M-D229E, had a curare IC_{50} of 42.1 nM, which is only three-fold more than that of the MWT (13 nM) and is comparable to previously reported studies (Hope et al., 1999). The presence of E or D at position 224 is not sufficient to determine curare potency, as ferret (Mochizuki et al., 2000), rat (Mair et al., 1998), dog (Jensen et al., 2006) and guinea pig (Lankiewicz et al., 1998) 5-HT_{3A} receptors all have E at this position, and curare has been reported to have high affinity for ferret, rat and dog receptors but low affinity for the guinea pig receptor (Fig. 1C).

Given that none of the individual point mutant receptors had curare potencies equal to that of the H-Loop C+1 chimera, we created a series of smaller chimeras (Fig. 2A). The first chimera H-Loop C which does not contain the V237I substitution, had a curare IC_{50} of 40 nM, suggesting that the V237I substitution is not required. The five point mutant chimera, H-Y217Q/R219K/M223I/S225I/Y228S, had a curare IC_{50} of 103 nM, which is significantly greater than that of the H-Loop C chimera, suggesting that the E224D substitution is partially required for high potency. The four point mutant chimera, H-Y217Q/M223I/E224D/Y228S, had an IC_{50} of 35nM, suggesting that neither the R219K nor the S225I substitutions are required to confer curare potency.

We further assessed the role of the Y217Q, M223I, E224D, Y228S substitutions in all possible two and three point mutant chimeric receptors containing the E224D substitution (Fig. 2B and 2C). The H-M223I/E224D/Y228S receptor had an IC_{50} (121 nM) four-fold lower than H-Y217Q/M223I/E224D (IC_{50} of 456 nM). Curare potency was the highest at the H-Y217Q/E224D/Y228S receptor (IC_{50} = 104 nM). The three point chimeras in which E224D and Y228S were present together, produced the lowest IC_{50}'s, suggesting a potential interaction between the two. Of the two point mutant chimeric receptors tested, the H-E224D/Y228S had the lowest IC_{50} value (271 nM). The H-M223I/E224D and the H-Y217Q/E224D chimeras had IC50's of 1,300 nM and 1,400 nM, respectively, thus having little effect on curare potency when compared to the HWT (IC_{50} = 1,817 nM). These results confirm the important role of a serine residue in position 228 for determining curare potency at the human receptor. Furthermore, results confirm all four substitutions are required to confer mouse-like curare potency at the human chimeric receptor.

The E224D mutation by itself lowers curare potency, yet its presence is required in the context of three other mouse-like substitutions to confer curare potency equal to that of H-Loop C+1. To examine the effect of mutating the other three residues in the absence of an E224 mutation, we created a single three point mutant chimera and a single two point mutant chimera (Fig. 2C and 2D). The H-Y217Q/M223I/Y228S chimera had a three-fold lower curare potency (IC_{50} of 175 nM) than the four point chimera, H-Y217Q/M223I/E224D/Y228S. The H-Y217Q/Y228S chimera possessed an IC_{50} of 353 nM, a three-fold decrease in potency compared to H-Y217Q/E224D/Y228S (Fig. 2D).

Furthermore, mutant thermodynamic analysis supports the existence of a significant interaction between residues 217, 223, and 228 with 224 with regard to function of the 5-HT_{3A} receptor, with a $\Delta\Delta G_{int}$ = -1.84 kcal/mol (Fig. 2E).

To confirm the combined role of specific Loop C and F residues in conferring curare potency at human and mouse receptors, we tested a chimera, H-K195E/V202I/Y217Q/M223I/E224D/Y228S, containing the four critical Loop C substitutions and the two Loop F substitutions identified in our previous study (Zhang et al., 2007) as being important for curare potency. This six point mutant human chimeric receptor had a mouse-like curare potency (IC_{50} = 6 nM) (Fig. 3A). Given that H-V237I is the point mutant receptor with the highest curare potency, we tested the hypothesis that the V237I mutation could substitute for the E224D mutation and maintain curare potency equal to that of H-Loop C (IC_{50} of 41 nM). The chimera, H-Y217Q/R219K/M223I/Y228S, had a curare IC_{50} of 101 nM, and the addition of the I237V mutation decreased curare potency (IC_{50} of 152 nM). The mutant, H-219K/V237I, was tested, since H-R219K had the second lowest IC_{50} of the seven point mutant receptors (Fig. 1B). This two point mutant chimera had a significantly higher IC_{50} (856 nM) (Fig. 3B) than either of the two receptors containing single mutations. This result suggests that in the context of other human/mouse substitutions, neither mutation is required to confer mouse-like potency at the human receptor.

Changes in curare IC_{50}'s in functional studies in wild-type versus mutant receptors may be a result of either mutation induced changes in binding and/or gating of the receptor. Thus, the next step was to investigate the role of these residues in binding of

curare at the 5-HT_{3A} receptor. All binding assays were carried out in oocyte membranes enriched with 5-HT_{3A} receptors. Saturation binding experiments were performed in a selected number of 5-HT_{3A} receptor constructs in order to measured binding affinity of [^{3}H]-BRL-43694 and displacement of [^{3}H]-BRL-43694 by curare (Table 1). K_d values for H-V202I (7.01 nM), H-E224D/Y228S (7.25 nM) and H-Y217Q/M223I/E224D/Y228S (12.6 nM) were significantly different from both MWT (3.53 nM) and HWT (2.6 nM) receptors. However, even the largest difference, which occurred between HWT and H-Y217Q/M223I/E224D/Y228S +V202I receptors (five-fold), was modest and not likely to account for differences in curare's displacement of [^{3}H]-BRL-43694 at the 5-HT_{3A} receptor.

In order to establish whether there is a correlation between functional effects of Loop C substitutions (Y217Q, M223I, E224D and Y228S) and binding affinity of curare at the 5-HT_{3A} receptor, we performed competition binding experiments with curare displacement of [^{3}H]-BRL-43694 binding. Overall, the results correlated well with those of the functional studies, with a few differences (Table 2). There was a 314-fold difference in curare affinities for MWT (K_i of 8.3 nM) and HWT (2,608 nM) 5-HT_{3A} receptors. However, while in functional studies substitutions in both Loops C and F are required to confer mouse-like curare potency, in binding studies, substitutions in Loop C (Y217Q/M223I/E224D/Y228S) alone are sufficient to confer mouse-like affinity of curare in human 5-HT_{3A} receptors (Tables 1 and 2). Another difference between binding and functional data was the effect of the addition of Y228S to the H-E224D background. While the K_i value (2,873 nM) for the two point mutant chimera (H-E224D/Y228S) was

significantly lowered relative to H-E224D (K_i of 432,000 nM), it was not lower than that of HWT (K_i of 2,608 nM). In electrophysiological recordings, the curare IC_{50} for H-E224D/Y228S (271 nM) was less than that of the HWT (1,817 nM). The point mutant receptor H-E224D had decreased curare affinity (K_i of 432,000 nM) when compared to HWT (K_i = 2,608 nM). The reciprocal mutations at the mouse receptor (M-E229D) resulted in a very modest change in receptor affinity to curare (Table 2).

Surprisingly, contrary to functional studies, the human mutant receptor containing the Loop F V202I single substitution had a 17-fold decreased curare affinity (K_i = 44,200 nM) when compared to the HWT (K_i = 2,608 nM) . In functional studies this substitution yielded a receptor with seven-fold increased curare potency when compared to the HWT. The reciprocal mutation at the mouse receptor (M-I207V) did not significantly alter curare affinity. However, when V202I is combined with the Y217Q, M223I, E224D and Y228S substitutions in the human receptor, the resulting chimera had a 1,524-fold decreased curare K_i of 29 nM, when compared to the receptor containing the single V202I substitution. Furthermore, the curare K_i of 29 nM is ~ 3.5 fold higher than that of MWT (8.3 nM). We used mutant thermodynamic analysis (Fig. 3C) to further investigate the coupling of H-Y217Q/M223I/E224D/Y228S and V202I. The results of the mutant thermodynamic analysis ($\Delta\Delta G_{int}$ = -1.93 kcal/mol) indicate there is indeed an interaction between the four residues in Loop C and the one residue in Loop F. Moreover, results suggest that the presence of a valine residue in position 202 is critical for both the maintenance of mouse-like affinity at the H-Y217Q/M223I/E224D/Y228S chimera as well as maintenance of characteristic curare affinity at the HWT receptor.

DISCUSSION

In previous studies, we demonstrated that both Loops C and F play a significant role in curare potency at the 5-HT_{3A} receptor, with substitution of either loop in the human receptor with mouse orthologs greatly enhancing potency of curare (Zhang et al., 2007). Loop C residues have been implicated in function of a number of receptors in the cys-loop family (Suryanarayanan et al., 2005; Zhang et al., 2006; Venkatachalan and Czajkowski, 2008). In this study, we identified four amino acid residues in Loop C that play a role in determining interspecies differences in curare potencies in human 5-HT_{3A} receptors. Changes in free energy calculated with mutant thermodynamic cycle analysis suggest interaction between amino acid residue at position 224 and residues at positions 217, 223 and 228, as well as an interaction between V202, in Loop F, with Loop C residues in conferring curare potency at the human 5-HT_{3A} receptor.

Inhibition of 5-HT currents by curare was enhanced in human chimeric 5-HT_{3A} receptors containing all four substitutions in Loop C (H-Y217Q/M223I/E224D/Y228S). These residues played a similar role in binding affinity, with the H-Y217Q/M223I/E224D/Y228S receptor having mouse-like curare affinity. Additionally, a number of chimeras containing substitutions not limited to Y217Q, M223I, E224D, Y228S had a curare potency under 200 nM, thus supporting the existence of interactions between multiple Loop C residues. In line with our observations, others have reported a mechanism that implicates multiple amino acids in determining binding affinity at ligand-gated ion channels, i.e., pairwise analysis of amino acids in the α and the γ/δ subunits of

the nACh receptor suggest an interaction of three amino acids in the *Naja mossambica mossambica* α-neurotoxin with several amino acids in the receptor subunits (Ackerman et al., 1998; Quiram et al., 2000). Other studies investigating actions of curare at nACh and 5-HT_3 receptors (Fu and Sine, 1994; Sine et al., 1995; Prince and Sine, 1996; Yan et al., 2006) point to the presence of critical intramolecular interactions. Moreover, alignment of amino acid residues in the 5-HT_3 receptor from different species, shows that relative curare potencies are not solely dependent on the presence of a glutamate or an aspartate at position 224 (Mair et al., 1998; Lankiewicz et al., 1998; Mochizuki et al., 2000; Jensen et al., 2006). Thus, while the identity of residue 224 is important, the role of this amino acid in receptor function is significantly affected by neighboring residues. As for the specific role of these residues, the intermolecular interactions are difficult to dissect given that there is also little overall consistency with the residues at the three remaining Loop C positions (217, 223, 228) across the species with respect to high and low curare potency (Mair et al., 1998; Mochizuki et al., 2000; Jensen et al., 2006).

The combination of the E224D and Y228S substitutions was particularly effective in increasing potency and binding affinity of the H-E224D 5-HT_{3A} receptor chimera. Both of these residues, 224 and 228, have been previously implicated in 5-HT_3 structure/function studies (Hope et al., 1999; Mochizuki et al., 1999; Schreiter et al., 2003). We found a modest difference between results of electrophysiological and radioligand binding assays; the H-E224D/Y228S chimera had a curare IC_{50} value significantly lower than that of the HWT receptor (271 nM and 1,817 nM, respectively), while Ki values at H-E224D/Y228S (2,873 nM) were slightly higher when compared to

the HWT (2,608 nM). These differences could be due to mutation-induced changes in gating. It is also possible that the E224-Y228 interaction has a more pronounced role in gating than in binding affinity. Further evidence of interactions between residues differentially affecting affinity and function is seen with the single substitution, H-V237I. Of all Loop C point mutants, H-V237I had the greatest effect on curare potency; however, this substitution was not required to confer potency or affinity of curare in the context of other Loop C residues. Moreover, it is important to remember that residue 237 is not technically in the binding domain, rather it is in the pre-TM1 domain, a region of the receptor critical to coupling of ligand binding to channel gating (Hu et al., 2003), thus further confirming a link between curare potency and residues important for gating of the 5-HT_3 receptor.

The most striking difference between functional and binding results was the curare Ki at H-V202I. This point mutant had a 17-fold greater curare K_i (44,240 nM) than the HWT receptor. Moreover, addition of the V202I mutation to the four point chimera, H-Y217Q/M223I/E224D/Y228S, had the opposite effect on curare affinity than it did on potency. In functional studies, Loop F residues contributed to increased curare potency when added to the H-Y217Q/M223I/E224D/Y228S background. In binding assays, addition of the V202I substitution to H-Y217Q/M223I/E224D/Y228S, resulted in a chimera with a 3.4-fold decreased curare affinity (29 nM). Thus, Loop F, while not contributing to mouse-like curare affinity at the human receptor, does play a role in both binding and function of the receptor. Other studies have reported that Loop F contributions to function of antagonists at the 5-HT_3 receptor are significant and that

electrostatic interactions involving Loop F residues may further stabilize docking (Yan et al., 2006; Thompson et al., 2005). Additionally, Pless and Lynch, (Pless and Lynch, 2009) reported that mutations in Loop F resulted in small but significant changes in antagonist affinity at the Glycine receptor.

There are a number of possible explanations for the differences in functional and binding results. First, structure/function studies have shown that the Loop F is a flexible loop that is likely important both binding and function of ligand-gated ion channels (Brejc et al., 2001; Newell and Czajkowski, 2003; Zhang et al., 2006; Padget and Lummis, 2008). The flexible Loop F is thought to undergo conformational changes that facilitate transition between the different states (bound to unbound, closed to open) in ligand-gated ion channels (Grutter et al., 2005). Moreover, it is know that curare exerts both antagonist and weak partial agonist functions in nACh receptors (Takeda and Trautmann, 1984; Morris et al., 1989; Steinbach and Chen, 1995), and displacement of [^{3}H]-BRL-43694 by curare could shift the state to a higher affinity desensitized state. As such, different states of the receptor may be assessed: closed to open and closed to desensitized in the functional and binding studies, respectively. Second, there is a possibility that the actual mutations may be altering the gating process to such an extent that the curare IC_{50} is altered as a function of gating and not binding. Third, curare is displacing 5-HT in the functional assay and BRL-43694 in binding assays. The amino acids contributing to binding of 5-HT and [^{3}H]-BRL-43694 may be different, and the mutations might affect the binding of each of these differently, independently of their effects on curare. Furthermore, the latter explanations may explain why amino acid

substitutions and interactions affect binding or function independently of where residues are located, whether they are in Loop C, Loop F or the pre-TM1 region.

We have created a number of mutant cycles to identify potential interactions between residues that confer high curare potency (Table 3). A free energy of interaction ($\Delta\Delta G_{int}$) is considered to be consistent with a direct physical interaction if its absolute value is greater than 1.0 kcal/mol. Fersht and co-workers (Schreiber and Fersht, 1995) have shown that $|\Delta\Delta G_{int}|$ values greater than 1.0 kcal/mol are consistent with close proximity (< 4 Å) of the residues in question. Using a cut-off value of $|\Delta\Delta G_{int}| > 1.0$ kcal/mol as our criterion, we find that all of the data are consistent with E224 making a direct physical interaction with Y217 and Y228

Homology models have been widely used to predict points of interaction between 5-HT_3 receptors and their respective ligands (Morris et al., 1998; Newell and Czajkowski, 2003; Joshi et al., 2006; Yan et al., 2006; Zhang et al., 2007; Padget and Lummis, 2008) as well as interactions of ligands and other cys-loop receptors (Schreiter et al., 2003; Grutter et al., 2005; Dutertre and Lewis, 2006). Models are based on the structure of the acetylcholine binding protein (AChBP), a structural homolog of the N-terminus of the nicotinic acetylcholine receptor (nAChR) (Brejc et al., 2001). The similarities between ligand-gated ion channels and the AChBP have been confirmed with the recent crystallization of the N-terminal domain of the α1 subunit of the nAChR (Dellisanti et al., 2007).

In constructing a structural model for the orientation of curare at the binding pocket of the 5-HT_{3A} receptor (Fig. 4), we used data from a previous study implicating

residues R92, E236, and N128 in curare-receptor interactions (Morris et al., 1998). Taking into consideration calculations from mutant thermodynamic cycle analysis, we propose a model of binding of curare at the 5-HT_{3A} receptor where the 2N group of the ligand sits between residues N128 and W90 of the human 5-HT_{3A} receptor and the 2'N group of the ligand directly interacts with residue E224. The role of W90 has been previously shown in binding of both BRL-43694 and curare (Morris et al., 1998; Yan et al., 2006). An electrostatic interaction between negatively charged amino acid residues in Loop C of the 5-HT_3 receptor and the amino group of the ligand has been proposed to stabilize docking at the binding pocket (Czajkowski et al., 1993; Boess et al., 1997) and E224 could serve this role. Moreover, the idea of a direct interaction between the ligand and residue 224 is corroborated by a previous study by Schreiter et al., (2003) in which fluorescence studies implicated residue 224 in both binding and possibly gating of the 5-HT_3 receptor. One area in which the model seems to differ from the experimental data is in regards to intramolecular interactions between Y217, Y228 and E224. Mutant thermodynamic cycle analysis gives strong evidence of a critical interaction between these residues. While this interaction is not as clear in the molecular model, it is important to keep in mind that homology models are based on static states (apo/antagonist or agonist) and may not accurately represent the dynamic nature of amino acid side chains. Thus, while invaluable to better understanding underlying interactions between ligands and their respective targets, models must be taken as close estimations in the context of additional experimental data.

Summary—Our experimental results support the hypothesis that interspecies differences in Loop C of the 5-HT_{3A} receptor are critical for conferring curare sensitivities at mouse and human receptors. Moreover, we identified four amino acid residues in the human receptor that when substituted with the mouse ortholog (Y217Q, M223I, E224D, and Y228S), are sufficient to confer mouse-like curare binding affinity at the human receptor. Our electrophysiology data shows that these same substitutions when coupled with the V202I substitution (in Loop F), produce a receptor with mouse-like curare potency. This suggests a critical role for Loop C in interspecies differences in both binding and gating, with a more pronounced effect on binding. The data also confirms our previous report (Zhang et al., 2007) of the importance of V202 in conferring curare potency at the human receptor. Finally, the study provides a more detailed picture of the molecular interactions that determine differences in pharmacological sensitivities of curare at human and mouse 5-HT_{3A} receptors.

Table 1 5-HT and Curare Potencies at Wild-Type, Chimeric, and Point Mutant Mouse and Human 5-HT_{3A} Receptors

Receptor	5-HT EC_{50} (mean ± S.E.) μM	5-HT Hill Slope (mean ± S.E.)	Curare IC_{50} (mean ± S.E.) nM	Curare Hill Slope (mean ± S.E.)
MWT [a]	1.02 ± 0.07	2.23 ± 0.37	12.99 ± 0.77	1.17 ± 0.09
H-K195E/V202I, Y217Q/M223I/E224D/Y228S	1.3 ± 0.04	2.28 ± 0.16	6.49 ± 0.49 [d]	1.15 ± 0.1
H-Loop C+1 [a]	3.3 ± 0.12 [b, i]	2.32 ± 0.21	40.77 ± 2.52	1.26 ± 0.08
H-Loop C	1.72 ± 0.06	2.53 ± 0.26	40.27 ± 2.53	1.15 ± 0.09
H-Y217Q/M223I/E224D/Y228S	2.94 ± 0.14 [b]	2.47 ± 0.3	35.31 ± 3.1	1.01 ± 0.09
H-Y217Q/R219K/M223I/Y228S	1.54 ± 0.13	1.25 ± 0.12	101.03 ± 3.1 [e]	1.37 ± 0.05
H-Y217Q/R219K/M223I/S225I/ Y228S	0.91 ± 0.09	1.7 ± 0.36	102.82 ± 8.2 [e]	0.99 ± 0.08
H-Y217Q/E224D/Y228S	3.47 ± 0.1 [b]	3.72 ± 0.42	104.2 ± 2.9 [f]	1.35 ± 0.05
H-M223I/E224D/Y228S	6.32 ± 0.7 [b]	1.92 ± 0.36	121.3 ± 7.12 [f, g]	1.32 ± 0.1
H-Y217Q/R219K/M223I/Y228S/ V237I	0.82 ± 0.06	3.06 ± 0.85	152.5 ± 7.31 [h]	1.57 ± 0.11
H-Y217Q/M223I/Y228S	2.51 ± 0.14 [c]	1.86 ± 0.19	175 ± 7.80 [e]	1.49 ± 0.1
H-Y217Q/Y228S	2.15 ± 0.18	1.77 ± 0.26	353.4 ± 23 [e]	1.37 ± 0.11
H-Y217Q/M223I/E224D	1.56 ± 0.08	2.03 ± 0.2	456.5 ± 28.92 [f]	1.13 ± 0.07
H-R219K/V237I	1.57 ± 0.07	1.89 ± 0.14	875.9 ± 46.3 [e]	1.45 ± 0.13
H-M223I/E224D	2.25 ± 0.13	1.97 ± 0.21	1305 ± 68.81 [f]	1.15 ± 0.04
H-Y217Q/E224D	2.59 ± 0.03 [b, i]	2.23 ± 0.14	1400 ± 45.13 [f]	1.32 ± 0.1
H-E224D/Y228S	5.04 ± 0.09 [b, i]	2.19 ± 0.2	270.8 ± 3.31 [d, e]	1.40 ± 0.04
HWT [a]	1.46 ± 0.04	3.42 ± 0.31	1817 ± 92.36	1.19 ± 0.08
H-Y217Q	1.79 ± 0.09	2.13 ± 0.28	1147 ± 23.8	1.56 ± 0.05
H-R219K	1.29 ± 0.1	1.47 ± 0.18	658.63 ± 15 [b]	1.48 ± 0.05
H-M223I	1.92 ± 0.04	2.15 ± 0.15	925.72 ± 56 [c]	1.14 ± 0.09
H-E224D	2.68 ± 0.11 [b, i]	2.07 ± 0.16	8982 ± 514 [b]	1.21 ± 0.09
H-S225I	2.05 ± 0.17	1.78 ± 0.24	2150 ± 100	1.31 ± 0.1
H-Y228S	2.95 ± 0.16 [b, i]	1.63 ± 0.16	915.2 ± 70 [c]	1.23 ± 0.12
H-V237I	2.65 ± 0.15 [b, i]	1.72 ± 0.14	380.9 ± 92.12 [b]	0.96 ± 0.07

[a] taken from Zhang et al., 2007

[b] $p < 0.001$ compared to HWT; [c] $p < 0.05$ compared to HWT; [d] $p < 0.01$ compared to HWT; [e] $p < 0.001$, compared to H-Loop C; [f] $p < 0.001$, compared to H-Y217Q/M223I/E224D/Y228S; [g] $p < 0.05$, compared to H-Y271Q/E224D/Y228S; [h] $p < 0.01$ compared to H-Loop C, Student Newman Keul's post hoc analysis. One-way ANOVAs are described in the Results or Figure Legends.

[i] $p < 0.001$, compared to MWT, Student's t-test.

Table 2 Comparison of Curare K_is for displacement of [^{3}H]-BRL-43694 at wild type, point mutant, and chimeric 5-HT_{3A}Rs

5-HT_{3A}R Construct	[^{3}H]-BRL-43694 Kd (nM)	Curare Ki (nM)	Curare Ki fold change from MWT	Curare Ki fold change from HWT
MWT	3.53 ± 0.32	8.33 ± 0.6 [b]	---	↓ 314
HWT	2.58 ± 0.61	2,608 ± 225 [a]	↑314	---
H-Y217Q/M223I/E224D/Y228S	4.31 ± 0.06	6.42 ± 0.63 [b]	1.3	↓ 407
H-E224D, Y228S	7.25 ±0.5 [a, b]	2,873 ± 422 [a]	↑346	1.1
H-E224D	5.76 ± 0.4	432,000 ± 42,975 [a, b]	↑52,048	↑165
M-D229E	6.90 ± 0.92	11.82 ± 1.01 [b]	1.4	↓ 221
H-V202I	7.01 ± 0.41 [a, b]	44,240 ± 6,473 [a, b]	↑5,330	↑16
M-I207V	6.20 ± 0.5	17.73 ± 2.1 [b]	↑2.1	↓ 147
H-Y217Q/M223I/E224D/Y228S + V202I	*12.60 ± 0.2* [a, b]	29.01 ± 3.6 [a, b]	↑3.4	↓ 90

ANOVA was performed, and it was significant, $p < 0.05$; [a]$p < 0.006$ compared to MWT; [b]$p < 0.006$ compared to HWT, two-tailed unpaired t-test with a Bonferroni correction factor.

Table 3 Double Mutant Thermodynamic Cycle Analysis for Residues in Loop C of the 5-HT_{3A} Receptor.

Receptor A	Receptor B	Receptor C	Receptor D	Cycle 1 ΔG	Cycle 2 ΔG	$\Delta\Delta G_{int}$
Y217Q	Y217Q/M223I/Y228S	Y217Q/E224D	Y217Q/M223I/E224D/Y228S	1.10	2.14	-1.03*
Y217Q	Y217Q/M223I/E224D	Y217Q/Y228S	Y217Q/M223I.E224D/Y228S	0.53	1.31	-0.78
M223I	Y217Q/M223I/Y228S	M223I/E224D	Y217Q/M223I/E224D/Y228S	1.00	2.09	-1.09*
E224D	Y217Q/E224D/Y228S	M223I/E224D	Y217Q/M223I/E224D/Y228S	2.67	2.09	0.58
E224D	M223I/E224D/Y228S	Y217Q/Y228S	Y217Q/M223I/E224D/Y228S	2.58	2.14	0.44
E224D	Y217Q/M223I/E224D	E224D/Y228S	Y217Q/M223I.E224D/Y228S	1.78	1.15	0.63
Y228S	M223I/E224D/Y228S	Y217Q/Y228S	Y217Q/M223I.E224D/Y228S	1.22	1.31	-0.09
Y228S	Y217Q/M223I/Y228S	E224D/Y228S	Y217Q/M223I/E224D.Y228S	1.00	1.15	-0.15

Cycles are Receptors A →B (Cycle 1) and Receptors C → D (Cycle 2). $\Delta\Delta G_{int} = \Delta G_B - \Delta G_A - (\Delta G_D - \Delta G_C)$.

(*) Indicates intramolecular interaction.

Figure 1. Role of individual amino acid substitutions in conferring curare potency at human and mouse 5-HT_{3A}Rs. A: Sequence alignment of residues in Loop C and Loop F of mouse and human 5-HT_{3A} receptors. Bold letters indicate differences in amino acids in the two receptors, and (*) indicates Loop F residues previously reported to play a role in curare potency (2). B: Concentration-response curves for curare were generated in oocytes expressing HWT, H-Loop C+1 chimera, and human-mouse point mutations corresponding to six interspecies differences in Loop C and one difference between Loop C and TM1 (n=4-7). Curare (1–100,000 nM) was co-applied with 5-HT (EC_{10}) for 30 s. C: Panel shows glutamate is a conserved residue in a number of species but does not appear to have a direct effect on curare potency as indicated to the right of the amino acid sequences.

Figure 1

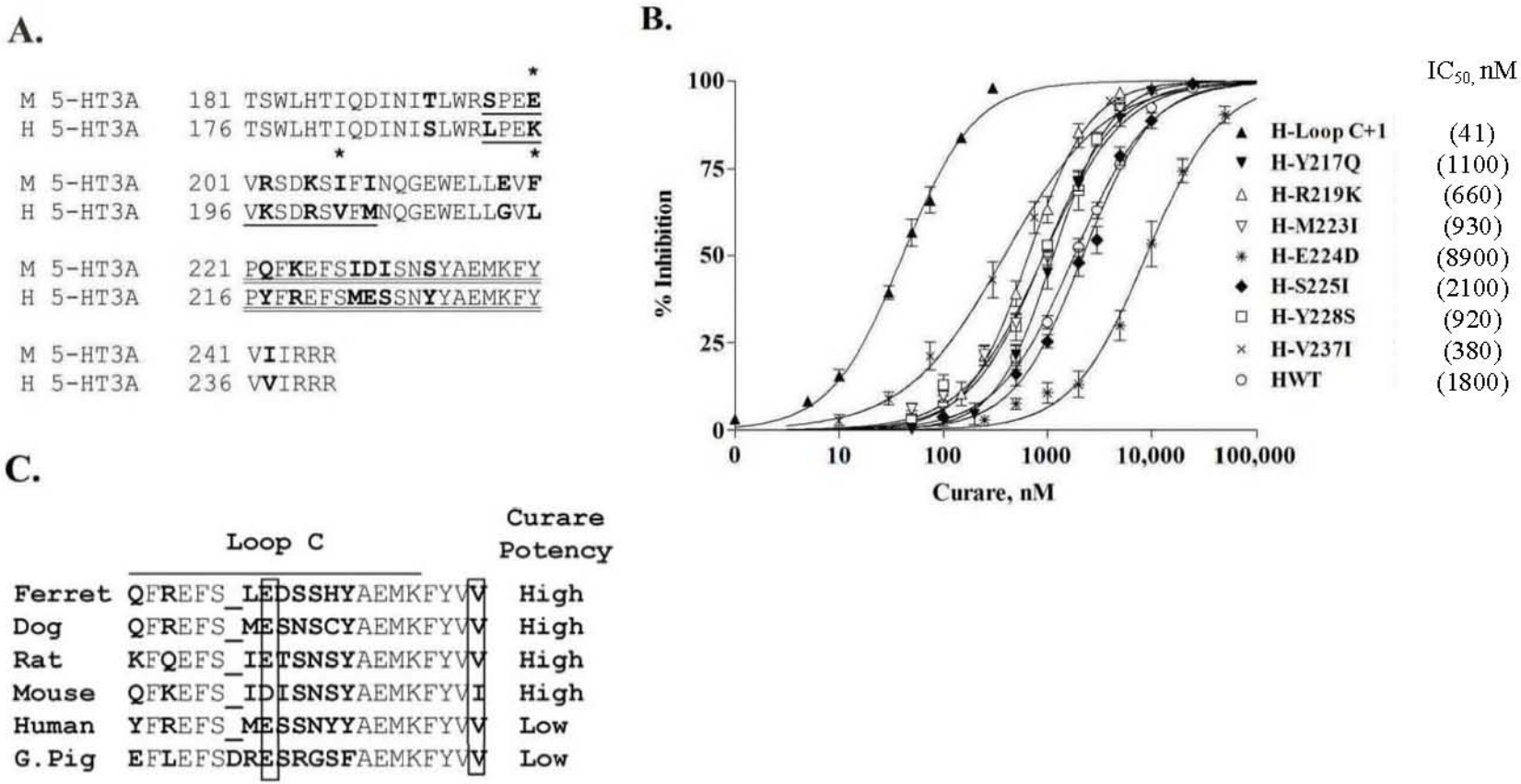
A.
M 5-HT3A 181 TSWLHTIQDINITLWRSPEE
H 5-HT3A 176 TSWLHTIQDINISLWRLPEK
M 5-HT3A 201 VRSDKSIFINQGEWELLEVF
H 5-HT3A 196 VKSDRSVFMNQGEWELLGVL
M 5-HT3A 221 PQFKEFSIDISNSYAEMKFY
H 5-HT3A 216 PYFREFSMESSNYYAEMKFY
M 5-HT3A 241 VIIRRR
H 5-HT3A 236 VVIRRR
B.
% Inhibition
Curare, nM
IC50, nM
H-Loop C+1 (41)
H-Y217Q (1100)
H-R219K (660)
H-M223I (930)
H-E224D (8900)
H-S225I (2100)
H-Y228S (920)
H-V237I (380)
HWT (1800)
C.
Loop C
Curare Potency
Ferret QFREFS_LEDSSHYAEMKFYVV High
Dog QFREFS_MESNSCYAEMKFYVV High
Rat KFQEFS_IETSNSYAEMKFYVV High
Mouse QFKEFS_IDISNSYAEMKFYVI High
Human YFREFS_MESSNYYAEMKFYVV Low
G.Pig EFLEFSDRESRGSFAEMKFYVV Low

Figure 2. Characterization of the role of residues in Loop C. Following analysis of the seven point-mutant chimera, a series of smaller chimeras were created to assess the role of combined Loop C substitutions in conferring mouse-like curare potency at the human 5-HT_3 receptor. Concentration-response curves for curare (1–100,000 nM) were generated in oocytes expressing human-mouse chimeric 5-HT_{3A}Rs (n=4-7). A: Curare inhibition of 5-HT-induced currents in a series of H-Loop C chimeric receptors compared to results from the H-Loop C+1 chimera. B: Curare inhibition of 5-HT-induced currents for three point mutant H-Loop C chimeras containing the E224D substitution. C: Curare inhibition of 5-HT-induced currents in the H-M223I/E224D/Y228S chimeras and in a series of two point mutant H-Loop C chimeras compared to results from the H-Y217Q/M223I/E224D/Y228S chimera. D: Panel shows that the two and three point chimeras that had the highest curare potencies were those containing both E224D and Y228S. E: Mutant thermodynamic cycle analysis for 5-HT_{3A} chimeric receptors with and without the E224D substitutions.

Figure 2

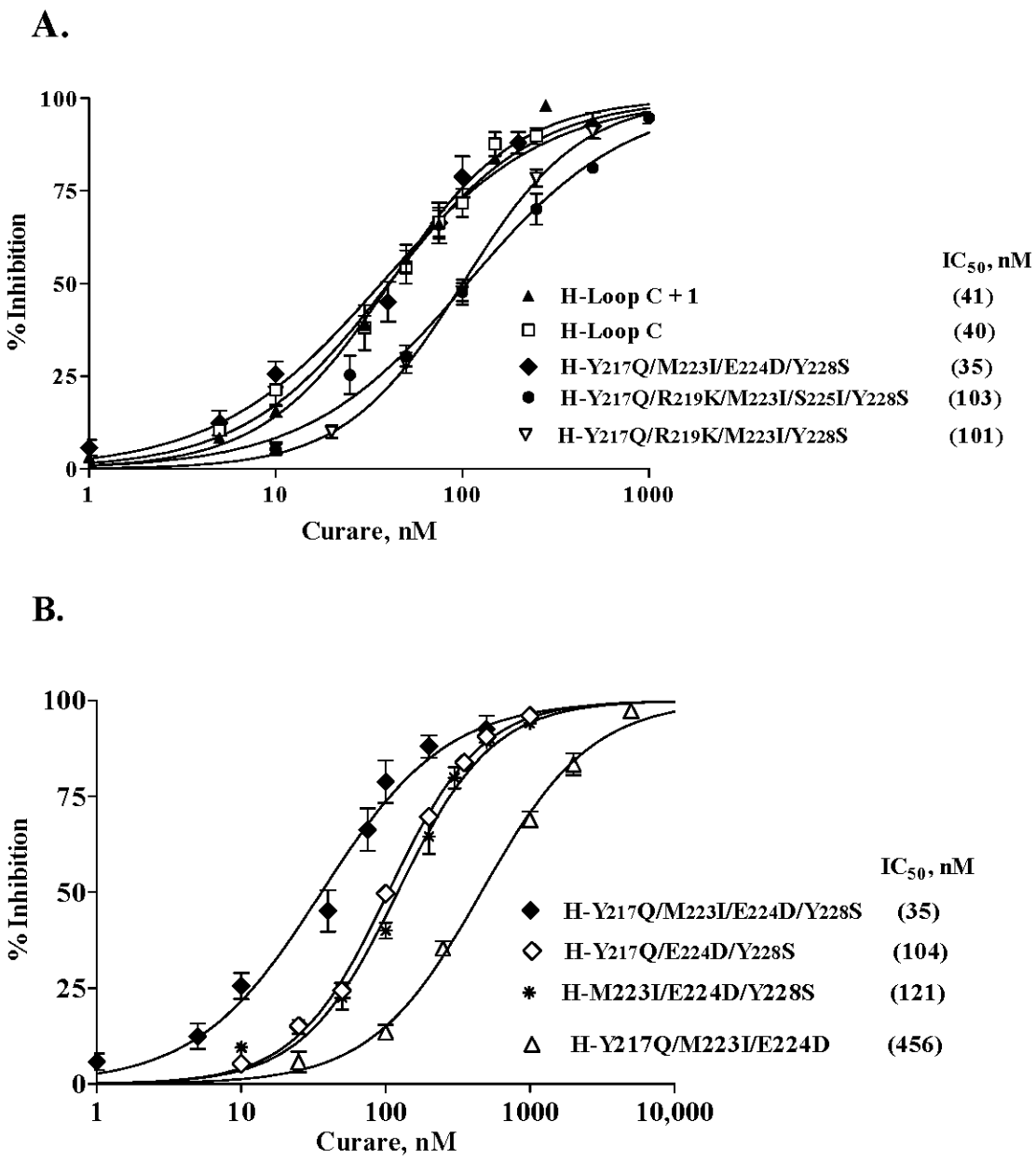
A.
100
75
50
25
0
% Inhibition
1
10
100
1000
Curare, nM
IC50, nM
H-Loop C + 1 (41)
H-Loop C (40)
H-Y217Q/M223I/E224D/Y228S (35)
H-Y217Q/R219K/M223I/S225I/Y228S (103)
H-Y217Q/R219K/M223I/Y228S (101)
B.
100
75
50
25
0
% Inhibition
1
10
100
1000
10,000
Curare, nM
IC50, nM
H-Y217Q/M223I/E224D/Y228S (35)
H-Y217Q/E224D/Y228S (104)
H-M223I/E224D/Y228S (121)
H-Y217Q/M223I/E224D (456)

C.

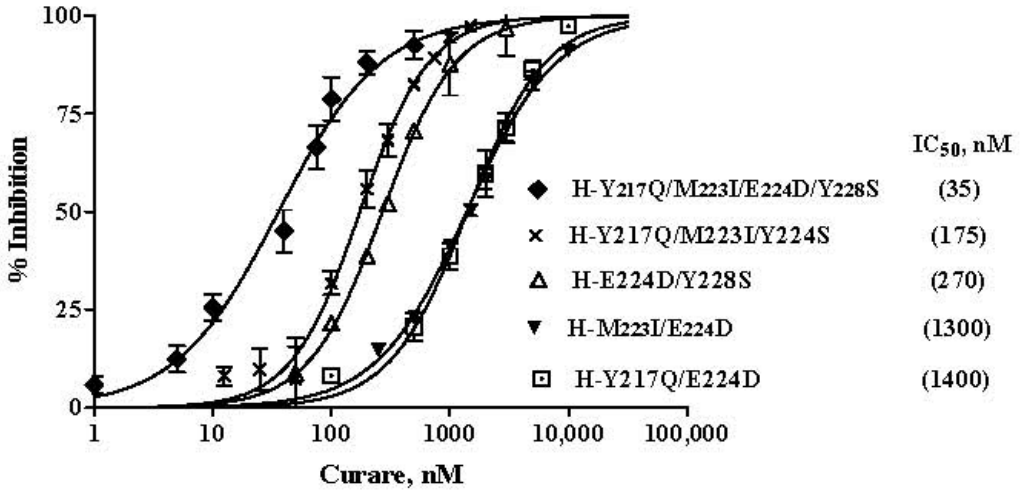

D.

YQ MI ED YS 35 nM

-- -- ED -- 8982 nM
-- MI ED -- 1305 nM
YQ MI ED -- 465 nM
-- MI ED YS 121 nM

YQ -- -- YS 353 nM
YQ -- ED YS 104 nM
-- MI ED YS 121 nM

YQ -- ED YS 104 nM
YQ MI -- YS 175 nM

E.

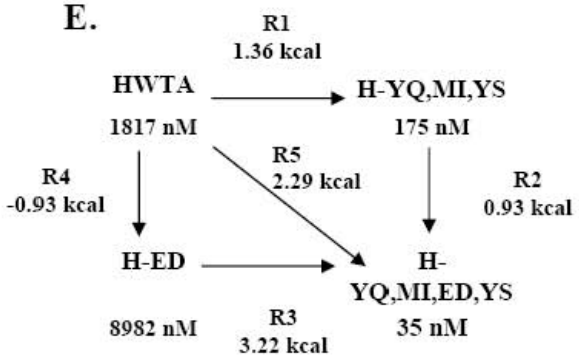

Figure 3. Loops C and F play a role in conferring mouse-like curare potency at the human receptor. Concentration-response curves where generated for curare (1-100,000 nM). Curare was co-applied with 5-HT (EC_{10}), for 30 s (n=4-7). A: Curare inhibition of 5-HT-induced current in chimeras with and without Loop F amino acid substitutions (K195E and V202I). B: Testing of five, three and two point Loop C chimeras containing the V237I and/or the R219K substitutions. C: Mutant thermodynamic cycle analysis using Ki values obtained from radioligand binding assays for $5\text{-}HT_{3A}$ receptor chimeras containing residue substitutions in Loop C and/or Loop F.

Figure 3

A.

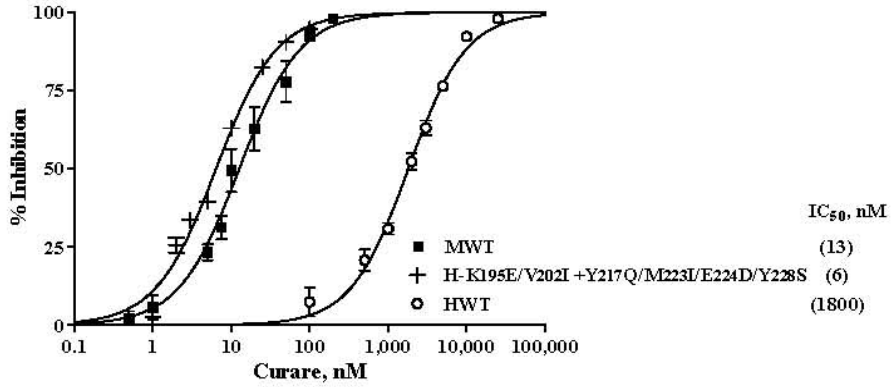
100
75
50
25
0
% Inhibition
0.1
1
10
100
1,000
10,000
100,000
Curare, nM
IC50, nM
MWT (13)
H-K195E/V202I +Y217Q/M223I/E224D/Y228S (6)
HWT (1800)

B.

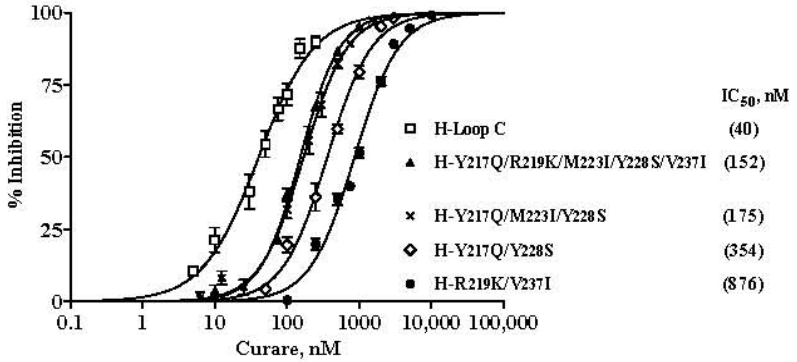
100
75
50
25
0
% Inhibition
0.1
1
10
100
1000
10,000
100,000
Curare, nM
IC50, nM
H-Loop C (40)
H-Y217Q/R219K/M223I/Y228S/V237I (152)
H-Y217Q/M223I/Y228S (175)
H-Y217Q/Y228S (354)
H-R219K/V237I (876)

C.

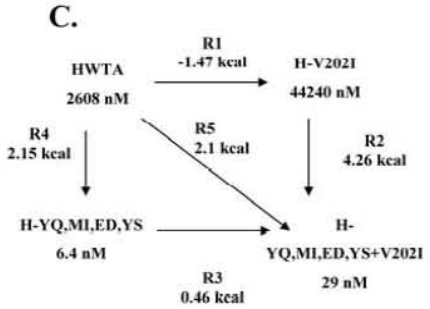
HWTA
2608 nM
R1
-1.47 kcal
H-V202I
44240 nM
R4
2.15 kcal
R5
2.1 kcal
R2
4.26 kcal
H-YQ,MI,ED,YS
6.4 nM
H-
YQ,MI,ED,YS+V202I
29 nM
R3
0.46 kcal

Figure 4. Molecular model of docking of curare at the human 5-HT_{3A} receptor ligand binding domain. Shown are several residues previously shown to be important for binding of curare at the mouse receptor (R92, E236, and N128) (21), along with residues E224, Y217, and Y228 characterized in the present study.

Figure 4

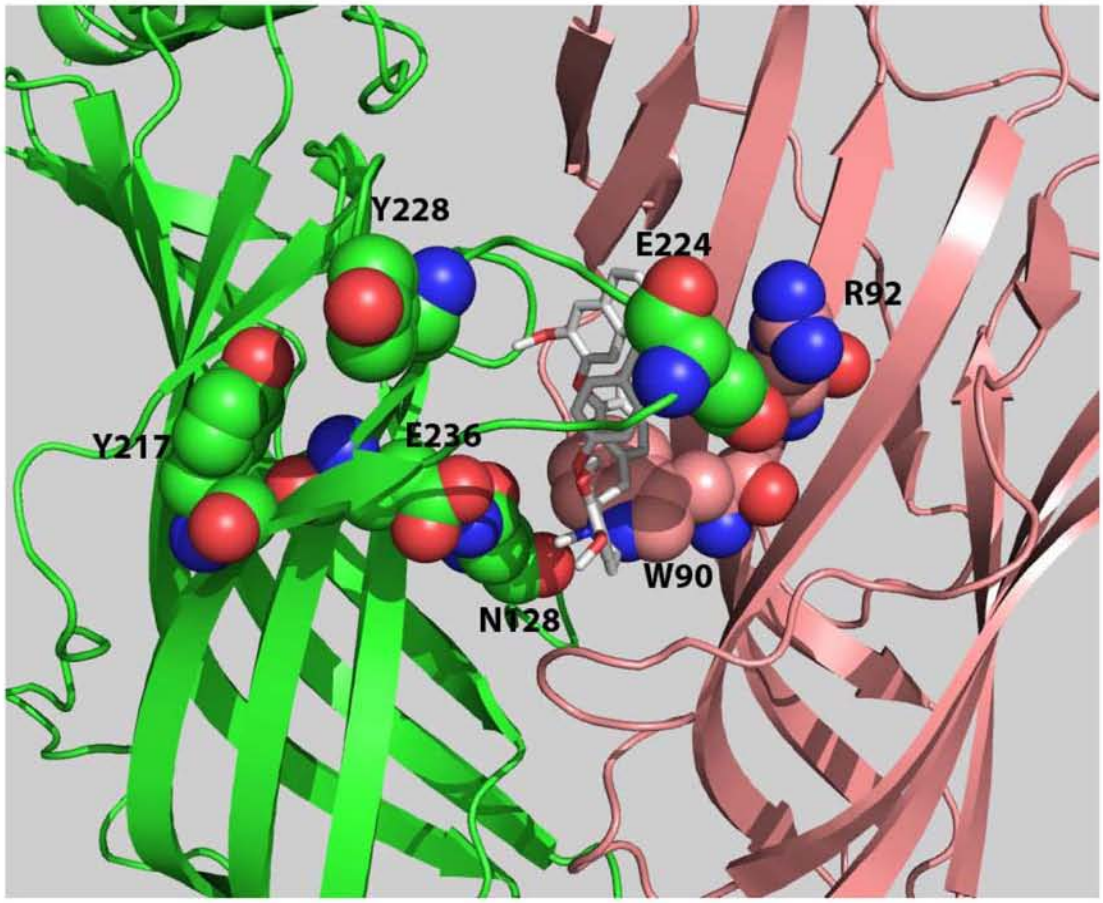

REFERENCES

Ackerman, E. J., Ang, E. T., Kanter, J. R., Tsigelny, I., and Taylor, P. J. (1998) Identification of pariwise interactions in the alpha-neurotoxin-nicotinic acetylcholine receptor complex through double mutant cycles. *J. Biol. Chem.* **273:** 10958-10964.

Ackers, G. K., and Smith, F. R. (1985) Effects of site-specific amino acid modification on protein interactions and biological function. *Annu. Rev. Biochem.* **54:** 597-629.

Akhondzadeh, S., Mohammadi, N., Noroozian, M., Karamghadiri, N., Ghoreishi, A., Jamshidi, A.-H., and Forghani, S. (2008) Added ondansetron for stable schizophrenia: A double blind, placebo controlled trial. *Schizophr. Res.* [Epub ahead of print].

Boess, F. G., Steward, K. J., Steele, J. A., Liu D., Reid, J., Glencorse, T. A., and Martin, I. L. (1997) Analysis of the ligand binding site of the 5-HT3 receptor using site directed mutagenesis: importance of glutamate 106. *Neuropharmacol.* **36:** 637–647.

Brejc, K., van Dijk, W. J., Klaassen, R. V., Schuurmans, M., van Der Oost, J., Smit, A. B., and Sixma, T. K. (2001) Crystal structure of an ACh-binding protein reveals the ligand-binding domain of nicotinic receptors. *Nature* **411:** 269-276.

Colquhoun, D. (1998) Binding, gating, affinity and efficacy: the interpretation of structure-activity relationships for agonists and of the affects of mutating receptors. *Br. J. Pharmacol.* **125:** 924-947.

Czajkowski, C., Kaufmann, C., and Karlin, A. (1993) Negatively charged amino acid residues in the nicotinic receptor delta subunit that contribute to the binding of acetylcholine. *Proc. Natl. Acad. Sci.U. S. A.* **90:** 6285–6289

Davies, P.A., Pistis, M., Hanna, M.C., Peters, J.A., Lambert, J.J., Hales, T.G., and Kirkness, E.F. (1999) The 5-HT_{3B} subunit is a major determinant of serotonin receptor function. Nature 397, 359-363.

de Oliveira-Pierce, A. N., Zhang, R., Machu, T. K. (2009) Colchicine: A Novel Positive Allosteric Modulator of the Human 5-Hydroxytryptamine3A Receptor. *J. Pharmacol., Exp. Ther.* **329:** 838-847.

Dellisanti, C. D., Yao, Y., Stroud, J. C., Wang, Z. Z., and Chen, L. (2007) Crystal structure of the extracellular domain of nAChR α-1bound to α-bungarotoxin at 1.94Å resolution. *Nat. Neurosci.* **10:** 953-962.

Dutertre, S., Lewis, R. J. (2006) Toxin insights into nicotinic acetylcholine receptors. Biochem. Pharmacol, **72:** 661– 670.

Ferrara, P., Gohlke, H., Price, D. J., Klebe, G., and Brooks, C. L. III (2004) Assessing scoring functions for protein-ligand interactions. *J. Med. Chem.* **47:** 3032-3047.

Fiebich, B. L., Akindi, R. S., Seidel, M., Geyer, V., Haus, U., MÜller, W., Stratz, T., and Candelario-Jalil, E. (2004) Expression of 5-HT_{3A} receptors in cells of the immune system. *Scand. J. Rheumatol. Suppl.* **119:** 9-11.

Fu, D. X., and Sine, S. M. (1994). Competitive antagonist bridge that a-y subunit interface of the acetylcholine receptor through quaternary ammonium-aromatic interactions. *J Biol. Chem.* **269:** 26152-26157.

Gasteiger, J., and Marsili, M. (1980) Iterative partial equalization of orbital electronegativity-A rapid access to atomic charges. *Tetrahedron.* **36:** 3219-3228.

Grutter, T., de Carvalho, L. P., Dufresne, V., Taly, A., Edelstein, S. J., and Changeux, J.-P. et al., 2005

Hansen, S., Sulzenbacher, G., Huxford, T., Marchot, P., Taylor, P., and Bourne, Y. (2005) Structures of *Aplysia* AChBP complexes with nicotinic agonists and antagonists reveal distinctive binding interfaces and conformations. *EMBO. J.* **24:** 3635-3646.

Hope, A. G., Belelli, D., Mair, I. D., Lambert, J. J., and Peters, J. A. (1999) Molecular Determinants of (+)-Tubocurarine Binding at Recombinant 5-Hydroxytryptamine$_{3A}$ Receptor Subunits. *Mol. Pharmacol.* **55:** 1037-1043.

Hu, X.-Q., Zhang, L., Stweart, R. R., and Weight, F. F. (2003) Arginine 222 in the Pre-Transmembrane Domain 1 of 5-HT$_{3A}$ Receptors Links Agonist Binding to Channel Gating. *J. Biol. Chem.* **278:** 46583-46589.

Jensen, T. N., Nielsen, J., Frederiksen, K., and Ebert, B. (2006) Molecular cloning and pharmacological characterization of serotonin 5-HT$_{3A}$ receptor subtype in dog. *Eur. J. Pharmacol.* **538:** 23-31.

Joshi, P. R., Suryanarayanan, A., Hazai, E., Schulte, M. K., Maksay, G., and Bikadi, Z. (2006) Interactions of Granisetron with an Agonist-Free 5-HT$_{3A}$ Receptor Model. *Biochem.* **45:** 1099-1105.

Lankiewicz, S., Lobitz, N., Wetzel, C. H., Rupprecht, R., Gisselmann, G., and Hatt, H. (1998) Molecular cloning functional expression, and pharmacological characterization of 5-hydroxytryptamine3 receptor cDNA and its splice variants from guinea pig. *Mol. Pharmacol.* **53:** 202-212.

Lowry, O. H., Rosebrough, N. J., Farr, A. L., and Randall, R. J. (1951) Protein measurement with the folin phenol reagent. *J. Biol. Chem.* **193:** 265-275.

Machu, T. K., Hamilton, M. E., Frye, T. F., Shanklin, C. L., Harris, M. C., Sun, H., Tenner Jr, T. E., Soti, F. S., and Kem, W. R. (2001) Benzylidene analogs of anabaseine display partial agonist and antagonist properties at the mouse 5-hydroxytryptamine(3A) receptor. *J. Pharmacol. Exp. Ther.* **299:** 1112-1117.

Mair, I. D., Lambert, J. J., Yang, J., Dempster, J., and Peters, J. A. (1998) Pharmacological characterization jof the rat 5-hydroxytryptamine type3 receptor subunit (r5-HT_{3A}(b)) expressed in Xenopus laevis oocutes. *Br. J. Pharmacol.* **124:** 1667-74.

Mochizuki, S., Miyake, A., and Furuichi, K. (1999) Identification of a domain affecting agonist potency of *meta*-chlorophenylbiguanide in 5-HT_3 receptors. *Eur. J. Pharmacol.* **369:** 125-132.

Mochizuki, S., Watanabe, T., Miyake, A., Saito, M. and Furuichi, K (2000) Cloning, expression, and characterization of ferret 5-HT(3) receptor subunit. *Eur. J. Pharmacol.* **399:** 97–106.

Morris CE, Montpetit MR, Sigurdson WJ, Iwasa K. (1989) Activation by curare of acetylcholine receptor channels in a murine skeletal muscle cell line. *Can J Physio Pharmacol* **67:** 152-158.

Morris, G., Goodsell, D., Huey, R., Hart, W., Belew, R., and Olson, A. (1998) Automated docking using Lamarckian genetic algorithm and an empirical free energy binding free energy function. *J. Comput. Chem.* **19:** 1639-1662.

Newell, J. G., and Czajkowski, C. (2003) The GABAA receptor alpha 1 subunit Pro-174-Asp191 segment is involved in GABA binding and channel gating. *J. Biol. Chem.* **278:** 13166-13172.

Padget, C. L., and Lummis, S. C. R. (2008) The F-loop of the GABAA Receptor γ2 Subunit Contributes to Bensodiazepine Modulation. *J. Biol. Chem.* **283:** 2702-2708.

Pettersen, E., Goddard, T., Huang, C., Couch, G., Greenblatt D, Meng E and Ferrin T (2004) UCSF Chimera: A visualization system for exploratory research and analysis. *J. Comput. Chem.* **25:** 1605-1612.

Pless, S. A., and Lynch, J. W. (2009) Ligand-specific conformational changes in the α1 glycine receptor ligand-binding domain. *J. Biol. Chem.* [Epub ahead of print].

Prince, R. J., and Sine, S. M. (1996) Molecular dissection of subunit interfaces in the acetylcholine receptor: identification of residues that determine agonist selectivity. *J Biol. Chem.* **271:** 25770-25777

Quiram, P.A., McIntosh, J. M., and Sine, S. M. (2000) Pairwise interactions between neuronal alpha(7) acetylcholine receptors and alpha-conotoxin PnIB. *J. Biol. Chem.* **275:** 4889-4896.

Reeves, D. C., and Lummis, S. C. (2002) The molecular basis of the structure and function of the 5-HT_3 receptor: a model ligand-gated ion channel (review). *Mol. Membr. Biol.* **19:** 11-26.

Sali, A., and Blundell, T. (1993) Comparative protein modeling by satisfaction of spatial restraints. *J. Mol. Biol.* **234:** 779-815.

Schreiber, G., and Fersht, A. (1995) Energetics of protein-protein interactions: Analysis of the barnase-barstar interface by single mutations and double mutant cycles. *J. Mol. Biol.* **248:** 478-486.

Schreiter ,C., Hovius, R., Costioli, M., Pick, H., Kallenberger, S., Schild, L., and Vogel, H. (2003) Characterization of the Ligand-binding Site of the Serotonin 5-HT_3 Receptor. *J. Biol. Chem.* **278:** 22709-22716.

Sine, S. M., Kreienkamp, H. J., Bren, N., Maeda, R., and Taylor, P. (1995). Molecular dissection of subunit interfaces in the acetylcholine receptor: identification of determinants of a-conotoxin Ml selectivity. *Neuron* **15:** 205-211

Steinbach, J. H., and Chen, Q. (1995) Antagonist and partial agonist actions of d-tubocurarine at mammalian muscle acetylcholine receptors. J. Neurosci. 15: 230-240.

Suryanarayanan, A., Joshi, P. R., Bikadi, Z., Mani, M., Kulkarni, T. R., Gaines, C., and Schulte, M. K. (2005) The Loop C Region of the Murine 5-HT_{3A} Receptor Contributes to the Differential Actions of 5-Hydroxytryptamine and m-Chlorophenylbiguanide. *Biochem.* **44:** 9140-9149.

Takeda, K., and Trautmann, A. (1984) A Patch-clamp Study of the Partial Agonist Actions of Tubocurarine on Rat Myotubes. J. Physiol. **349:** 353-374.

Thompson, A. J., and Lummis, S. C. R. (2007) The 5-HT_3 receptor as a therapeutic target. *Expert Opin. Ther. Targets* **11**: 527-540.

Thompson, A. J., Price, K. L., Reeves, D. C., Chan, S. K., Chau, P. L., and Lummis, S. C. (2005) Locating an Antagonist in the 5-HT_3 Receptor binding Site Using Modeling and Radioligand Binding. J. Biol. Chem. **250:** 20476-20482.

Unwin, N. (1998) The nicotinic acetylcholine receptor of the Torpedo electric ray. *J. Struct. Biol.* **121:** 181-190.

Venkatachalan, S. P., and Czajkowski, C. (2008) A conserved salt bridge critical for GABAA receptor function and loop C dynamics. *P.N.A.S.* **105:** 13604-13609.

Yan, D., and White, M. M. (2005) Spatial orientation of the antagonist granisetron in the ligand binding site of the 5-HT_3 receptor. *Mol. Pharmacol.* **68:** 365-371.

Yan, D., Meyer, J.K., and White, M. M. (2006) Mapping residues in the ligand-binding domain of the 5-HT_3 receptor onto d-tubocurarine structure. *Mol. Pharmacol.* **70:** 571-578.

Yan, D., Schulte, M. K., Bloom, K. E., and White, M. M. (1999) Structural Features of the Ligand-binding Domain of the Serotonin 5-HT_3 Receptor. *J. Biol. Chem.* **274:** 5537-3341.

Zhang, R., Wen, X., Militante, J., Hester, B., Rhubottom, H. E., Sun, H., Leidenheimer, N. J., Yan, D., White, M. M., and Machu, T. K. (2007) The role of loop F residues in determining differential d-tubocurarine potencies in mouse and human 5-hydroxytryptamine 3A receptors. *Biochem.* **46:** 1194-1204.

Zhang, R., White, N. A., Soti, F. S., Kem, W. R., and Machu, T. K. (2006) N-Terminal Domains in Mouse and Human 5-Hydroxytryptamine$_{3A}$ Receptors Confer Partial Agonist and Antagonist Properties to Benzylidene Analogs of Anabaseine. *J. Pharmacol. Exp. Ther.* **317:** 1276-1284.

Zhang, R., White, N. A., Soti, F. S., Kem, W. R., and Machu, T. K. (2006) N-Terminal Domains in Mouse and Human 5-Hydroxytryptamine$_{3A}$ Receptors Confer Partial

Agonist and Antagonist Properties to Benzylidene Analogs of Anabaseine. *J. Pharmacol. Exp. Ther.* **317:** 1276-1284.

Footnotes:

This manuscript is taken from a dissertation submitted to the University of North Texas Health Science Center in partial fulfillment of the requirements for the Doctor of Philosophy degree. This study was supported by National Institute of Neurological Disorders and Stroke grant NS043438.

CHAPTER III

PHYSICOCHEMICAL REQUIREMENTS OF AMINO ACIDS IN THE 5-HYDROXYTRYPTAMINE$_{3A}$ RECEPTOR FOR BINDING OF AND GATING BY BENZYLIDENE ANALOGS OF ANABASEINE

PREFACE

Analogs of benzylidene-anabaseine (BA) have different actions at human and mouse 5-HT$_{3A}$ receptors. The BA analog containing a hydroxyl group at the 2' position, 3-(2-hydroxy,4-methoxybenzylidene)-anabaseine (2-OHMBA), acts as a partial agonist at the mouse receptor and as an antagonist at the human receptor. The previous chapter discussed how specific residues in Loops C and F of the 5-HT$_{3A}$ receptor ligand binding domain affect binding affinities of *d*-Tubocurarine (curare) between the species. In the present chapter, the role of residues in the same region of the receptor will be investigated regarding the differential pharmacology of 2-OHMBA at mouse and human receptors. Not surprisingly, the studies described in this chapter demonstrate that some of the same residues identified as critical for differences in curare sensitivities also play a significant role in differential pharmacology of 2-OHMBA at mouse and human 5-HT$_{3A}$ receptors.

CHAPTER III

PHYSICOCHEMICAL REQUIREMENTS OF AMINO ACIDS IN THE 5-HYDROXYTRYPTAMINE$_{3A}$ RECEPTOR FOR BINDING OF AND GATING BY BENZYLIDENE ANALOGS OF ANABASEINE

A.N. de Oliveira-Pierce[1], Ran Zhang[1, 2], William R. Kem[3], and Tina K. Machu[1]

1. Department of Pharmacology and Neuroscience, University of North Texas Health Science Center, 3500 Camp Bowie Blvd., Fort Worth, TX 76107

2. Department of Immunology, The University of Texas, M. D. Anderson Cancer Center, 7455 Fannin St., Houston, TX 77054

3. Department of Pharmacology and Therapeutics, University of Florida, College of Medicine, Gainesville, FL 32610

Running head: Actions of Benzylidene Analogs of Anabaseine at the 5-HT$_{3A}$R

Address correspondence to: A.N. de Oliveira-Pierce, Department of Pharmacology and Neuroscience, University of North Texas Health Science Center, 3500 Camp Bowie Blvd., Fort Worth, TX 76107. Tel: 817-735-2190; Fax: 817-735-0408; E-mail: aoliveir@hsc.unt.edu

Abbreviation List: 5-Hydroxytryptamine (5-HT); 5-hydroxytryptamine$_{3A}$ receptor (5-HT$_{3A}$); modified Barth's solution (MBS); vesicle dialysis buffer (VDB); nicotinic acetylcholine receptor (nAChR); ligand binding domain (LBD); mouse wild-type 5-

Hydroxytryptamine$_{3A}$ receptor (MWT); human wild-type 5-Hydroxytryptamine$_{3A}$ receptor (HWT); 3-(2-hydroxy,4-methoxybenzylidene)-anabaseine (2-OHMBA); 3-(2,4-dimethoxybenzylidene)-anabaseine (DMXBA); 1-Methyl-N-[(3-endo)-9-methyl-9-azabicyclo[3.3.1]non-3-yl]-1H-indazole-3-carboxamide hydrochloride (BRL-43694), Benzylidene-anabaseine (BA).

ABSTRACT

In previous reports, we demonstrated that 3-(2-hydroxy,4-methoxybenzylidene)-anabaseine (2-OHMBA) is a partial agonist at the mouse (5-Hydroxytryptamine$_{3A}$) 5-HT$_{3A}$ receptor and a competitive antagonist at the human receptor. Through site-directed mutagenesis, we identified two residues (I207 and I228) in the ligand binding domain of the mouse receptor, which when mutated to the corresponding human receptor amino acids, resulted in loss of partial agonist activity and gain of competitive antagonist actions. Mutation of a third residue, I209, resulted in reduced potency. We also reported that a –OH at the 2' position of the benzylidene ring was necessary for optimal partial agonist activity. In the present study we used two-electrode voltage clamp electrophysiological recordings and radioligand binding assays to determine the physicochemical requirements of amino acids in the mouse receptor at positions 207, 209, and 228 for gating by 2-OHMBA, and the amino acid with which the 2-OH moiety interacts. Of the 28 point mutant receptors tested, 16 exhibited 5-HT mediated currents. Of the 16, only M-I207L, M-I209M/L, and M-I228A/L were gated by 2-OHMBA. EC$_{50}$'s ranged from 0.43 to 28.8 μM and efficacies range from 10% to 1,231%. In all the remaining mutant receptors, 2-OHMBA inhibited 5-HT mediated currents. We performed double mutant thermodynamic cycle analysis, pairing a mutated mouse receptor at residue 207, 209, or 228 with substitution of -OCH3 and -OH at the 2' position of the benzylidene-anabaseine (BA) compound and measured displacement of

[^{3}H]-BRL-49364. Results suggest that the 2–OH interacts directly with I228, a residue in Loop C of the LBD, to effect gating in the mouse 5-HT_{3A} receptor.

INTRODUCTION

The 5-Hydroxytryptamine$_3$ receptor (5-HT$_3$R) is a cationic ligand-gated ion channel that mediates fast synaptic neurotransmission (Ropert and Guy, 1991; Ronde and Nichols, 1998; Thompson and Lummis, 2006). This receptor is a member of the cys-loop family of ligand-gated ion channels (LGIC's) (Maricq et al., 1991) along with the nicotinic acetylcholine (nAChR), γ-aminobutyric acid$_A$ (GABA$_A$R), glycine receptors (GlyR) (Grenningloh et al., 1987; Schofield et al., 1987) and Zn^{2+} regulated ion channels (Davies et al., 2003). Five 5-HT$_3$ receptor subunits have been cloned (A-E) (Belelli et al., 1985; Maricq et al., 1991; Niesler et al., 2007). Receptors forming A-homomers or A/B-heteromers have been shown to have functional significance in the central and peripheral nervous systems (Thompson and Lummis, 2006). Receptors containing subunits C-E are found predominantly in the gastrointestinal tract and in dorsal root ganglia; however, their function remains poorly understood (Holbrook et al., 2009). The ligand binding domain (LBD) for all LGICs is located in the N-terminus at the interface between subunits and consists of six loops (A-F). Loops A-C form the principal component of the LBD and Loops D-F form the complementary component of the LBD (Thompson and Lummis, 2006).

Anabaseine is a toxic compound extracted from the nemertine worm that acts primarily as an agonist at central and peripheral nAChR's (de Fiebre et al., 1995; Kem et al., 1997). A derivative of anabaseine, 3-(2,4-dimethoxybenzylidene)-anabaseine (DMXBA), acts as an antagonist at both human and mouse 5-HT$_{3A}$ receptors with IC$_{50}$'s

of 3.1 ± 0.2 μM and 15.7 ± 0.9 μM, respectively (Machu et al., 2001; Zhang et al., 2006). BA analogs have been used previously to probe binding and function of the α7 nAChR receptor (Papke et al., 2005), and residues in Loops C and F have been reported to play a significant role in differential pharmacology of these compounds across species (Stokes et al., 2004). An analog of DMXBA in which the 2' position of the benzylidene ring is replaced with -OH, 3-(2-hydroxy, 4-methoxybenzylidene)-anabaseine (2-OHMBA), acts as a potent antagonist at the human receptor with an IC_{50} of 1.5 ± 0.1 μM. However, despite the fact that human and mouse 5-HT_{3A} receptors share 84% amino acid identity, 2-OHMBA acts as a partial agonist at the mouse receptor with an EC_{50} of 2.0 ± 0.3 μM (Machu et al., 2001). Previously, we reported that the distal 1/3 of the N-terminus of the 5-HT_{3A} receptor plays a critical role in interspecies differential pharmacology of 2-OHMBA (Zhang et al., 2006) and that residues I207, I209 and I228 are critical for partial agonist activity at the mouse receptor (Machu et al., 2009).

In the present study, we further investigated the physicochemical properties of residues required for partial agonist activity of 2-OHMBA by substituting the Ile at 207, 209 and 228 with amino acids of different hydropathies, polarities and molecular volumes. Mouse 5-HT_{3A} point mutant receptors were tested using two-electrode voltage clamp electrophysiology in order to determine which amino acid substitutions are capable of maintaining partial agonist activity of this BA analog in the mouse receptor. Another part of our experiments builds on structure-function studies that have identified a pharmacophore required for coupling of ligand binding to channel gating of the 5-HT_3 receptor. This pharmacophore is thought to consist of a hydrogen bond acceptor, an

amine group, an aromatic group and a charged group (Daveu et al., 1999). We demonstrated that the –OH in the 2' position of 2-OHMBA is likely involved in the formation of a hydrogen bond with the receptor. Substitutions with –F or $–CH_3$ abolished partial agonist activity of the BA compound and created antagonist activity at MWT. We used double-mutant thermodynamic cycle analysis to determine whether the 2' -OH directly interacts with residues 207, 209 or 228. Double-mutant thermodynamic cycle analysis has been previously used to establish orientation and points of interaction between ligands and amino acids in cys-loop receptors, e.g., *d*-Tubocurarine and nACh (Pedersen and Papineni, 1995; Willcoxson et al., 2002) and 5-HT_3 receptors (Yan et al., 2006), granisetron and 5-HT_3Rs (Yan and White, 2005), and α-Neurotoxin and nAChRs (Malany et al., 2000). In the present study, we present evidence of an interaction between the 2' -OH of 2-OHMBA and residue 228 in Loop C of the mouse 5-HT_{3A}R.

EXPERIMENTAL METHODS

Analogs of 3-Benzylideneanabaseine. Syntheses of DMXBA and its analogs were performed as previously described in Kem et al. (2004). Stock solutions of 1-10 mM were made with water, were aliquoted, and stored at -20 °C. Prior to use, compounds were diluted to desired concentrations in modified Barth's solution (MBS) containing (in mM) NaCl 88, KCl 1, NaHCO3 2.4, HEPES 10, MgSO4 0.82, Ca(NO3)2 0.33, and CaCl2 0.91 (pH 7.5) for electrophysiology studies, or in vesicle dialysis buffer (VDB) containing (in mM) NaCl 96, MOPS 10, EDTA 0.1, and 0.02% NaN3 (pH 7.5)VDB for radioligand binding studies. Compounds were not exposed to strong light due to the light sensitivity of BA analogs.

Isolation of Xenopus laevis Oocytes. X. laevis frogs were kept in tanks of dechlorinated tap water on a 12-h light/12-h dark cycle at 18 °C and fed a diet of Xenopus Express sinking frog food once per week. Frogs were anesthetized by immersion for 20 min. in ice cold 0.12% 3-aminobenzoic acid ethyl ester solution, pH 6.5-7.5, adjusted with sodium bicarbonate. Ovarian tissue was removed through a small incision in the frog's abdomen and placed in MBS. Tissue was manually separated into smaller clumps and subjected to chemical dissection and defolliculation by gently rocking the clumps in a medium containing 2 mg/ml Collagenase Type 2 and in (mM) NaCl 83, KCl 2, MgCl2 1, and HEPES 10 (pH 7.5) for 2 hours. Chemical dissection was repeated using new media and new Collagenase solution. Oocytes were washed with MBS and stored in incubation media composed of ND 96, containing (in mM) NaCl 96,

KCl 2, CaCl2 1.8, MgCl2 1 and HEPES 5 (pH 7.5), plus 10 mg/l streptomycin, 50 mg/l gentamycin, 10000-units/l penicillin, 96 mg/l sulfamethoxazole, 19 mg/l trimethoprim, 0.5 mM theophylline, and 2 mM sodium pyruvate.

Construction of Chimeric Receptors. Mouse and human 5-HT_{3A} receptor cDNAs, provided by Drs. D. Julius and A. Miyake, respectively, were subcloned into pCR-Script™ Amp SK(+)$^{-}$ (Stratagene, La Jolla, CA) or pcDNA 3.1($^{-}$) (Invitrogen, Carlsbad, CA). Introduction of restriction enzyme cleavage sites, digestion of cDNAs, and subsequent ligation of appropriate fragments were performed as previously described (Zhang et al., 2007). Mutant cDNAs were confirmed by dideoxynucleotide sequencing at the Biotechnology Core Facility at Texas Tech University, Lubbock, TX.

Transcription of cDNA to cRNA. The wild-type and mutant 5-HT_{3A}R cDNAs were linearized with NotI, extracted with phenol-chloroform, precipitated with sodium acetate and ethanol, and re-suspended in diethyl pyrocarbonate (DEPC)-treated water. The cDNAs were then transcribed with the T3 or T7 mMESSAGE mMACHINE (Ambion, Austin, TX).

Microinjection of Oocytes with 5-HT_3 Receptor cRNA. Aliquots of cRNA were centrifuged at 15,000*g*, and the ethanol was removed with a tuberculin syringe. Pellet was air dried and resuspended in DEPC-treated water to yield concentrations of 25-100 ng of cRNA/50 nl. The cRNA was drawn up into a micropipette (10–20 μm tip size). A volume of 50 nl, cRNA was injected into the animal/vegetal pole equator of each oocyte. Oocytes were stored in incubation medium in Corning cell well plates (Corning Glass Works,

Corning, NY) at room temperature. Electrophysiological recordings took place during 2-7 days following injection.

Electrophysiological Recordings. Oocytes were perfused (2 ml/min) in a 100 µl volume recording chamber with MBS via a roller pump (Cole-Parmer Instrument, Co., Chicago, IL). Oocytes were then impaled with two glass electrodes (1.2 mm outside diameter and 1–10-megaohm resistance) filled with 3 M KCl. A Warner Instruments Model OC-725B or OC-725C oocyte clamp (Hamden, CT) was used to voltage clamp oocytes at -70 mV, and clamping currents were plotted on a strip chart recorder (Cole Parmer Instrument, Co., Chicago, IL). To examine agonist or partial agonist effects, 5-HT or BA analogs were diluted to desired concentration in MBS and applied to oocytes for 30 s. To examine antagonist effects, BA analogs were also diluted in MBS and co-applied with 5-HT. Applications of 5-HT, BA analogs, or 5-HT plus BA analogs were performed every 5 min.

Membrane Purification. Oocytes were injected with 100 ng HWT or MWT cRNA and tested for expression with two-electrode voltage clamp electrophysiology on day two. Oocytes were homogenized with a hand-held glass potter (~50 *Xenopus laevis* oocytes) in ice-cold VDB, 0.1 ml per oocyte + 10 ul of protease inhibitor cocktail set III (Calbiochem, La Jolla, CA). The homogenate was centrifuged for 10 min at 800 g. The supernatant was collected, the pellet was re-suspended in VDB (0.1 ml/oocyte) and re-centrifuged at 800 g for 10 min. Supernatants were combined and centrifuged for 1 hour at 38,800 g. The membrane pellet was re-suspended in VDB (2-8 ml depending on expression) and divided

into several batches for storage at -20 °C. The Lowry assay (Lowry et al., 1951) was used to measure protein concentration.

Radioligand Binding Assays. Membrane homogenate (~ 8-15 μg/tube) was incubated at 37 °C for 2 hours with [^{3}H]-BRL-43694 (0.1 – 30 nM) for K_d determination. K_i values were determined by incubating aliquots of membrane at 37 °C for 2 hours with the BA analog (1 nM – 2 mM) and [^{3}H]-BRL-43694 at the respective K_d. Non-specific binding was measured with 50 μM MDL-7222 (3-tropanyl-3, 5-dichlorobenzoate), a 5-HT_{3A} receptor competitive antagonist. Membranes with bound radioligand were transferred to Whatman GF/B filters (Whatman, Clifton, NJ) and washed with VDB (pH 7.5) by rapid vacuum filtration. Filters were individually incubated in 3 ml of Econo-Safe™ scintillation cocktail (Research International Products, Mt Prospect, IL), and radioactivity was measured via scintillation spectrometry.

Data Analysis. Control values for electrophysiology experiments were obtained by averaging the 5-HT mediated response before and after the response to BA analog or 5-HT plus BA analog. For generation of concentration response curves for 5-HT or BA analog, currents were expressed as a percentage of the maximal 5-HT (25 μM) response. Inhibition by BA analogs was calculated by subtracting the current obtained from 5-HT plus BA from the average current obtained with 5-HT alone; the difference was divided by the average 5-HT mediated current, and the quotient was multiplied by 100.

Graphpad Prism (San Diego, CA) was used to calculate EC_{50}'s, IC_{50}'s, K_d's, K_i's and Hill coefficients. The equation used to calculate EC_{50}'s and IC_{50}'s was $I/I_{control} = 1/[1+[D/E(I)C_{50}]^{n}]$, where I is current, $I_{control}$ is the control current, D is the drug

concentration, EC_{50} is the concentration of drug that produces 50% of the maximal response, IC_{50} is the concentration of drug that produces 50% inhibition of the response, and n is the Hill coefficient. Specific binding was calculated as X*Bmax /(K_d+X), where X is the radioligand concentration, Bmax is the maximum specific binding/mg protein, and K_d is the dissociation constant (-1/slope). Values for the equilibrium dissociation constants (K_i's) were calculated from the IC_{50}'s and equation was K_i = (IC_{50})/(1+([ligand]/K_d)), where IC_{50} is the concentration of unlabeled drug needed to block 50% of the specific binding, K_d is the affinity of the radioligand for the receptor, and [ligand] is the concentration of the unlabeled drug, One-way analysis of variance (ANOVA) and Tukey-Kramer post-hoc analyses were performed by Instat (San Diego, CA).

In the double mutant thermodynamic cycle analysis, the interaction coefficient (Ω) was calculated using the equation: $\Omega = (K_{W,L1}/K_{W,L2})/(K_{M,L1}/K_{M,L2})$, where K is the dissociation constant obtained from radioligand binding assays, W is the wild-type receptor, M is the mutant receptor, and L1 and L2 are the BA compounds being compared. A Ω value significantly different from 1 suggests a direct interaction between the amino acid residue in the receptor and the functional group of the ligand (Yan et al., 2006).

RESULTS

Analogs of benzylidene-anabaseine have differential actions at mouse and human 5-HT_{3A}R's (Machu et al., 2001; Zhang et al., 2006). In previous studies we reported that the 2' functional groups in these compounds play a critical role in partial agonist function and in efficacy of the BA analogs in the mouse receptor and that both the 2' and 4' groups are important determinants of potency in apparent competitive antagonism of the BA analogs in the human receptor (Machu et al., 2001; Zhang et al., 2006). Results of the present study confirmed that the 2' –OH group is required for partial agonist function of 2-OHMBA at the mouse receptor. Substitution of the 2' –OH with –F or $–CH_3$ resulted in loss of agonist function and gain in antagonist activity (Fig. 1). A $–CH_3$ group has a similar molecular volume as –OH, whereas –F is a hydrogen bond acceptor, but not a hydrogen bond donor. The observation that substitution with –CH3 or –F caused loss of partial agonist activity suggests that size at the 2' position is not the critical determinant. Furthermore, the –OH is likely a hydrogen bond donor to an amino acid in the LBD that effects gating.

We identified two Ile residues in the mouse 5-HT_{3A} receptor, one in Loop F (I207) and one in Loop C (I228), which when individually mutated to the corresponding human receptor amino acids, resulted in loss of partial agonist activity and gain of antagonist function of 2-OHMBA in the mutant receptor (Machu et al., 2009). In the present study, we assessed the physicochemical properties of amino acids at each of the three positions in the mouse receptor that confer partial agonist activity of 2-OHMBA.

We systematically substituted I207 with all other 18 amino acid residues. All receptor constructs were expressed in *Xenopus* oocytes, and two-electrode voltage clamp electrophysiological recordings were performed. All mutant receptors were first tested for function with 5-HT (25 μM) and 2-OHMBA (25 μM). Of the 19, 11 were neither gated by 5-HT nor 2-OHMBA. Serotonin concentration response curves were performed in the remainder (Fig. 2B). Serotonin EC_{50} values ranged from 0.52 μM to 31.8 μM. Some of the EC_{50} values were significantly different than that of MWT, with the largest fold change of 23.4, occurring with M-I207A. Testing for 2-OHMBA function revealed that most substitutions, with the exception of the I207L, resulted in loss of partial agonist activity and gain in antagonist activity of this BA analog (Fig. 2C and 2D). Potencies for antagonist function of 2-OHMBA at the point mutant receptors ranged from 1.65 μM to 7.33 μM. In M-I209L, there was a significant but moderate decrease in both potency (EC_{50} of 6.2 μM) and efficacy (44%) when compared to MWT (EC_{50} of 2.0 μM and 63% efficacy) (Fig. 2D).

For I209, we substituted amino acids with different hydrophobicities, molecular volumes and polarities: Ala, Leu, Met, and Tyr. Serotonin evoked currents in M-I209L/A/M and 2-OHMBA evoked currents in evoked currents in the I209L and M point-mutant receptors. The M-I209Y receptor did not respond to either 5-HT or 2-OHMBA. Functional receptors had 5-HT potencies ranging from 0.73 μM to 4.53 μM (Fig. 3A). Interestingly, 2-OHMBA maintained partial agonist activity at most point mutants tested, albeit with significantly decreased potency (EC_{50} of 12.2 μM) and <10% efficacy for M-I209M (Fig. 3B). Both 5-HT and 2-OHMBA elicited currents at the M-

I209L point-mutant with EC_{50}'s of 4.53 and 6.64 μM, respectively (Fig. 3A and 3B). Another interesting result was the fact that the M-I209A point mutant responded to 5-HT with increased potency (EC_{50} of 0.73 μM) (Fig. 3A) when compared to the MWT (EC_{50} of 1.36 μM), while 2-OHMBA concentrations (4-25 μM) had significantly decreased efficacy (<20%) (data not shown). Functional tests using higher 2-OHMBA concentrations (100 μM) must be conducted to confirm these results and accurately calculate potency.

We examined the effect of mutations in position 228, in Loop C. As with I209 point-mutants, we substituted I228 for amino acids with different hydrophobicities, molecular volumes and polarities: Ala, Leu, Gln, and Cys. The mutant receptors M-I228A and M-I228L responded to 5-HT and 2-OHMBA. M-I228Q and M-I228C did not respond to either 5-HT or 2-OHMBA. While most of the EC_{50} values for point-mutant receptors were different than that of the MWT, the M-I228L substitution appeared to have the most significant effect on 5-HT potency with an EC_{50} of 27.84 μM (Fig. 4A). This result was surprising given the fact that the Ile-Leu substitution was the most conserved mutation tested. As for the effect of the I228L mutation on the function of 2-OHMBA, in agreement with the I207L and I209L substitutions, partial agonist activity was maintained with a moderate decrease in potency (EC_{50} of 14.1 μM), when compared to the MWT (2.0 μM), and with no apparent changes in efficacy. Similar to the Ile-Met substitution in position 207, a previous testing of M-I228M reported loss of partial agonist activity and gain in antagonist activity of 2-OHMBA with an IC_{50} of 11.3 μM (Machu et al., 2009) (Fig. 4C). However, unlike the I207A, the I228A point mutation had

a surprising effect on agonist function. While EC_{50} values for 2-OHMBA between M-I228A and MWT were not significantly different (2.1 μM and 2.0 μM, respectively), efficacy of 2-OHMBA was 18.6 fold greater at M-I228A than at the MWT. Thus, 5-HT appears to function as a partial agonist at this mutant receptor (Fig. 4D).

We further examined residues 207 and 228 as likely candidates for direct interactions with the –OH. We also assessed D229, given that possible interactions between residue D229 and 5-HT_3 receptor ligands have been previously reported, (Thompson et al., 2005; Suryanarayanan et al., 2005). Binding studies were done with M-I207V, M-I228M, D228E, and D229A point-mutant receptors using 2-OHMBA AND DMXBA. Mutations were paired with changes in the BA analog, 2'-OH or 2'-OCH3, respectively. In radioligand binding studies, affinities for [^{3}H]-BRL-43694 ranged from 2.58 nM to 15.8 nM (Table 2). Most were significantly different from MWT (K_i of 3.53 nM). However, the largest fold-change was 4.5 and not likely to greatly impact displacement by 2-OHMBA or DMXBA. The K_i values for MWT, HWT, M-I207V, M-I228, M-D229E, and M-D229A ranged from 12.1 nM to 1,200 nM for DMXBA and 40.2 nM to 726.2 nM for 2-OHMBA, respectively, with most values being significantly different from MWT. Using double-mutant thermodynamic cycle analysis, we compared changes in interaction coefficients between the BA analog having a –OH at the 2' position and the analog having a $–OCH_3$ in the 2' position. BA analogs had an Ω value of 0.4 between MWT and M-I207V receptors, indicating there is no direct interaction between the Ile-207 residue and the 2' –OH (Fig. 5A). The analysis for Loop C residue Ile-228 on the other hand, indicates this Ile residue plays a critical role in direct

interaction between the 2' –OH and the MWT with an Ω value of 32.7 (Fig. 5B). Results for residue 229 also indicate a possible interaction with the 2' –OH group, as the Ω for the DMXBA/2-OHMBA/MWT/D229E cycle had a value of 1.8 (Fig. 5C). However, given the Ω value of 32.7 for I228, a Ω value of 1.8 indicates the D229 residue is likely not as critical in direct interactions with –OH.

DISCUSSION

The 2'-OH moiety at 2-OHMBA is critical for partial agonist function of this compound at the mouse 5-HT_{3A} receptor, with substitutions of the BA analog with -F or -CH3 producing no partial agonism, but instead inhibition of 5-HT elicited currents (Fig. 1). These results are in agreement with previous reports that DMXBA, a BA analog with a 2'-OCH3, did not elicit currents at MWT, but did antagonize 5-HT mediated currents. Also reported was that 4-OHMBA, a BA analog with a 4'-OH group, while capable of activating MWT receptors, had decreased efficacy (~24%) when compared to 2-OHMBA (~63%) (Machu et al., 2001). Substitution with a –CH3 at the 2' position created a compound with no agonist function at the MWT, suggesting that the similar molecular weight between the –OH and the –CH3 groups is not sufficient to confer partial agonist function to this compound. Based on previous studies, the existence of a hydrogen bond between 5-HT_3Rs and their ligands is required for binding of both agonists and antagonists (Daveu et al., 1999). Considering we have demonstrated that the 2'-OH is critical for gating of this receptor by BA, we propose that this group functions as a hydrogen bond donor, as substitution of the 2' –OH moiety with –F, a hydrogen bond acceptor, created a BA analog that did not gate the MWT receptor.

Another interesting finding of this study was that the 2' moiety of the BA analog appears to be involved in direct interaction with residues in Loop C of the mouse 5-HT_{3A}R, with an Ω value for I228M of 32.7 (Fig. 5B). The identity of the amino acid in position 228 was not only critical for direct interaction with the 2'-OH, but also for

partial agonist activity of 2-OHMBA. The substitution with Leu maintained partial agonist activity of 2-OHMBA, and the Ala substitution affected function of 5-HT, turning this otherwise potent full agonist compound into a partial agonist at the mouse receptor. These results are similar to those observed in a study by Suryanarayanan et al., (2005), in which the I228A mutation caused a significant increase in 5-HT EC_{50} and converted 5-HT into a partial agonist with lower efficacy than 2-methyl-5-HT. These results further confirm that residue 228 is critical for gating by 2-OHMBA and binding at the MWT receptor.

Double mutant thermodynamic cycle analysis of residue D229 of the mouse 5-HT_{3A} receptor suggested that while this residue is not as critical for direct interaction with the 2'-OH of 2-OHMBA, given its Ω value of 1.8 when substituted with Ala, and a Ω value of 0.05 when substituted with Glu, it does have a significant role in binding of the drug. A substitution with the human reciprocal mutant, D229E, caused a decrease in affinity of [^{3}H]-BRL-43694 (~2-fold), DMXBA (~2.5-fold), and 2-OHMBA (~4.3-fold) when compared to MWT (Table 2). Substitutions with Ala also caused decreased affinity of these compounds with the highest decrease being ~17.2-fold for DMXBA. These data are comparable to results from a previous study reporting that the D229A substitution decreased affinity of both 5-HT (~140-fold) and [^{3}H]-BRL-43694 (~8-fold) at the MWT 5-HT_3 receptor (Suryanarayanan et al., 2005). Another study with similar changes in affinity as a result of Ala substitution was done by Thompson et al. (2005); they reported an ~12.3-fold decreased affinity for [^{3}H]-BRL-43694. Additionally, homology models suggest that residues 229 and 230 at the mouse receptor are important for stabilization of

the ligand binding domain and may underly inherent differences in intramolecular interactions in mouse and human 5-HT_{3A} receptors (Reeves et al., 2002; Thompson et al., 2005). Collectively, these results indicate an important role for an Asp residue in position 229 of the mouse receptor for actions of a number of 5-HT_3 ligands, including BA analogs.

In addition to further establishing the role of Loop C in both function and binding of BA analogs at the 5-HT_{3A} receptor, this study enabled us to demonstrate that even though residues in Loop F do not appear to directly interact with the 2'-OH moiety, the presence of an Ile at this position, as well as at position 209, are critical for function of 2-OHMBA. At residue 207, the only substitution capable of maintaining partial agonist of 2-OHMBA was the Ile to Leu mutation. This suggests that specific physicochemical characteristics are required for partial agonist function of this compound. Side chains of Ile have been previously implicated in trafficking of both, nAChR's and 5-HT_3R's (Castillo et al., 2005), and in creating hydrophobicity at the binding pocket (Chang and Weiss, 1998). Furthermore, since Ile and Leu have nearly identical molecular weights (MW), it is possible that MW in addition to hydrophobicity play an important role in gating of 5-HT_3. One way in which our data differs from a previous report by Thompson et al., (2005), in which it was suggested that I207 forms a hydrogen bond with [^{3}H]-BRL-43694, is that double-mutant thermodynamic cycle analysis using radioligand binding data produced an Ω of 0.4. This would indicate no direct hydrogen bond between the 2'-OH group of 2-OHMBA and I207. This data does not, however, eliminate the possibility that this group forms a hydrogen bond with another moiety of this compound. Another

important point is that while residues 207 and 209 may not be directly interacting with the 2'-OH group of 2-OHMBA, they do play a critical role in gating as substitution of Ile with most amino acids ablated agonist function of this compound. Additionally, it is possible that a direct interaction between –OH and the amino acid is not taking place, but rather that 2'–OH interacts with a keto group, and that absence of an Ile or a Leu induces a conformational change. This change could be responsible for steric hindrance of the molecule and subsequent ablation of gating by anabaseine. Thus, these residues may play a role in the overall conformational changes that couple binding with activation of the 5-HT_{3A} receptor.

Actions of 2-OHMBA at the mouse receptor were altered by point-mutations at residue 209, with the only substitution to maintain partial agonist activity with comparable efficacies being Ile to Leu. Once again, the physicochemical properties of these amino acids appear to play a critical role in the function of this compound. One difference between these two residues (207 and 209) was that the Ile to Met substitution at the 207 position changed the actions of 2-OHMBA from partial agonist to antagonist, while at the 209 receptor, partial agonist activity was maintained, albeit with $< 10\%$ efficacy. In summary, our data supports involvement of both Loops C and F in gating of the mouse 5-HT_{3A} receptor by 2-OHMBA while identifying Loop C as the critical component in formation of a hydrogen bond with the 2'-OH group of this BA analog.

Table 1 Testing of mouse 5-HT_{3A} point mutant receptors for pharmacological effects of 5-HT and 2-OHMBA.

Point Mutant	5HT	2-OHMBA	
	EC_{50} (µM)	EC_{50} (µM)	IC_{50} (µM)
*I207L	0.52	6.01	N/A
I207M	0.78	N/A	6.83
I207C	2.17	N/A	2.22
†I207V	2.88	N/A	3.93
I207Q	5.64	N/A	1.52
I207T	7.02	N/A	1.82
I207K	19.71	N/A	1.96
I207A	31.8	N/A	1.35
*†I209M	4.45	12.23	N/A
*I209L	4.53	6.24	N/A
£I209A	0.73	N/A	--
*I228A	0.43	0.21	N/A
*I228L	1.8	14.12	N/A
†I228M	3.54	N/A	11.33
I228C	N/A	N/A	N/A
I228Q	N/A	N/A	N/A

N/A = not applicable
MWTA EC_{50} for 5-HT = 1.36 µM and EC_{50} for 2-OHMBA = 2.0 µM
***Maintenance of 2-OHMBA partial agonist activity.**
£Additional testing with higher 2-OHMBA concentrations required in order to calculate an accurate IC_{50}.
†Taken from Machu et al., 2009.

Table 2 Binding affinities for displacement of [^{3}H]-BRL-43694 by BA analogs in wild-type and point mutant 5-HT$_{3A}$R's.

5-HT$_{3A}$R Construct	[^{3}H]-BRL-43694 K_d (nM)	DMXBA K_i (nM)	2-OHMBA K_i
MWT	3.53 ± 0.3	33.7 ± 3.91 [b]	58.8 ± 4.3 [b]
HWT	2.58 ± 0.61	1200 ± 112 [a]	726.2 ± 94.42 [a]
M-I207V	6.23 ± 0.52 [a, b]	58.32 ± 6.83 [b]	40.23 ± 3.9 [b]
M-I228M	5.82 ± 0.2 [a, b]	12.12 ± 1.8 [a]	690.5 ± 51.02 [a, b]
M-D229E	6.9 ± 0.91 [a]	83.13 ± 12.02 [b]	255.72 ± 16.6 [a, b]
M-D229A	15.8 ± 0.32 [a, b]	578.8 ± 38.71 [a, b]	51.72 ± 7.01 [b]

ANOVA was performed, and it was significant $p < 0.05$. [a]$p < 0.01$ compared to MWT; [b]$p < 0.01$ compared to HWT, two-tailed unpaired t-test with a Bonferroni correction factor.

Figure 1. –OH is required for partial agonist activity of BA at MWT 5-HT_{3A}R's. MWT 5-HT_{3A}R inhibition of 5-HT (EC_{50}) by BA analogs in which the 2' –OH has been substituted with –F or –CH3. Insert shows concentration response curve for 2-OHMBA (n=4-7).

Figure 1

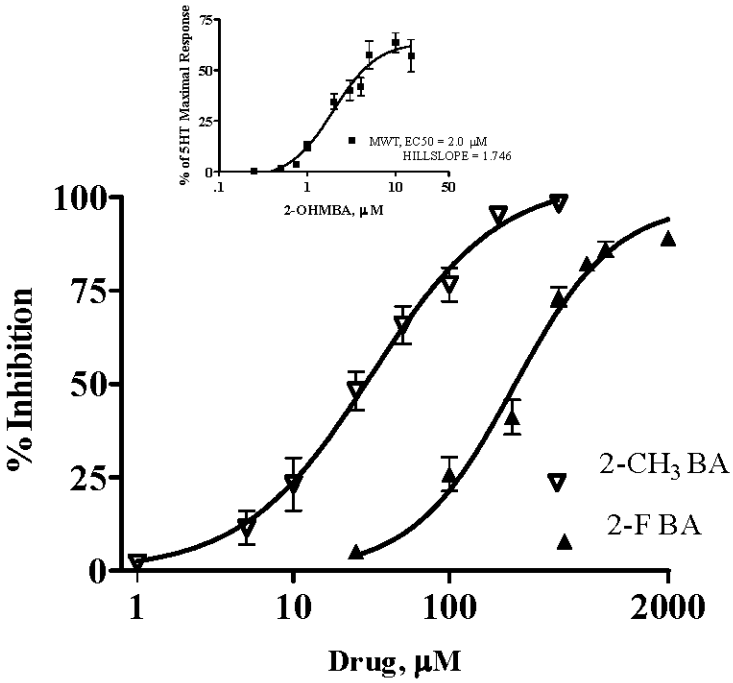

IC_{50} (µM), HILLSLOPE

2-CH_3 BA (31.4, 1.064)

2-F BA (257.3, 1.345)

Figure 2. Actions of 5-HT and 2-OHMBA at MWT and M-I207X point mutant 5-HT_{3A}Rs. A: Residues in or near Loops C and F of the mouse and human 5-HT_{3A}R's are aligned. (*) indicate the I207, I209, I228 and D229 residues in the mouse and human orthologs V202, M204, M223 and E229. B: 5-HT concentration response curves for MWT and functional M-I207X point mutant 5-HT_{3A}R's (n=4-7). M-I207V is the human reciprocal mutant. C: Inhibition of 5-HT by 2-OHMBA at M-I207X point mutant 5-HT_{3A}R's. 2-OHMBA (0.5-100 μM) was co-applied with 5-HT (EC_{50}) for 30 s. D: 2-OHMBA concentration response curve for MWT and M-I207L 5-HT_{3A}R's (n=4-7). M-I207L was the only I207X point mutant to maintain partial agonist activity of 2-OHMBA.

Figure 2

A.


Loop B
Loop F
Loop C
Mou 185 HTIQDINITLWRSPEEVRSDKSIFTNQGEWELLEVFPQFKEFSTDTS
Hum 180 HTIQDINISLWRLPEKVKSDRSVFMNQGEWELLGVLPYFREFSMESS
Loop C
Mou 232 NSYAEMKFYVIIRRR
Hum 227 NYYAEMKFYVVIRRR

B.

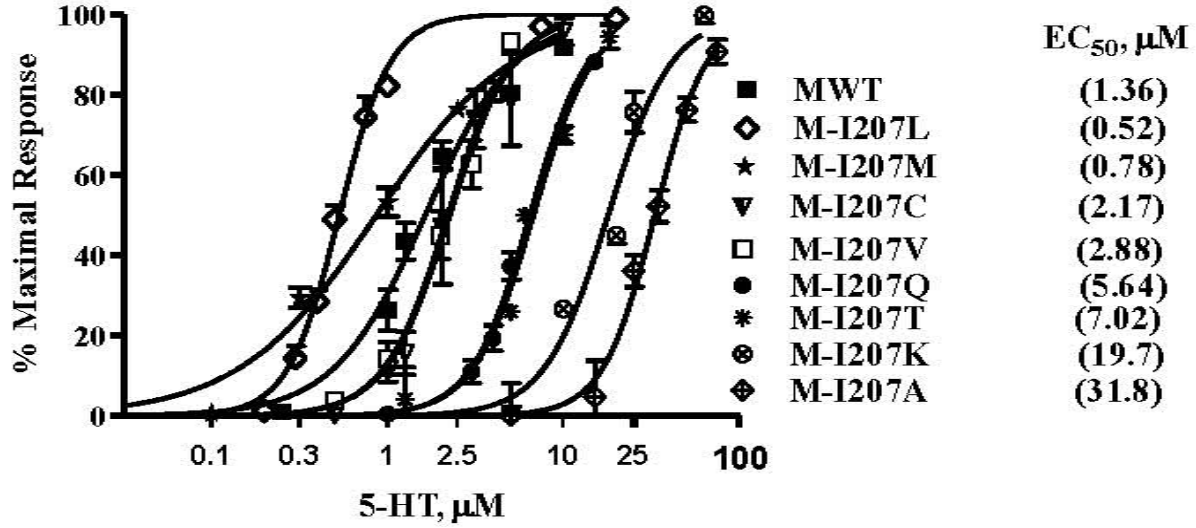
% Maximal Response
100
80
60
40
20
0
0.1
0.3
1
2.5
10
25
100
5-HT, µM
EC50, µM
MWT (1.36)
M-I207L (0.52)
M-I207M (0.78)
M-I207C (2.17)
M-I207V (2.88)
M-I207Q (5.64)
M-I207T (7.02)
M-I207K (19.7)
M-I207A (31.8)

C.

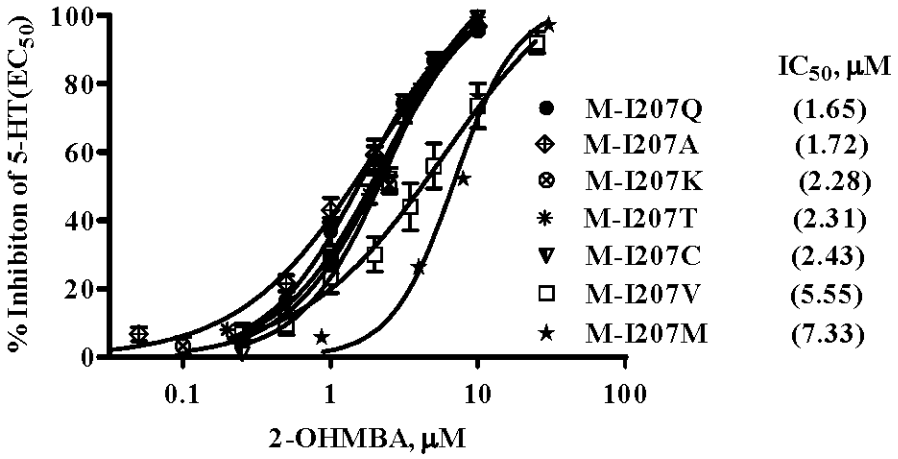
% Inhibiton of 5-HT(EC50)
100
80
60
40
20
0
0.1
1
10
100
2-OHMBA, μM
IC50, μM
M-I207Q (1.65)
M-I207A (1.72)
M-I207K (2.28)
M-I207T (2.31)
M-I207C (2.43)
M-I207V (5.55)
M-I207M (7.33)

D.

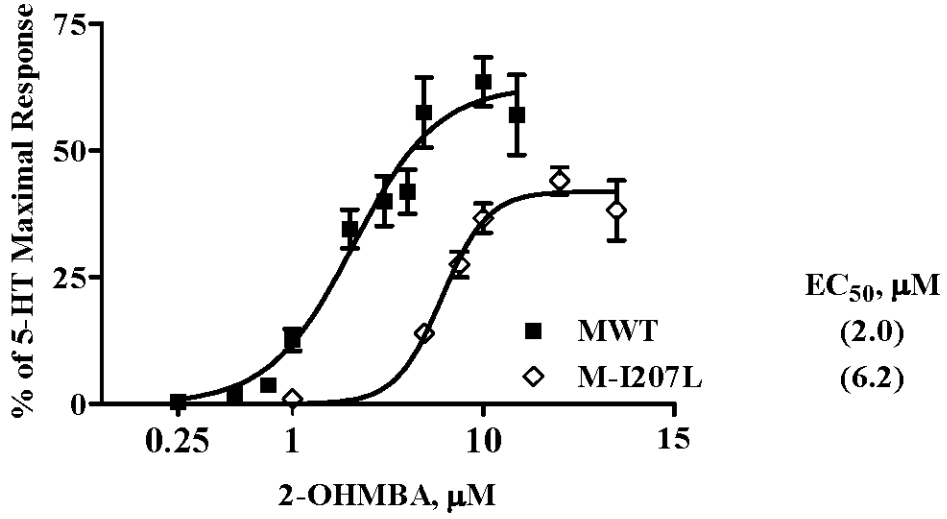
% of 5-HT Maximal Response
75
50
25
0
0.25
1
10
15
2-OHMBA, μM
EC50, μM
MWT (2.0)
M-I207L (6.2)

Figure 3. Actions of 5-HT and 2-OHMBA at MWT and M-I209X point mutant 5-HT_{3A}R's. A: Concentration-response curve for 5-HT were generated in oocytes expressing MWT and M-I209X 5-HT_{3A}R's (n=4-7). M-I209M is the human reciprocal mutant. The M-I209Y point mutant receptor did not respond to 5-HT concentrations (0.5-25 μM). B: 2-OHMBA concentration response curve for MWT, M-I209L and M-I209M 5-HT_{3A}R's (n=4-7). M-I209Y/A did not respond to 2-OHMBA concentrations (0.25-100 μM). M-I209M maintained partial agonist activity but with efficacy < 10%.

Figure 3

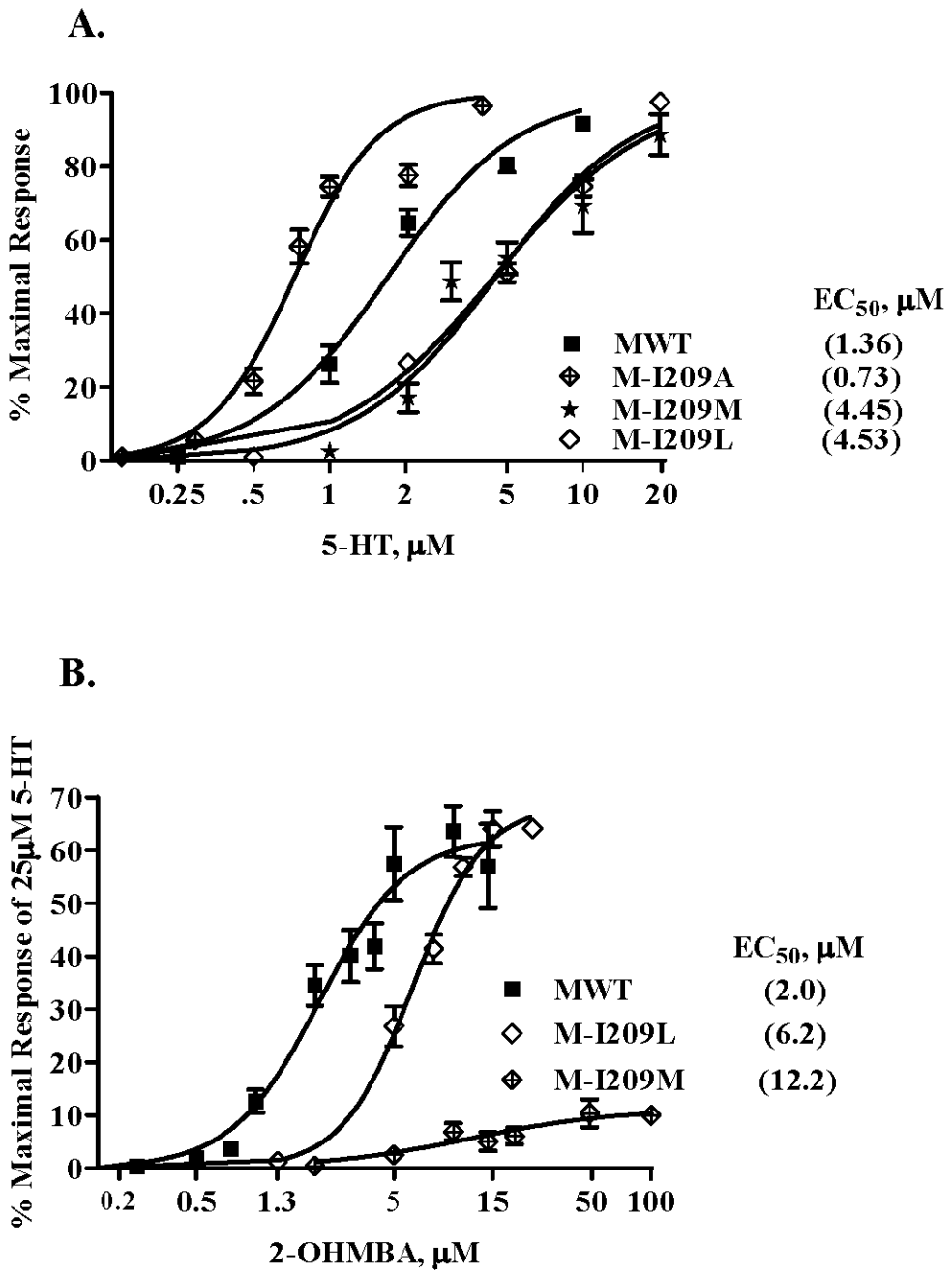
A.
% Maximal Response
100
80
60
40
20
0
0.25
.5
1
2
5
10
20
5-HT, µM
EC50, µM
MWT (1.36)
M-I209A (0.73)
M-I209M (4.45)
M-I209L (4.53)
B.
% Maximal Response of 25µM 5-HT
70
60
50
40
30
20
10
0
0.2
0.5
1.3
5
15
50
100
2-OHMBA, µM
EC50, µM
MWT (2.0)
M-I209L (6.2)
M-I209M (12.2)

Figure 4. Actions of 5-HT and 2-OHMBA at MWT and M-I228X point mutant 5-HT_{3A}R's. A: Concentration-response curve for 5-HT were generated in oocytes expressing MWT and M-I228X 5-HT_{3A}R's (n=4-7). M-I228M is the human reciprocal mutant. M-I228C/Q did not respond to 5-HT concentrations (0.5-25 μM). B: 2-OHMBA concentration response curve for M-I228L 5-HT_{3A}R showing maintenance of partial agonist activity of 2-OHMBA with the same efficacy, but lower potency when compared to MWT (n=4-7). 2-OHMBA (0.25-100 μM) response is calculated as a percentage of maximal response to 5-HT (25 μM). C: Inhibition of 5-HT by 2-OHMBA at the M-I228M point mutant 5-HT_{3A}R. 2-OHMBA (0.5-100 μM) was co-applied with 5-HT (EC_{50}) for 30 s. D: Concentration response curve for M-I228A shows this substitution produced a receptor with very strong agonist activity of 2-OHMBA with similar potency, but much higher efficacy than 5-HT.

Figure 4

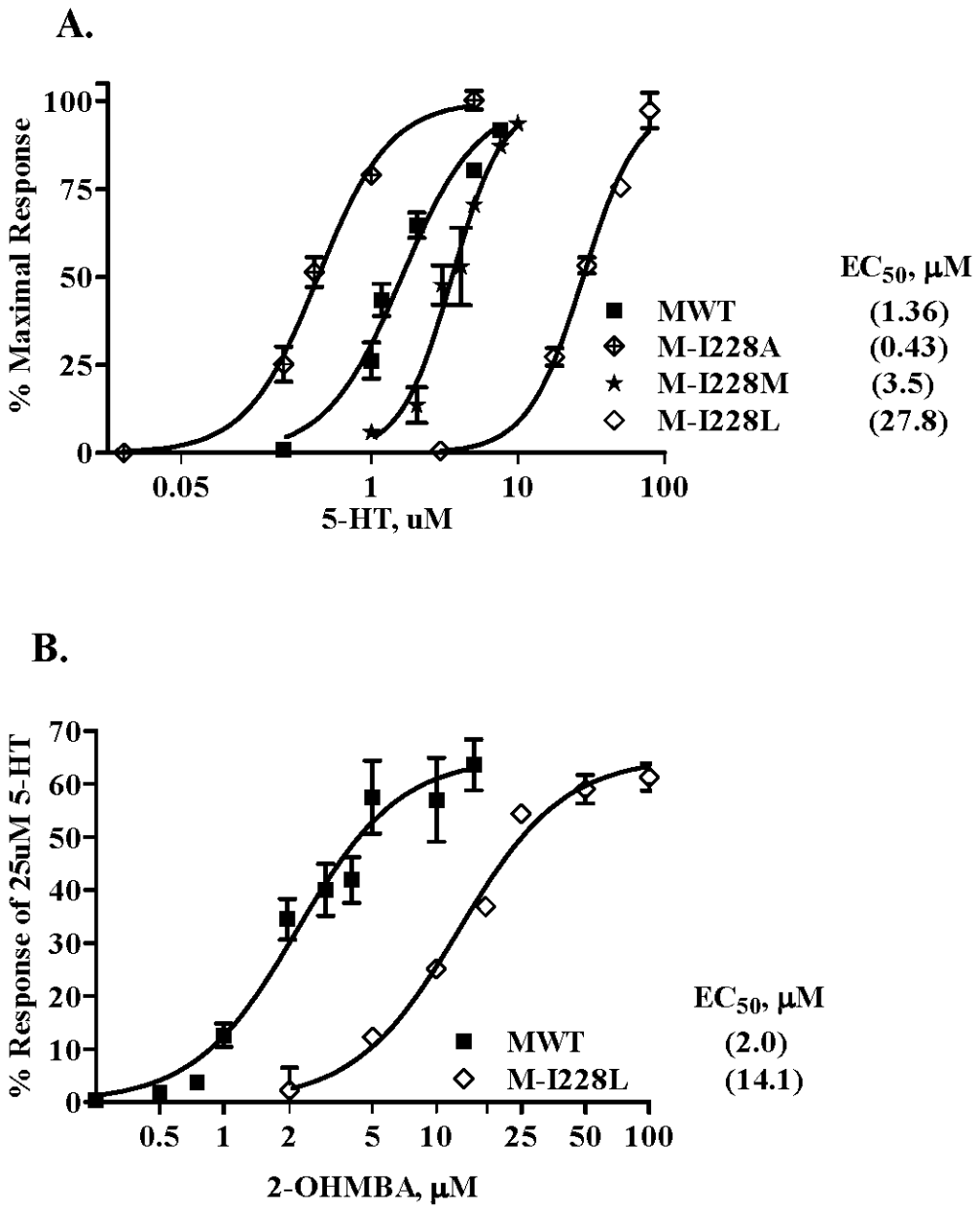
A.
% Maximal Response
100
75
50
25
0
0.05
1
10
100
5-HT, uM
EC50, µM
MWT (1.36)
M-I228A (0.43)
M-I228M (3.5)
M-I228L (27.8)
B.
% Response of 25uM 5-HT
70
60
50
40
30
20
10
0
0.5
1
2
5
10
25
50
100
2-OHMBA, µM
EC50, µM
MWT (2.0)
M-I228L (14.1)

C.

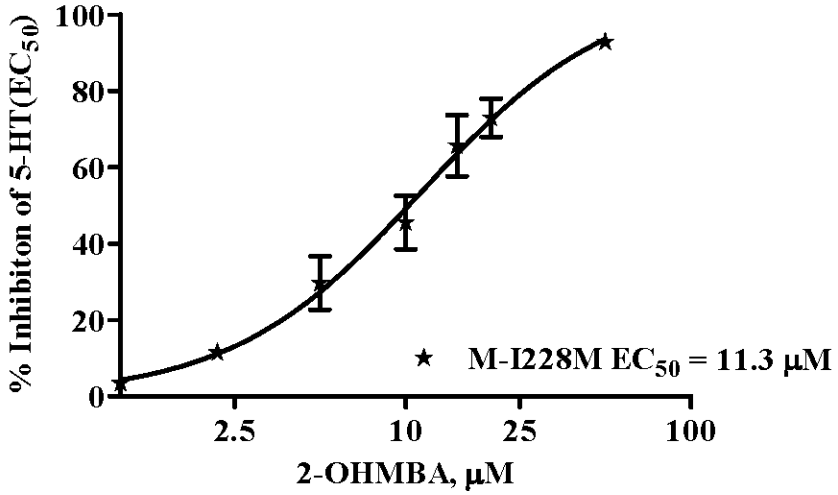
% Inhibiton of 5-HT(EC50)
100
80
60
40
20
0
2.5
10
25
100
2-OHMBA, µM
M-I228M EC50 = 11.3 µM

D.

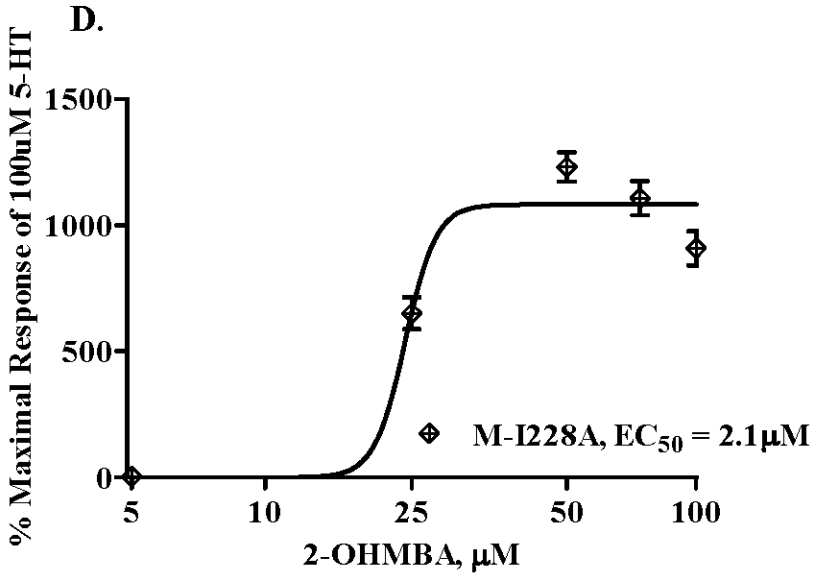
% Maximal Response of 100uM 5-HT
1500
1000
500
0
5
10
25
50
100
2-OHMBA, µM
M-I228A, EC50 = 2.1µM

Figure 5. Double Mutant Thermodynamic Cycle Analysis using K_i values obtained from radioligand binding assays where 2-OHMBA or DMXBA displaced [^{3}H]-BRL-43694. Analysis of interaction between residues in the mouse 5-HT_{3A}R with the 2' functional group of BA analogs. B: Analysis of interaction between residues of the mouse 5-HT_{3A}R with the 2' functional group of BA analogs. (A) residue 207, (B) residue 228, (C and D) residue 229.

Figure 5

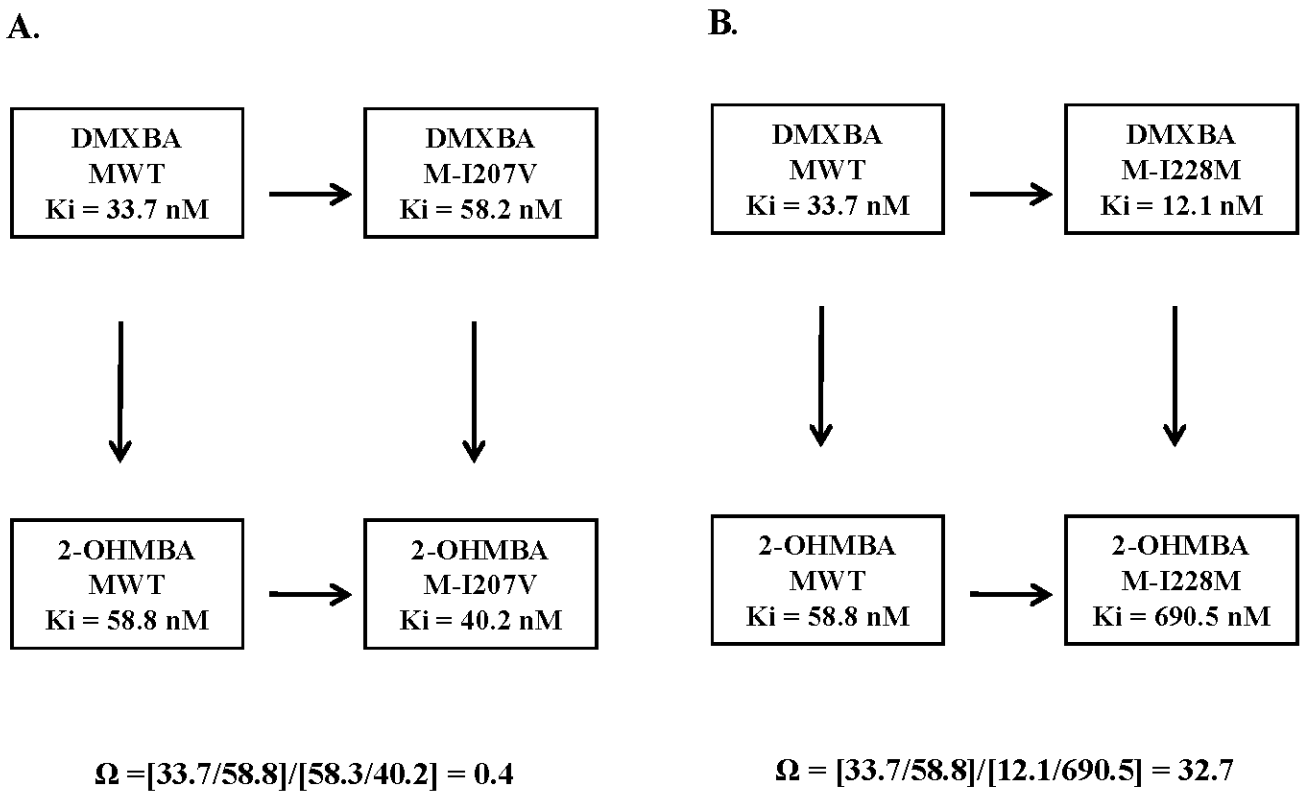
A.
DMXBA MWT Ki = 33.7 nM
DMXBA M-I207V Ki = 58.2 nM
2-OHMBA MWT Ki = 58.8 nM
2-OHMBA M-I207V Ki = 40.2 nM
Ω =[33.7/58.8]/[58.3/40.2] = 0.4
B.
DMXBA MWT Ki = 33.7 nM
DMXBA M-I228M Ki = 12.1 nM
2-OHMBA MWT Ki = 58.8 nM
2-OHMBA M-I228M Ki = 690.5 nM
Ω = [33.7/58.8]/[12.1/690.5] = 32.7
C.
DMXBA MWT Ki = 33.7 nM
DMXBA M-D229E Ki = 83.1 nM
2-OHMBA MWT Ki = 58.8 nM
2-OHMBA M-D229E Ki = 255.7 nM
Ω = [33.7/58.8]/[83.1/255.7] = 1.8
D.
DMXBA MWT Ki = 33.7 nM
DMXBA M-D229A Ki = 578.8 nM
2-OHMBA MWT Ki = 58.8 nM
2-OHMBA M-D229A Ki = 51.7 nM
Ω = [33.7/58.8]/[578.8/51.7] = 0.05

REFERENCES

Belelli, D., Balcarek, J. M., Hope, A. G., Peters, J. A., Lambert, J. J., and Blackburn, T. P. (1985) Cloning and functional expression of a human 5-Hydroxytryptamine type 3A receptor subunit. *Mol. Pharmacol.* **48:** 1054-1062.

Daveu, C., Bureau, R., Baglin, I., Prunier, H., Lancelot, J. C., and Rault, S. (1999) Definition of a Pharmacophore for Partial Agonists of Serotonin 5-HT Receptors. *J. Chem. Inf. Comput. Sci.* **39:** 362-369.

Davies, P. A., Wang, W., Hales, T. G., and Kirkness, E. F. (2003) A Novel Class of Ligand-gated Ion Channel Is Activated by Zn^{2+}. *J. Biol. Chem.* **278:** 712-171.

de Fiebre, C. M., Meyer, E. M., Henry, J. C., Muraskin, S. I., Kem, W. R., and Papke, R. L. (1995) Characterization of a series of anabaseine-derived compounds reveals that the 3-(4)-dimethulaminocinnamylidine derivative is a selective agonist at neuronal nicotinic alpha 7/125I-alpha-bungatotoxin receptor subtypes. *Mol. Pharmacol.* **47:** 164-171.

Ferrara, P., Gohlke, H., Price, D. J., Klebe, G., and Brooks, C. L. III (2004) Assessing scoring functions for protein-ligand interactions. *J. Med. Chem.* **47:** 3032-3047.

Gasteiger, J., and Marsili, M. (1980) Iterative partial equalization of orbital electronegativity- A rapid access to atomic charges. *Tetrahedron.* **36:** 3219-3228.

Grenningloh, G., Gundelfinger, E., Schmitt, B., Betz, H., Darlison, M. G., Barnard, E. A., Schofield, P. R., and Seeburg, P. H. (1987) Glycine vs GABA receptors. *Nature* **330:** 25-26.

Hansen, S., Sulzenbacher, G., Huxford, T., Marchot, P., Taylor, P., and Bourne, Y. (2005) Structures of *Aplysia* AChBP complexes with nicotinic agonists and antagonists reveal distinctive binding interfaces and conformations. *EMBO. J.* **24:** 3635-3646.

Holbrook, J. D., Gill, C. H., Zebda, N., Spences, J. P., Leyland, R., Rance, K. H., Trinh, H., Balmer, G., Kelly, F. M., Yusaf, S. P., Coutenay, N., Luck, J., Rhodes, A., Modha, S., Moore, S. E., Sanger, G. J., and Gunthorpe, M. J. (2009) Characterisation of 5-HT_{3C}, 5-HT_{3D} and 5-HT_{3E} receptor subunits: evolution, distribution and function. *J. Neurochem.* **108:** 384-396.

Kem, W. R., Mahnir, V. M., Papke, R. L., and Lingle, C. J. (1997) Anabaseine is a potent agonist upon muscle and neuronal α-bungarotoxin sensitive nicotinic receptors. *J. Pharmacol. Exp. Ther.* **283:** 979-992.

Kem, W. R., Mahnir, V. M., Prokai, L., Papke, R. L., Cao, X., LeFrancois, S., Wildeboer, K., Prokai-Tatrai, K., Porter-Papke, J., and Soti, F. (2004) Hydroxy Metabolites of the Alzheimer's Drug Candidate 3-[(2,4-Dimethoxy)Benzylidene]-Anabaseine Dihydrochloride (GTS21): Their Molecular Properties, Interactions with Brain Nicotinic Receptors, and Brain Penetration. *Mol. Pharmacol.* **65:** 56-67.

Lowry, O. H., Rosebrough, N. J., Farr, A. L., and Randall, R. J. (1951) Protein measurement with the folin phenol reagent. *J. Biol. Chem.* **193:** 265-275.

Machu, T. K., Hamilton, M. E., Frye, T. F., Shanklin, C. L., Harris, M. C., Hongwei, S., Tenner Jr., T. E., Soti, F. S., and Kem, W. R. (2001) Bensylidene Analogs of

Anabaseine Display Partial Agonist and Antagonist Properties at the Mouse 5-Hydroxytryptamine3A Receptor. *J. Pharmacol. Exp. Ther.* **299:** 1112-1119.

Machu, T. K., Zhang, R., Hayrapetyan, Y., Hayrapetyan, V., White, M. M., and Kem, W. R. (2009) Amino Acids in Loops C and F of the Mouse 5-Hydroxytryptamine$_{3A}$ Receptor Confer Partial Agonist Activity to 3-(2-hydroxy, 4-methoxybenzylidene)-anabaseine. (To be submitted).

Malany, S., Osaka, H., Sine, S. M., and Taylor, P. (2000) Orientation of α-Neurotoxin at the Subunit Interfaces of the Nicotinic Acetylcholine Receptors. *Biochem.* **39:** 15388-15398.

Maricq, A. V., Peterson, A. S., Brake, A. J., Myers, R. M., and Julius, D. (1991) Primary structure of functional expression of the 5-HT$_3$ receptor, a serotonin-gated ion channel. *Science* **254:** 432-437.

Morris, G., Goodsell, D., Huey, R., Hart, W., Belew, R., and Olson, A. (1998) Automated docking using Lamarckian genetic algorithm and an empirical free energy binding free energy function. *J. Comput. Chem.* **19:** 1639-1662.

Niesler, B., Walstab, J., Combrink, S., Moller, D., Kapeller, J., Rietdorf, J., Bonisch, H., Gothert, N., Rappold,, G., and Bruss, M. (2007) Characterization of the Novel Human Serotonin Subunits 5-HT$_{3C}$, 5-HT$_{3D}$, and 5-HT$_{3E}$. *Mol. Pharmacol.* **72:** 8-17.

Papke, R. L., McCormack, T. J., Jack, B. A., Wang, D., Bugaj-Gaweda, C., Schiff, H. C., Buhr, J. D., Waber A. J., and Stokes, C. (2005) Rhesus monkey α7 nicotinic

acetylcholine receptors: comparisons to human α7 receptors expressed in *Xenopus* oocytes. *Eur. J. Pharmacol.* **524:** 11-18.

Pedersen, S. E., and Papineni, R. V. L. (1995) Interaction of *d*-Tubocurarine Analogs with the Topedo Nicotinic Acetylcholine Receptor. *J. Biol. Chem.* **270:** 31141-31150.

Pettersen, E., Goddard, T., Huang, C., Couch, G., Greenblatt D, Meng E and Ferrin T (2004) UCSF Chimera: A visualization system for exploratory research and analysis. *J. Comput. Chem.* **25:** 1605-1612.

Ronde, P., and Nichols RA (1998) High Calcium Permeability of Serotonin 5-HT_3 Receptors on Presynaptic Nerve Terminals from Rat Striatum. *J. Neurochem.* **70:** 1094-1103

Ropert, N., and Guy, N. (1991) Serotonin Facilitates GABAergic transmission in the CA1 region of the rat hippocampus in vitro. *J. Physiol.* **441:** 121-136.

Sali, A., and Blundell, T. (1993) Comparative protein modeling by satisfaction of spatial restraints. *J. Mol. Biol.* **234:** 779-815.

Schofield, P. R., Darlison, M. G., Fujita, N., Burt, D. R., Stephenson, F. A., Rodriguez, H., Rhee, L., Ramachandran, J., Reale, A., Glencorse, T., Seeburg, P. H., and Barnard, E. A. (1987) Sequence and functional expression of the $GABA_A$ receptor shows a ligand-gated receptor super-family. *Nature* **328:** 221-227.

Stokes, C., Papke, J. K. P., Horenstein, N. A., Kem, W. R., McCormack, R. J., and Papke, R. L. (2004) the structural basis for GTS-21 selectivity between human and rat nicotinic α7 receptors. *Mol. Pharmacol.* **66:** 14-24.

Suryanarayanan, A., Joshi, P. R., Bikdi, Z., Mani, M., Kulkarni, T. R., Gaines, C., and Schulte, M. K. (2005) The Loop C Region of the Murine 5-HT Receptor Contributes to the Differential Actions of 5-Hydroxytryptamine and *m*-Chlorophenylbiguanide. *Biochem.* **44:** 9140-9149.

Thompson, A. J., Price, K. L., Reeves, D. C., Chan, S. L., Chau, P.-L., and Lummis, S. C. R. (2005) Locating an Antagonist in the 5-HT_3 Receptor Binding Site Using Modeling and Radioligand Binding. *J. Biol. Chem.* **280:** 20476-20482.

Thompson, A. J., and Lummis, S. C. (2006) 5-HT_3 Receptors. *Curr. Pharm. Des.* **12:** 3615-3630.

Willcoxson, I., Hong, A., Whisenant, R., Edwards, J., Wang, H., Sarkar, H., and Pedersen, S. (2002) Orientation of *d*-tubocurarine in the muscle nicotinic acetykcholine receptor-binding site. *J. Biol. Chem.* **277:** 42249-42258.

Yan, D., and White, M. M. (2005) Spatial orientation of the antagonist granisetron in the ligand binding site of the 5-HT_3 receptor. *Mol. Pharmacol.* **68:** 365-371.

Yan, D., Meyer, J. K., White, M. M. (2006) Mapping Residues in the Ligand-Binding Domain of the 5-HT_3 Receptor onto *d*-Tubocurarine Structure. *Mol. Pharmacol.* **70:** 571-578.

Zhang, R., White, N. A., Soti, F. S., Kem, W. R., and Machu, T. K. (2006) N-Terminal Domains in Mouse and Human 5-Hydrosytryptamine$_{3A}$ Receptor Confer Partial Agonist and Antagonist Properties to Benzylidene Analogs of Anabaseine. *J. Pharmacol. Exp. Ther.* **317:** 1276-1284.

Zhang, R., Wen, X., Militante, J., Hester, B., Rhubottom, H. E., Sun, H., Leideheimer, N. J., Yan, D., White, M. M., and Machu, T. K. (2007) The Role of Loop F Residues in Determining Differential *d*-Tubocurarine Potencies in Mouse and Human 5-Hydroxytryptamine 3A Receptors. *Biochem.* **46:** 1194-1204.

Footnotes:

This manuscript is taken from a dissertation submitted to the University of North Texas Health Science Center in partial fulfillment of the requirements for the Doctor of Philosophy degree. This study was supported by National Institute of Neurological Disorders and Stroke grant NS043438.

CHAPTER IV

FINAL CONCLUSIONS

Agonist binding at the 5-Hydroxytryptamine$_3$ (5-HT$_3$) receptor induces opening of a cationic channel permeable to Na^+, K^+ and Ca^{2+} (Yang, 1990; Rondé and Nichols, 1998; Panicker et al., 2002). However, the specific molecular rearrangements associated with gating mechanisms are largely unknown. Investigation of the architecture and intramolecular interactions of the 5-HT$_3$ receptor is vital to developing a better understanding of coupling of ligand binding to channel gating.

The bulk of the present work was done to identify key amino acids in Loops C and F of the ligand binding domain that account for differential that account for differential pharmacology of curare and 2-OHMBA in mouse and human receptors, as well as to define points of interaction between 2-OHMBA and the 5-HT$_{3A}$ receptor. Studies were conducted using chimeric and point-mutant receptors, and results demonstrated the importance of Loops C and F in the N-terminus in pharmacological function of curare and analogs of benzylidene-anabaseine (de Oliveira-Pierce, unpublished; Zhang et al., 2006; Machu et al., 2009). The study also identified specific residues responsible for interspecies differences in binding and function. In all experiments described in this dissertation in which whole N-terminal switches between mouse and human receptors were done, altered function of 2-OHMBA and curare was

observed. The end result was the creation mouse chimeric receptors with human like sensitivities and vice-versa. These results are in agreement with other studies that reported residues in the N-terminus are directly related to ligand recognition at the binding site (Karlin and Akabas, 1998; Brejc et al., 2001).

One important finding of these studies was that amino acid residues identified in chapters 2 and 3 overlap, e.g., mouse 207 (Loop F), 228and 229 (Loop C), (human orthologs 202, 224 and 225). Furthermore, in a previous study, a potential domain within Loop C was identified as responsible for interspecies differences in *m*-CPBG for human and rat 5-HT_3 receptors (Mochizuki et al., 1999). These results suggest some degree of commonality in the overall conformational changes and molecular interactions associated with binding and function of the ligands studied.

Residues 207 and 209 in Loop F of the mouse receptor were identified as critical for partial agonist function of 2-OHMBA. Results suggest these residues do not directly interact with the 2'-OH moiety of 2-OHMBA, however, as with curare, they appear to be partially responsible for interspecies pharmacological differences. This is likely occurring due to downstream conformational changes triggered by ligand binding.

Another important finding of this study was the identification of residue 228 in Loop C of the mouse receptor as the residue likely interacting with the 2'-OH group of 2-OHMBA. Furthermore, the only amino acids in position 228 that resulted in maintenance of partial agonist activity of 2-OHMBA as well as full agonist activity of 5-HT were Leu or Ile, suggesting physicochemical properties in the side chain of these isomers promote

conformational changes that enable formation of a hydrogen bond between ligand and receptor.

In summary, the data collected for both studies has further enabled the development of a better molecular model for ligand binding at the 5-HT_{3A} binding domain. Residues implicated in this model are shared with residues involved in binding of other 5-HT_3 ligands (Yan and White, 2005; Yan et al., 2006), supporting the idea of overall commonality in molecular interactions between the receptor and different ligands. Findings of this body of work will likely improve our understanding of the underlying molecular interactions of a number of potentially therapeutic compounds targeting the 5-HT_{3A} receptor. One specific example of where this knowledge would be helpful is the use of Tropisetron (ICS 205-930) for the treatment of pain disorders. Serotonin plays a role in nociceptive input regulation. Platelets, mast cells and serotonergenic nerve endings (located in the amygdala, hippocampus and other brain regions) (van Hooft et al., 2000) release 5-HT activating primary afferent fibers. The end result of this process being the sensation of pain. While tropisetron has proven effective in blocking this process, it also interferes with GABAA function (Eglen et al., 1996; Thompson et al., 2007). A better understanding of the underlying mechanisms of the 5-HT_3 receptor would allow us to develop more specific antagonists and potentially eliminate some of the unwanted side-effects associated with this drug.

REFERENCES

Brejc, K., van Dijk, W.J., Klaassen, R.V., Schuurmans, M., van Der Oost, J., Smit, A.B., and Sixma, T.K. (2001) Crystal structure of an ACh-binding protein reveals the ligand-binding domain of nicotinic receptors. *Nature* **411:** 252-255.

Eglen, R. M., and Bonhaus, D. W. (1996). 5-Hydroxytryptamine $(5\text{-HT})_3$ receptors: molecular biology, pharmacology and therapeutic importance. *Curr. Pharm. Des.* **2**, 367-374.

Karlin, A., and Akabas, M.H. (1998) Substituted-cysteine accessibility method. *Methods Enzymol.* **293:** 123-145.

Mochizuki, S., Miyake, A., and Furuichi, K. (1999) Identification of a domain affecting agonist potency of *meta*-chlorophenylbiguanide in 5-HT_3 receptors. *Eur. J. Pharmacol.* **369:** 125-132.

Panicker, S., Cruz, H., Arrabit, C., and Slesinger, P.A. (2002) Evidence for a Centrally Located Gate in the Pore of a Serotonin-Gated Ion Channel. *J. Neurosci.* **22:** 1629-1639.

Rondé, P, and Nichols R. A. (1998) High Calcium Permeability of Serotonin 5-HT_3 Receptors on Presynaptic Nerve Terminals from Rat Striatum. *J. Neurochem.* **70:** 1094-1103.

Thompson AJ, Lummis SCR. (2007). The 5-HT_3 receptor as a therapeutic target. *Expert Opin. Ther. Targets* **11**, 527-540.

Van Hooft, J. A., and Viverberg, H. P. M. (2000). 5-HT_3 receptors and neurotransmitter release in the CNS: a nerve ending story? *Trends Neurosci.* **23**, 605-610.

Yan, D., and White, M. M. (2005) Spatial orientation of the antagonist granisetron in the ligand binding site of the 5-HT_3 receptor. *Mol. Pharmacol.* **68:** 365-371.

Yan, D., Meyer, J. K., White, M. M. (2006) Mapping Residues in the Ligand-Binding Domain of the 5-HT_3 Receptor onto *d*-Tubocurarine Structure. *Mol. Pharmacol.* **70:** 571-578.

Yang, J. (1990) Ion permeation through 5-hydroxytryptamine-gated channels in neuroblastoma N18 cells. *J. Gen. Physiol.* **96:** 1177-1198.

Zhang, R., White, N. A., Soti, F. S., Kem, W. R., and Machu, T. K. (2006) N-Terminal Domains in Mouse and Human 5-Hydrosytryptamine$_{3A}$ Receptor Confer Partial Agonist and Antagonist Properties to Benzylidene Analogs of Anabaseine. *J. Pharmacol. Exp. Ther.* **317:** 1276-1284.

APPENDIX

Colchicine: A Novel Positive Allosteric Modulator of the Human 5-Hydroxytryptamine$_{3A}$ Receptor

de Oliveira-Pierce AN, Zhang R and Machu TK

Department of Pharmacology and Neuroscience, University of North Texas Health Sciences Center

Fort Worth, TX (ANOP, RZ, TKM)

Department of Pharmacology and Neuroscience, Texas Tech University,

Lubbock, TX (RZ, TKM)

Running Title: Colchicine Actions in Human and Mouse 5-HT$_{3A}$Rs

Corresponding Author:

Andreia Naomi de Oliveira-Pierce

Department of Pharmacology and Neuroscience

University of North Texas Health Sciences Center

3500 Camp Bowie Blvd., Fort Worth, TX 76107

TEL: 817-735-2190 FAX: 817-735-0408

e-mail: aoliveir@hsc.unt.edu

Text Pages: 20

Tables: 3

Figures: 7

References: 39

Number of words in abstract: 218

Number of words in introduction: 666

Number of words in discussion: 1475

Abbreviations:

5-hydroxytryptamine (5-HT); 5-hydroxytryptamine$_{3A}$ receptor (5-HT$_{3A}$); modified Barth's solution (MBS); vesicle dialysis buffer (VDB); nicotinic acetylcholine receptor (AchR); ligand-gated ion channels (LGICs); ligand binding domain (LBD); gamma-aminobutyric acid (GABA).

Recommended section assignment: Neuropharmacology

ABSTRACT

The actions of colchicine were examined with the two-electrode voltage clamp technique and radioligand binding assays in mouse and human 5-HT_{3A}Rs expressed in *Xenopus* oocytes. Colchicine inhibited 5-HT evoked currents in oocytes expressing mouse 5-HT_{3A}Rs, with an IC_{50} of 59.5 $\pm$ 3 μM. In contrast to the mouse receptor, co-application of colchicine with 5-HT (< 1 μM) strongly enhanced 5-HT-evoked currents in oocytes expressing human 5-HT_{3A}Rs. Colchicine applied alone did not induce detectable current. In the presence of 0.5 μM 5-HT, the potentiation was concentration dependent and reached the maximum (~ 100%) when 750 μM colchicine was applied. However, colchicine-dependent inhibition can be observed at 5-HT concentrations > 1 μM. In oocyte membranes expressing mouse or human receptors, binding studies with colchicine (25 nM – 1 mM) revealed no displacement of [3H]- BRL-43694, suggesting that actions of colchicine do not occur at the ligand binding domain. Functional effects of colchicine on both receptors occurred in the absence of preincubation and after cold temperature incubation, suggesting that the microtubule depolymerizing effects of colchicine play no role in modulation of receptor function. Studies with interspecies chimeric receptors demonstrated that the distal one-third of the N-terminus is responsible for the bi-directional modulation by colchicine. Collectively, these results suggest that colchicine modulates receptor function through Loops C and/or F through a gating mechanism.

INTRODUCTION

The 5-Hydroxytryptamine$_3$ receptor (5-HT$_3$R) belongs to the superfamily of ligand-gated ion channels (LGICs) (Maricq et al., 1991) and shares a number of structural, and functional homologies with other members, such as the nicotinic acetylcholine receptor (nAChR), γ-aminobutyric acid$_A$ receptor (GABA$_A$R) and glycine receptor (GlyR) (Grenningloh et al., 1987; Schofield et al., 1987). To date, five 5-HT$_3$ receptor subunits have been cloned (A-E) (Maricq et al., 1991; Belelli et al., 1995; Niesler et al., 2007). Receptors composed of A-homomers and A/B-heteromers have been shown to have functional significance in the central and peripheral nervous systems, (see review by Thompson and Lummis, 2006) and a recent study reported expression of functional A/C-, A/D- and A/E- heteromers (Niesler et al., 2007). The ligand binding domain (LBD) is located in the N-terminus at the interface between subunits and consists of six loops: A- F. Loops A-C form the principal component of the LBD, and Loops D-F form the complementary component of the LBD (reviewed by Thompson and Lummis, 2006). Homology models using the AChBP and biochemical studies have identified important residues for ligand-binding on both the primary (Loops A-C) and the complementary (Loops D-F) interfaces of the binding site (Schreiter et al., 2003; Thompson et al., 2005).

The homomeric 5-HT$_{3A}$R is a good model system for exploring the ligand recognition sites of LGICs. Significant homology exists between the 5-HT$_{3A}$Rs among the six cloned species (80% to 95%). Interestingly, these small differences in amino acid composition are responsible for striking interspecies variation of responses to numerous drugs which act at the 5-HT recognition site, including curare (Miyake et al., 1995; Zhang et

al., 2007), 2-methyl 5-HT (Maricq et al., 1991; Belelli et al., 1995), 1-phenylbiguanide (PBG) (Maricq et al., 1991), and benzylidene analogs of anabaseine (Zhang et al., 2006). Loops C and F have been implicated in interspecies differential potency of curare and *m*-clorophenylbiguanidine (Mochizuki et al., 1999; Hope et al., 1999; Zhang et al., 2007), and agonist function of 2-OHMBA (Zhang et al., 2006). The differential sensitivity of these drugs among interspecies 5-HT_{3A}Rs can be used to localize ligand binding domain(s) or gating residues through the use of interspecies chimeras and point mutations.

An important feature of all LGICs is the allosteric regulation of receptor function by various compounds. For example, PNU-120596 potentiates (Bertrand et al., 2008), while steroids either potentiate or inhibit the function of neuronal nAChRs (Paradiso et al., 2001). More allosteric modulators have been found for $GABA_A$Rs than for any other LGIC. Such ligands include barbiturates, picrotoxin, progesterone metabolites, as well as benzodiazepines (BZDs) and non BZDs, which act at the BZD recognition site (review by Sigel and Buhr, 1997 and Da Settimo et al., 2007). Tropeines allosterically modulate the activity of GlyRs (Maksay et al., 2008).

The 5-HT_{3A}R is allosterically modulated by numerous drugs. Most of these drugs fall in the class of alcohols and anesthetics, and therefore, are not selective for the 5-HT_{3A}R. Examples of drugs that potentiate 5-HT_{3A}R-mediated currents include trichloroethanol (Lovinger et al., 2000), and volatile anesthetics (Machu and Harris, 1994). However, to date, 5-hydroxyindole and its analogues (van Hooft, et al., 1997) are the only reported selective allosteric modulators of 5-HT_{3A}R function, albeit with weak potentiating actions effective only in the millimolar concentration range.

Colchicine is a microtubule depolymerizing agent that competitively antagonizes $GABA_A$Rs (Bueno and Leidenheimer, 1998) and GlyRs (Machu, 1998). In the present study, we determined the actions of colchicine on 5-HT_{3A}Rs. We found that colchicine inhibits the mouse 5-HT_{3A}R with a similar potency to that observed in the $GABA_A$R and α2 GlyR (Bueno and Leidenheimer, 1998; Machu, 1998). Radioligand binding assays show colchicine does not displace [^{3}H]-BRL-43694, a competitive antagonist that binds at the 5-HT_{3A}R agonist recognition domain. More importantly, we found that colchicine potentiates the function of the human 5-HT_{3A}R at low 5-HT concentrations and antagonizes the receptor at higher 5-HT concentrations. By constructing interspecies chimeras, we identified 63 amino acid fragments within the distal one-third of the N-termini of the receptors that confer colchicine's potentiating actions.

METHODS

Isolation of *Xenopus laevis* oocytes

X. laevis frogs were kept in tanks of dechlorinated tap water on a 12-hr light/dark cycle at 19 °C and fed a diet of dehydrated liver in *Xenopus* I chow three times per week. Frogs were anesthetized by immersion in cold 0.12% 3-aminobenzoic acid ethyl ester for 20 minutes. After removal through a small surgical incision in the frog's abdomen, ovarian lobes were placed in modified Barth's Solution (MBS) containing (in mM) NaCl 88, KCl 1, $NaHCO_3$ 2.4, HEPES 10, $MgSO_4$ 0.82, $Ca(NO_3)_2$ 0.33, and $CaCl_2$ 0.91 (pH 7.5).

Ovarian lobes were manually dissected into clumps of four to ten oocytes and were then subjected to chemical separation and defolliculation. Clumps of oocytes were placed in medium containing 2 mg/ml collagenase Type 2 and (in mM) NaCl 83, KCl 2, $MgCl_2$ 1, and HEPES 10 (pH 7.5) and gently rocked for two hours. Oocytes were then removed to fresh collagenase medium and rocked gently for an additional two hours. Lastly, oocytes were rinsed with MBS and stored in incubation media composed of ND96, containing (in mM) NaCl 96, KCl 2, $CaCl_2$ 1.8, $MgCl_2$ 1, and HEPES 5 (pH 7.5), plus 10 mg/l streptomycin, 50 mg/l gentamicin, 10,000 units/l penicillin, 96 mg/l sulfamethoxazole, 19 mg/l trimethoprim, 0.5 mM theophylline, and 2 mM sodium pyruvate.

Construction of Chimeric Receptors:

Mouse and human 5-HT_{3A}R cDNAs, provided by Drs. D. Julius and A. Miyake, respectively, were subcloned into pCR-Script™ Amp SK(+)$^-$ (Stratagene, La Jolla, CA). Three unique restriction enzyme cleavage sites, Nru I, Spe I, and Nar I, were introduced in both mouse and human 5-HT_{3A}R cDNAs by site-directed mutagenesis (U.S.E. mutagenesis

kit, Pharmacia Biotech Inc., Piscataway, N.J.) of the nucleotides encoding the conserved residues: Thr 181 and Arg 244 in the mouse receptor cDNA and Thr 176 and Arg 239 in the human receptor cDNA, respectively. Numbering of the amino acids in the two receptors began with the initiating methionine. Primers were used to introduce Spe I and Nar I, and selection pressure for the mutagenesis was performed as previously described in Zhang et al., (2006). Chimeric cDNAs were confirmed by dideoxynucleotide sequencing at the Biotechnology Core Facility at Texas Tech University, Lubbock, TX.

Transcription of cDNA to cRNA.

The wild-type and chimeric cDNAs were linearized with BamH I , extracted with phenol-chloroform, precipitated with sodium acetate and ethanol, and resuspended in diethyl pyrocarbonate (DEPC) treated water. The cDNAs were then transcribed with T3 mMESSAGE mMACHINE (Ambion, Austin, TX).

Microinjection of oocytes with 5-HT_3 receptor cRNAs

An aliquot of cRNA was centrifuged at 15,000 x g and the ethanol removed with a tuberculin syringe. After air-drying, the pellet was resuspended in a volume of DEPC water to yield a concentration of 5-30 ng of cRNA/50 nl. The cRNA was drawn up into a micropipette (10-20 μm tip size). Fifty nl of cRNA were injected into the animal/vegetal pole equator of each oocyte. Oocytes were stored in incubation medium in Corning cell well plates (Corning Glass Works, Corning, N.Y.) at room temperature. Incubation medium was changed daily. Oocytes were recorded from day two through day seven following injection.

Electrophysiological recordings

Oocytes were perfused in a 100 μl volume chamber with MBS via a roller pump (Cole-Parmer Instrument, Co., Chicago, IL). Oocytes were impaled with two glass electrodes (1.2 mm outside diameter and 1-10 megaohm resistance) filled with 3 M KCl. Oocytes were voltage clamped to -70 mV with a Warner Instruments Model OC-725C oocyte clamp (Hamden, CT). Clamping currents were plotted on a strip chart recorder (Cole Parmer Instrument, Co., Chicago, IL). Serotonin, in the absence or presence of colchicine, was dissolved in MBS and applied to the oocytes for 30 s. For the cold temperature experiments, oocytes were incubated at least two hours prior to recording and were continuously perfused with ice-cold MBS during recording.

Membrane Purification

Oocytes were injected with 100 ng HWT or MWT cRNA and tested for expression using two-voltage clamp electrophysiology on day three. Oocytes were homogenized with a hand-held glass potter (~50 *Xenopus laevis* oocytes) in ice-cold vesicle dialysis buffer VDB containing (in mM) NaCl 96, MOPS 10, EDTA 0.1, and 0.02% NaN3 (pH 7.5), 0.1 ml per oocyte + 10 ul of protease inhibitor cocktail set III (Calbiochem, La Jolla, CA). The homogenate was centrifuged for 10 min at 800 g. The supernatant was collected, the pellet was resuspended in VDB (0.1 ml/oocyte) and recentrifuged at 800 g for 10 min. Supernatants were then combined and centrifuged for 1 hour at 38,800 g. The membrane pellet was resuspended in VDB (2-8 ml depending on expression) and divided into several batches for storage at -80 °C. Protein content was measured with the Lowry assay (Lowry et al., 1951).

Radioligand Binding Assays

For Kd determinations, membrane homogenate was incubated at 37 °C for 2 hours with [3H]-BRL-43694 (0.1 nM – 23 μM). Specific binding was calculated as X*Bmax /(Kd+X), where X = radioligand concentration, Bmax = maximum specific binding/mg protein, and Kd = dissociation constant (-1/slope). For Ki determinations, aliquots of membrane were incubated at 37 °C for 2 hours with colchicine (25 nM – 1 mM) and [3H]-BRL-43694 at the Kd of MWT (3.5 nM) and HWT (2.6 nM) respectively. Non-specific binding was measured with MDL-7222 (3-tropanyl-3, 5-dichlorobenzoate), a 5-HT_{3A} receptor competitive antagonist.

Data Analysis

Graphpad Prism (San Diego, CA) was used to calculate Kd, Ki, Bmax, EC_{50} and IC_{50} values, and Hill coefficients. Graphpad Instat was used to perform t-tests, one-way analysis of variance (ANOVA), Student's t-test and post-hoc tests.

RESULTS

Colchicine Inhibits 5-HT-Evoked Currents in *Xenopus* Oocytes Expressing Mouse 5-HT$_{3A}$ Rs. Figure 1A illustrates typical responses of the mouse 5-HT$_{3A}$R to colchicine. In the absence of preincubation, colchicine clearly inhibited 5-HT-mediated responses in oocytes expressing the mouse 5-HT$_{3A}$R. Colchicine quickly washed out, as a baseline response was obtained with the next application of 5-HT alone. A colchicine concentration response curve was generated in oocytes expressing the mouse 5-HT$_{3A}$R (Fig. 1B). When co-applied with 0.5 μM 5-HT, which generates 10% of the maximum current (EC_{10}), colchicine inhibited 5-HT-mediated currents in a concentration dependent manner at concentrations ranging from 3 to 300 μM. The colchicine concentration that reduced 5-HT mediated currents by 50% (IC_{50}) was 59.5 ± 3 μM. To examine whether microtubule depolymerization was involved in the colchicine inhibitory action at the mouse 5-HT$_{3A}$R, the temperature sensitivity of the colchicine effect was measured (Table 1). For at least 2 h prior to recording, oocytes were incubated in ice-cold MBS, which completely depolymerizes oocyte microtubules (Gard, 1991). Colchicine at 50 and 200 μM inhibited 5-HT mediated currents by 43% and 82% in oocytes incubated at 4°C for 2 h (Table 1), which is virtually identical to that observed in oocytes maintained at room temperature (43% and 80%, respectively).

Antagonism by Colchicine at Mouse 5-HT$_{3A}$Rs. In order to determine the mechanism(s) through which colchicine inhibits mouse 5-HT$_{3A}$Rs, we performed additional electrophysiological experiments, as well as radioligand binding experiments. In the first set of experiments, we recorded 5-HT (0.25 - 500 μM) concentration response curves in the

presence of increasing concentrations of colchicine, 200, 1000, and 10,000 μM (Fig. 2). In the presence of increasing concentrations of competitive antagonists, 5-HT concentration response curves shift rightward, with increases in 5-HT EC_{50}'s; maximal current amplitudes are achieved in the presence of sufficient concentrations of 5-HT. In contrast, non-competitive antagonists reduce the maximal response to 5-HT, even at very high 5-HT concentrations, and cause no shift in the 5-HT EC_{50}'s. In Fig. 2A, the 5-HT concentration response curves were shifted to the right as concentrations of colchicine increased. However, the inhibitory effect of colchicine (1000 and 10,000 μM) was not completely overcome as 5-HT concentrations were increased. Therefore, it is not possible to determine from these experiments the mechanism(s) through which colchicine inhibits receptor function. The EC_{50} of 5-HT was 0.93 ± 0.04 μM in the absence of colchicine. In the presence of colchicine, 200, 1000 and 10,000 μM, the EC_{50}'s for 5-HT were 3.7 ± 0.3, 13.4 ± 2.4, and 81.4 ± 3.3 μM, respectively.

To determine whether colchicine has any competitive action at the ligand binding domain for 5-HT, we performed radioligand binding assays, Fig 2 and Table 2. In Fig. 2B, saturation binding experiments were performed with the 5-HT_3R competitive antagonist, [3H]-BRL-43694; a Kd of 3.53 ± 0.3 nM was obtained. In Fig. 2C, colchicine (25 nM to 1mM) did not displace [3H]-BRL-43694 (3.5 nM). These results suggest that colchicine does not act at the 5-HT recognition site.

Allosteric modulation of ligand-gated ion channels produce shifts in agonist concentration response curves, resulting in altered agonist EC_{50}'s in electrophysiological studies and in binding studies (Sigel and Buhr, 1997). For example, benzodiazepine

agonists such as diazepam produce shifts in the GABA or GABA agonist, muscimol, concentration response curves of the $GABA_A$ receptor to the left, and benzodiazepine inverse agonists produce rightward shifts of the GABA or muscimol concentration response curves. Benzodiazepines produce these changes by altering the affinity of GABA and other GABA agonists at their recognition site. To determine whether colchicine alters the affinity of 5-HT, we measured the displacement of [3H]-BRL-43694 by 5-HT (0.25 nM – 500 μM) in the absence and presence of colchicine (300 and 1000 μM) (Table 2). A similar approach has been used to examine PNU-69176E's allosteric modulation of 5-HT displacement of [3H]-mesulergine at the 5-HT recognition site of the 5-HT2C receptor (Im et al., 2003). We reasoned that if colchicine decreases the affinity of 5-HT at the 5-HT recognition site in the mouse receptor, then the potency of 5-HT in displacing [3H]-BRL-43694 would be reduced. In the absence of colchicine, the 5-HT K_i was 311 $\pm$ 0.5 nM. Colchicine (200 and 1000 μM) significantly increased the K_i values of 5-HT to 406 $\pm$ 0.37 and 1250 $\pm$ 150 nM, respectively (Table 2). These results suggest that colchicine acts at an allosteric site to modulate mouse $5\text{-}HT_{3A}$ receptor function.

Effects of Colchicine on 5-HT-Evoked Currents in *Xenopus* Oocytes Expressing Human $5\text{-}HT_{3A}$Rs. In contrast with the mouse receptor, colchicine (300 μM) enhanced currents evoked by 5-HT (0.5 μM), an ~ EC_5 (Fig. 3A) in the human $5\text{-}HT_{3A}$ receptor. The EC_{50} for 5-HT is 1.39 $\pm$ 0.06 μM. Stimulation occurred in the absence of preincubation. Colchicine quickly washed out, as a baseline response was observed with the next application of 5-HT (0.5 μM). To further explore the potentiating effects of colchicine on

human 5-HT_{3A}R function, a colchicine (10 μM to 1000 μM) concentration response curve was generated in the presence of 0.5 μM 5-HT (Fig. 3B). Colchicine enhanced 5-HT-evoked currents at concentrations as low as 25 μM, and the potentiation reached the maximum when the colchicine concentration was increased to 750 μM (~ 100%). A colchicine EC_{50} of 226.6 ± 25.1 μM was obtained. Colchicine (200 μM or 10 mM) in the absence of 5-HT produced no detectable current in oocytes expressing the human 5-HT_{3A}R (data not shown). Therefore, colchicine enhances human receptor function at a site other than the 5-HT recognition site.

Potentiating Effect of Colchicine at the Human 5-HT_{3A}R is 5-HT-Concentration Dependent and Microtubule Independent. Figure 3C shows the percent change induced by colchicine (300 μM) of 5-HT (0.5- 10 μM) mediated currents. Colchicine enhanced 0.5 μM 5-HT mediated currents, but had no effect on 1 μM 5-HT (~ EC_{20}) evoked currents. At 3 and 10 μM 5-HT, colchicine had inhibitory actions. As a putative positive allosteric modulator, colchicine's enhancement of receptor function would be predicted to decrease as 5-HT concentrations increased. As probability of opening is increased with higher 5-HT gating concentrations, there is less ability of a positive allosteric drug to increase it further. The inhibition of human receptor function at high concentrations of 5-HT is likely due to an additional inhibitory site on the receptor. We predict that this site has a lower affinity for colchicine than the positive allosteric site. At high concentrations of 5-HT, the positive allosteric modulation of colchicine (300 μM) would be masked, leaving the inhibitory effects to predominate.

To further examine the putative stimulatory and inhibitory colchicine sites on the human 5-HT_{3A} receptor, we performed binding assays. In Fig. 4A, saturation binding experiments were done with the 5-HT_3R competitive antagonist, [3H]-BRL-43694; a Kd of 2.58 ± 0.6 nM was obtained. In Fig. 4B, colchicine (25 nM to 1mM) did not displace [3H]-BRL-43694 (2.6 nM). These results also suggest that colchicine does not act at the 5-HT recognition site of the human receptor. We next examined the ability of colchicine to alter the displacement of [3H]-BRL-43694 by 5-HT (Table 2). In the absence of colchicine, the 5-HT K_i was 1530 ± 230 nM. Colchicine (300 μM) significantly decreased the K_i value of 5-HT to 738 ± 0.64 nM. In contrast, colchicine (1000 μM) increased the K_i value of 5-HT to 2940 ± 240 nM. These results suggest that colchicine acts at two possible allosteric sites on the human 5-HT_{3A} receptor.

To test whether colchicine potentiates the function of the human receptor through a microtubule dependent mechanism, oocytes were incubated in ice-cold MBS for at least 2 h prior to recording (Table 1). Colchicine (300 μM) enhanced 0.5 μM 5-HT-mediated currents by 90.3 ± 4.3%, which is not significantly different than that (79.3 ± 8.7%) recorded in oocytes at room temperature. Likewise, colchicine (300 μM) induced inhibition of 10 mM 5-HT mediated responses was similar between oocytes incubated for 2 hours on ice (39 ± 7.9%) and oocytes maintained at room temperature (34 ± 5.1%).

The Species-Selective Colchicine Actions on Mouse and Human 5-HT_{3A}Rs are Conferred by Their N-terminal Extracellular Domains. We have determined that colchicine is both a positive allosteric modulator and inhibitor of the human receptor, while it is an antagonist of the mouse receptor. Studies using nACh/5-HT3 receptor chimeras

have shown that the ligand binding domains of the receptors are in the N-terminus (Eiselé et al., 1993; Craig et al., 2004). To correlate species-differential colchicine actions to defined structural domains of 5-HT_{3A}Rs, we constructed four chimeric receptor cDNAs as previously published (Zhang et al., 2006). The first chimera was designated H239M and contains the entire N-terminal domain of human receptor cDNA and the balance of the mouse 5-HT_{3A}R cDNA. The second chimera, M244H , is a mirror image of the first and consists of the entire N-terminal domain of mouse receptor cDNA and the balance the human receptor cDNA. The third chimera, M181H239M is the mouse receptor cDNA in which the distal one-third of the N-terminus is replaced by human receptor cDNA, and the fourth corresponding human receptor chimera is H176M244H, in which the distal one-third of the human receptor cDNA is replaced by mouse receptor cDNA.

These chimeric receptors, along with their parental receptors, mouse wild-type receptor (MWT) and human wild-type receptor (HWT), were expressed in *Xenopus* oocytes, and the responses to 5-HT (0.5 μM) or 5-HT (0.5 μM) plus colchicine (300 μM) were measured. Serotonin concentration response curves were performed, and EC_{50} values and Hill coefficients for each receptor construct are listed in Table 2. Percent change induced by colchicine is represented in Fig. 5. In receptors containing the human receptor N-terminus, colchicine enhanced 5-HT evoked currents. Potentiation of 64.3 $\pm$ 3.5 and 52.8 $\pm$ 5% were observed in HWT and H239M receptors, respectively. Potentiation of 35.3 $\pm$ 3.3% was measured in M181H239M receptors, which suggests that the distal one-third of the N-terminus is sufficient to confer positive allosteric modulation by colchicine. However, the enhancement produced by colchicine was significantly less in the M181H239M than the

HWT receptor, suggesting that residues in the other two-thirds of the human receptor N-terminus may play a role in determining colchicine's efficacy. Inhibition by colchicine (300 μM) was produced in receptors containing the mouse receptor N-terminus. Inhibition of 91.7 ± 1.8, 83.4 ± 2.6, and 91.7 ± 1.1% were determined in MWT, M244H, and H176M244H receptors, respectively. Thus, replacement of the distal one-third of the human receptor with that of the mouse receptor was sufficient to confer colchicine-induced inhibition.

The Distal One-Third of the N-termini of 5-HT_{3A}Rs Confer Positive Allosteric Modulation in the Human Receptor and Competitive Antagonism in the Mouse Receptor. To characterize further the role of the distal one-third of the N-terminus in the species-selective colchicine action, we performed colchicine concentration response curves in MWT, HWT, H176M244H, and M181H239M receptors. In Fig. 6A, colchicine concentration response curves were conducted in the presence of 0.5 μM 5-HT, an EC_{10} for both MWT and H176M244H receptors. Colchicine inhibited 0.5 μM 5-HT mediated currents with the same potency in both receptor constructs, suggesting that replacement of the last one-third of human receptor with that of the mouse receptor is sufficient to generate a receptor that is virtually identical to the MWT receptor in its direction of modulation by and sensitivity to colchicine. In Fig. 6B, a representative tracing of the inhibitory action of colchicine (300 μM) at the H176M244H receptor is shown.

The actions of colchicine at the MWT receptor were compared with that at the M181H239M receptor (Fig. 7A). A 1 μM 5-HT concentration, which represents ~ an EC_{50} for both receptor constructs, was used. An EC_{50} concentration of 5-HT was chosen

for two reasons. In the MWT receptor, 1 μM 5-HT mediated currents were predicted to be inhibited in a concentration dependent manner. Secondly, in the human receptor, an EC_{50} concentration of 5-HT would *not* be predicted to produce currents that could be enhanced by colchicine, given that 1 μM 5-HT (EC_{20}) in the human receptor was unaffected by colchicine (Fig. 3C). If anything, the actions of colchicine on 1 μM 5-HT mediated currents in M181H239M might be predicted to be slightly inhibitory, given the inhibition of 45% and 27% of 3 μM (EC_{85}) and 10 μM (EC_{100}) 5-HT in HWT receptor (Fig. 3C). In Fig. 7A, the MWT receptor is inhibited by colchicine with an IC_{50} of 96.5 ± 6 μM, whereas the M181H239M receptor was unaffected by colchicine (10-500 μM). These results demonstrate that replacement of the distal one-third of the mouse receptor with that of the human receptor is sufficient to remove the inhibitory actions of colchicine in the mouse receptor.

A full concentration response curve was generated in the M181H239M receptor in Fig. 7B. Colchicine (25- 1000 μM) enhanced 5-HT mediated currents in the chimeric receptor, with an EC_{50} of 296.4 ± 97.4%, with a slightly smaller potency and less efficacy than that seen in the HWT receptor. Thus, in the $5\text{-}HT_{3A}R$, if the distal one-third of the N-terminus is human-like, potentiating actions of colchicine will be observed. However, amino acids in the first two-thirds of the N-terminus may play a role in determining colchicine efficacy. Figure 7C is a typical tracing of the allosteric modulatory actions of colchicine (300 μM) in the M181H239M receptor.

DISCUSSION

A number of studies investigating the relationships between members of the superfamily of LGICs and cytoskeleton intermediary proteins suggest that their associations play an important role in receptor distribution and function (review by Chen and Olsen, 2007; Antolik et al., 2007; Sun et al., 2008). In the present study we investigated colchicine, a chemical compound more commonly known for its microtubule-depolymerizing actions. Previous studies reported that colchicine acts as a competitive antagonist at the Gly α1 and α2 receptors (Machu, 1998) and at $GABA_A$Rs (Bueno and Leidenheimer, 1998). The antagonism at these receptors was independent of the microtubule depolymerizing function of colchicine. Results from the present study show that colchicine inhibits 5-HT currents at the mouse 5-HT_{3A}R, while at the human 5-HT_{3A}R, both potentiation and inhibition are observed. Furthermore, the potency of colchicine at the mouse 5-HT_{3A}R is similar to that seen at the $GABA_A$R and slightly higher than that at the GlyR α2.

Concordant with results reported for the GlyRα2 and the $GABA_A$Rs, the actions of colchicine at the 5-HT_{3A}R are independent of microtubule depolymerization. Depolymerization of microtubules with colchicine takes at least 1.5 h to reach equilibrium at 30 ^{o}C (Owellen et al., 1972). Therefore, colchicine would not be expected to produce an immediate effect on the function of 5-HT_{3A}Rs if it were working through a microtubule dependent mechanism. As predicted, colchicine's inhibition of mouse 5-HT_{3A}R function occurred in the absence of preincubation. Other evidence that colchicine acts directly at the mouse 5-HT_{3A}R include experiments conducted under cold temperatures. Oocyte

microtubules are known to be completely depolymerized after 2 h of incubation at 4 ^{o}C (Gard, 1991). Additionally, microtubule depolymerization induced by colchicine does not occur at cold temperatures (Wilson et al., 1974). No significant change in colchicine-induced inhibition was observed in 5-HT-mediated currents in oocytes incubated on ice for 2 h. Furthermore, both potentiating and inhibitory effects of colchicine on the human 5-HT_{3A}R were preserved in oocytes incubated on ice for 2 h. Our results do not exclude the possibility that microtubules play a role in the synaptic localization of LGICs, rather they demonstrate a direct effect of this microtubule-depolymerizing agent on yet another member of the LGIC family.

Another major finding of the present study is that colchicine acts in a dissimilar manner at mouse and human 5-HT_{3A}Rs, despite the fact that they share 84% amino acid identity. In the human receptor, colchicine enhances 5-HT mediated currents at low 5-HT concentrations and inhibits function at higher 5-HT concentrations. In contrast, colchicine has inhibitory actions at the mouse receptor. Colchicine did not displace [3H]-BRL 43694 binding in mouse or human 5-HT_{3A} receptors, and therefore does not act at the ligand recognition site. In agreement with the binding experiments, colchicine applied in the absence of 5-HT did not produce any detectable currents in mouse or human receptors. We suggest that colchicine acts at an allosteric site to produce opposing actions in human and mouse receptors, i.e., as an agonist and inverse agonist, respectively. Results of our radioligand binding assays strengthen this hypothesis. When colchicine (300 μM and 1000 μM) was co-applied with 5-HT, a significant decrease in the potency of 5-HT at the MWTA receptor was observed. However in the HWTA

receptor, 300 μM co-application of colchicine resulted in a significant increase in 5-HT potency while 1000 μM co-application of colchicine led to a significant decreased in 5-HT potency (table 2). These findings parallel the bi-directional modulation of $GABA_AR$ function by ligands binding to the BZD recognition site (reviewed in Sigel and Buhr, 1997). BZD analogs are agonists, antagonists, or inverse agonists, but we are unaware of any single compound subserving a function as agonist in one $GABA_AR$ subunit combination and inverse agonist in another.

Further examination of the potentiating actions of colchicine at the human 5-$HT_{3A}R$ revealed that potentiation decreased as the concentration of co-applied 5-HT increased, which is similar to results obtained with BZD agonists at the $GABA_AR$. However, unlike BZD's actions at the $GABA_AR$, when co-applied with 5-HT concentrations >1 μM, colchicine acted as an inhibitor at the human receptor, thus suggesting that a second inhibitory allosteric site may exist in the human 5-$HT_{3A}R$. If a second site exists in the mouse receptor, it would have a lower affinity than the human receptor for colchicine, based on the lack of inhibitory action of colchicine (10 – 500 μM) at mouse chimeric receptor M181H239M. Such a putative site could exist in any part of the receptor, but a channel binding domain is doubtful, given that the transmembrane (TM) two domains which contain the pore lining residues are identical between the two species.

A major goal of the present study was to investigate the amino acid domains responsible for the switch between positive allosteric modulation in the human 5-$HT_{3A}R$ and inverse agonism in the mouse receptor by colchicine. The agonist binding domain of

cys-loop receptors is located in the N-terminus at the interface of two subunits. Loops A, B, and C are in the principal component of the LBD, and Loops D, E, and F are on the complementary face of the binding domain (Brejc et al., 2001). In addition to agonist ligands, allosteric modulators are also known to bind to the N-terminus domain of cys-loop receptors, with the best known example being BZDs, which bind to the interface of α/γ subunits of $GABA_A$Rs (Siegel, 2002). Loops C and F have been reported to play a critical role in differential pharmacological actions of drugs on both 5-HT_{3A} and $GABA_A$Rs (Zhang et al., 2006, Zhang et al., 2007; Padgett and Lummis, 2008). There are 16 differences between mouse and human receptors in the distal third of the N-terminus, seven in Loop C and nine in or within proximity of Loop F. To explore the N-terminus as the potential location for the colchicine binding site, we created mouse-human and human-mouse chimeric receptors. The first set of chimeras consisted of whole N-terminal substitutions. The function of the mouse-human chimera, in which the N-terminus was mouse-like, was inhibited by colchicine. In contrast, the function of the mirror image human-mouse chimera receptor was enhanced by colchicine. The distal one-third of the N-terminus was substituted in the second set of chimeras. Substitution of the distal one-third of the human receptor with that of the mouse yielded a chimera, H176M244H, whose function was inhibited by colchicine in the presence of 0.5 μM 5-HT; the IC50s were similar for H176M244H and MWT. The converse effects were observed in the mirror image chimera, M181H239M, in which the distal one-third of the N-terminus of the mouse receptor was replaced with that of the human receptor. These results suggest that the site responsible for colchicine's allosteric modulation of function

at low gating concentrations of 5-HT is located in the distal one-third of the N-termini of mouse and human 5-HT_{3A} receptors.

The underlying mechanism through which Loops C and/or F determine the direction of allosteric modulation of colchicine in mouse and human 5-HT_{3A}Rs remains to be determined. Our binding and electrophysiological studies demonstrated that colchicine does not compete with [3H]-BRL-43694 and 5-HT, respectively, at the 5-HT recognition site. Since every subunit interface is identical in the 5-HT_{3A}R, colchicine and BRL-43694 would be expected to compete, should they both bind at the junction of two subunit interfaces. Thus, these results strongly suggest that amino acid differences in the N-terminus of mouse and human 5-HT_{3A}Rs exert their differential actions by affecting gating, not binding. These loops have also been shown to play a significant role in modulation of GABA-induced currents by BZDs and other drugs binding at the BZD binding site on the $GABA_A$R (Sancar et al., 2007; Padgett and Lummis, 2008). The role of Loops C and F in the GABA-BZD modulatory mechanism differs from the proposed role of these loops in colchicine modulation in that Loops C and F likely induce conformational changes that affect gating of the 5-HT_{3A}R. In the $GABA_A$Rs these loops are thought to not only affect gating, but also play a direct role in stabilization of BZD binding site. The binding site(s) for colchicine in the mouse and human 5-HT_{3A} receptors could be in regions of the N-terminus that do not form the ligand binding domains or in the transmembrane domains. Residues in TM1 and TM2 domains of the α7 nAChR have recently been identified as strong candidates for binding of positive allosteric modulators (Young et al., 2008).

A number of clinical compounds targeting the 5-HT_{3A}R are currently in use (see review by Thompson and Lummis, 2007). A better understanding of the mechanisms underlying binding, gating, and allosteric modulation of this receptor can potentially advance drug development. The data from this study further supports existing evidence of a critical role for Loops C and F in function of the 5-HT_{3A}R and introduces colchicine as a powerful tool in dissecting the molecular interactions in the 5-HT_{3A}R that are responsible for receptor modulation.

ACKNOWLEDGEMENTS

The authors would like to thank Ankita Singh for her assistance with the colchicine radioligand binding assays.

REFERENCES

Antolik C, Catino DH, O'Neill AM, Resneck WG, Ursitti JA, Bloch RJ (2007) The actin binding domain of ACF7 binds directly to the tetratricopeptide repeat domain of rapsyn. *Neurosci* **145**: 56-65.

Belelli D, Balcarek JM, Hope AG, Peters JA, Lambert JJ and Blackburn TP (1995) Cloning and functional expression of a human 5-Hydroxytryptamine type $_{3A}$ receptor subunit. *Mol Pharmacol* **48**: 1054-1062.

Bertrand D, Bertrand S, Cassar S, Gubbins E, Li J, and Gopalakrishnan M (2008) Positive Allosteric Modulation of the α7 Nicotinic Acetylcholine Receptor: Ligand Interactions with Distinct Binding Sites and Evidence for a Prominent Role of the M2-M3 Segment. *Mol Pharmacol* **74**: 1407-1416.

Brejc K, van Dijk WJ, Klaassen RV, Schuurmans M, van Der Oost J, Smit AB and Sixma TK (2001) Crystal structure of an ACh-binding protein reveals the ligand-binding domain of nicotinic receptors. *Nature* **411**: 269-276.

Bueno OF and Leidenheimer NJ (1998) Colchicine inhibits $GABA_A$ receptors independently of microtubule depolymerization. *Neuropharmacol* **37**: 383-390.

Chen ZW and Olsen RW (2007) $GABA_A$ receptor associated proteins: a key factor regulating $GABA_A$ receptor function. *J Neurochem* **100**: 279-294.

Craig PJ, Bose S, Zwart R, Beattie RE, Folly EA, Johnson LR, Bell E, Evans NM, Benedetti G, Pearson KH, McPhie GI, Volsen SG, Millar NS, Sher E and Broad LM (2004) Stable expression and characterization of a human alpha 7 nicotinic

subunit chimera: a tool for functional high-throughput screening. *Eur J Pharmacol* **502**: 31-40.

Da Settimo F, Taliani S, Trincavelli ML, Montali M and Martini C (2007) GABA A/Bz receptor subtypes as targets for selective drugs. *Curr Med Chem* **14**: 2680-2701.

Eisele′ JL, Bertrand S, Galzi JL, Deillers-Thiery A, Changeux JP and Bertrand D (1993) Chimaeric nicotinic-serotonergic receptor combines distinct ligand binding and channel specificities. *Nature* **336**: 479-483.

Gard DL (1991) Organization, nucleation, and acetylation of microtubules in Xenopus laevis oocytes: a study by confocal immunofluorescence microscopy. *Dev Biol* **143**: 346-362.

Grenningloh G, Gundelfinger E, Schmitt B, Betz H, Darlison MG, Barnard EA, Schofield PR and Seeburg PH (1987) Glycine vs GABA receptors. *Nature* **330**: 25-26.

Hope AG, Belelli D, Mair ID, Lambert JJ and Peters JA (1999) Molecular Determinants of (+)-Tubocurarine Binding at Recombinant 5-Hydroxytryptamine$_{3A}$ Receptor Subunits. *Mol Pharmacol* **55**: 1037-1043.

Im WB, Chio CL, Alberts GL and Dinh DM (2003) Positive Allosteric Modulator of the Human 5-HT2C Receptor. *Mol Pharmacol* **64**: 78-84.

Lovinger DM, Sung KW and Zhou Q (2000) Ethanol and trichloroethanol alter gating of 5-HT3 receptor-channel in NCB-20 neuroblastoma cells. *Neuropharmacol* **39**: 561-570.

Lowry OH, Rosebrough NJ, Farr AL and Randall RJ (1951) Protein measurement with the folin phenol reagent. *J Biol Chem* **193**:265-275.

Machu TK and Harris RA (1994) Alcohols and anesthetics enhance the function of 5-hydroxytryptamine3 receptors expressed in Xenopus laevis oocytes. *J Pharmacol Exp Ther* **271**: 898-905.

Machu TK (1998) Colchicine competitively antagonizes glycine receptors expressed in Xenopus oocytes. *Neuropharmacol* **37**: 391-396.

Maksay G, Nenes P, Vincze Z and Biro T (2008) Synthesis of (nor)tropeine (di)esters and allosteric modulation of glycine receptor binding. *Bioorg Med Chem* **16**: 2086-2092.

Maricq AV, Peterson AS, Brake AJ, Myers RM and Julius D (1991) Primary structure and functional expression of the 5-HT_3 receptor, a serotonin-gated ion channel. *Science* **254**: 432-436.

Miyake A, Mochizuki S, Takemoto Y and Akuzawa S (1995) Molecular cloning of human 5- Hydroxytryptamine$_3$ receptor: heterogeneity in distribution and function among species. *Mol Pharmacol* **48**: 407-416

Mochizuki S, Miyake A and Furuichi K (1999) Identification of a domain affecting agonist potency of *meta*-chlorophenylbiguanide in 5-HT_3 receptors. *Eur J Pharmacol* **369**: 125-132.

Niesler B, Walstab J, Combrink S, Möller D, Kapeller J, Rietdorf J, Bönisch H, Göthert M, Rappold G, Brüss M (2007). Characterization of the Novel Human Serotonin Subunits 5-HT3C, 5-HT3D, and 5-HT3E. *Mol Pharmacol* **72:** 8-17.

Owellen RJ, Owens AH and Donigian DW (1972) The binding of vincristine, vinblastine, and colchicine to tubulin. *Biochem. Biophys Res Comm* **47**: 685-691.

Padgett CL and Lummis SCR (2008) The F-loop of the $GABA_A$ Receptor γ2 Subunit Contributes to Benzodiazepine Modulation. *J Biol Chem* **283**: 2702-2708.

Paradiso K, Zhang J and Steinbach JH (2001) The C terminus of the human nicotinic alpha4beta2 receptor forms a binding site required for potentiation by an estrogenic steroid. *J Neurosci* **21**: 6561-6568.

Sancar F, Ericksen SS, Kucken AM, Teisseré and Czajkowski C (2007) Structural Determinants for High-Affinity Zolpidem Binding to GABA-A receptors. *Mol Pharmacol* **71**: 38-46.

Schofield PR, Darlison MG, Fujita N, Burt DR, Stephenson FA, Rodriguez H, Rhee L, Ramachandran J, Reale A, Glencorse T, Seeburg PH and Barnard EA (1987) Sequence and functional expression of the $GABA_A$ receptor shows a ligand-gated receptor super-family. *Nature* **328**: 221-227.

Schreiter C, Hovius R, Costioli M, Pick H, Kellenberger S, Schild L and Vogel H (2003) Characterization of the ligand-binding site of the 5-HT_3 receptor. *J Biol Chem* **278**: 22709-22716.

Siegel E (2002) Mapping of the benzodiazepine recognition site on GABA(A) receptors. *Curr Top Med Chem* **2**: 833-839.

Sigel E and Buhr A (1997) The benzodiazepine binding site of $GABA_A$ receptors. *Trends Pharmacol Sci* **18**: 425-429.

Sun H, Hu XQ, Emerit MB, Schoenebeck JC, Kimmel CE, Peoples RW, Miko A and Zhang L (2008) Modulation of 5-HT3 receptor desensitization by the light chain of microtubule-associated protein 1B expressed in HEK 293 cells. *J Physiol* **586**: 751-762.

Thompson AJ, Price KL, Reeves DC, Chan SL, Chau PL and Lummis SCR (2005) Locating an antagonist in the 5-HT3 receptor binding site using modeling and radioligand binding. *J Biol Chem* **280**: 20476-20482.

Thompson AJ and Lummis CR (2006) 5-HT_3 receptors. *Curr Pharm Des* **12**: 3615-3630.

Thompson AJ and Lummis CR (2007) The 5-HT_3 receptor as a therapeutic target. *Expert Opin Ther Targets* **11**: 527-540.

van Hooft JA, van der Haar E and Vijverberg HP (1997) Allosteric potentiation of the 5-HT3 receptor-mediated ion current in N1E-115 neuroblastoma cells by 5-hydroxyindole and analogues. *Neuropharmacol* **36**: 649-53.

Wilson L, Bamburg JR, Mizel SB, Grisham LM and Creswell KM (1974) Interaction of drugs with microtubule proteins. *Fed Proc* **33**: 158-166.

Young GT, Zwart R, Walker AS, Sher E and Millar NS (2008) Potentiation of α7 nicotinic receptors via an allosteric transmembrane site. *Proc Natl Acad Sci* **105:** 14686-14691.

Zhang R, White NA, Soti FS, Kem WR, Machu TK (2006). N-Terminal Domains in Mouse and Human 5-Hydroxytryptamine$_{3A}$ Receptors Confer Partial Agonist and Antagonist Properties to Benzylidene Analogs of Anabaseine. *J Pharmacol Exp Ther* **317:** 1276-1284.

Zhang R, Wen X, Militante J, Hester B, Rhubottom HE, Sun H, Leidenheimer NJ, Yan D, White MM, Machu TK. (2007). The role of loop F residues in determining differential d-tubocurarine potencies in mouse and human 5-hydroxytryptamine$_{3A}$ receptors. *Biochem* **46:** 1194-1204.

FOOTNOTES

This study was supported by National Institute of Neurological Disorders and Stroke grant NS043438.

LEGENDS FOR FIGURES

Figure 1. Antagonist potency of colchicine at the mouse 5-HT_{3A}R. A: Representative tracings of currents produced in a single oocyte expressing mouse 5-HT_{3A}Rs. Serotonin, 0.5 μM was applied for 30 s to obtain a baseline current. Serotonin, 0.5 μM, was applied in the absence or presence of colchicine (300 μM) for 30 s. An inhibition of ~92 % of the 0.5 μM 5-HT induced baseline current was observed for the receptor. Washout of colchicine inhibition was observed with the next application of 5-HT five min later. B: A concentration-response curve for colchicine was generated in oocytes expressing mouse 5-HT_{3A}Rs (n=4-7). Colchicine (1-300 μM) was co-applied with 0.5 μM 5-HT for 30 s. An IC_{50} of 59.5 ± 3 μM was obtained. The Hill coefficient was 1.3 ± 0.08.

Figure 2. Colchicine antagonizes mouse 5-HT_{3A}Rs. A: Concentration-response curves for colchicine were generated in oocytes expressing the mouse 5-HT_{3A}R (n=3-5). Serotonin concentration response curves were generated in the presence of colchicine 0, 200, 1000 and 10,000 μM. The EC_{50}s generated for each of the curves were 0.93 ± 0.04, 3.7 ± 0.3, 13.4 ± 2.4, and 81.4 ± 3.3 μM, respectively. B: [^{3}H]-BRL-43694 binding to MWTA 5-HT_{3A} receptor rich membranes. Membranes were incubated for 2 hours with increasing concentrations of [^{3}H]-BRL-43694 (0.1 nM – 23 nM). Total (▼), specific (■) and non-specific (▲) binding. Non-specific binding was measured with MDL-7222 (3-tropanyl-3, 5-dichlorobenzoate), and specific binding was calculated by subtracting non-specific from total binding. Scatchard plot of the binding data shown. The Kd (3.5 ±

0.3 nM) was calculated as the negative reciprocal of the slope of three separate experiments. C: Colchicine displacement of [^{3}H]-BRL-43694 binding to MWTA 5-HT_{3A} receptor rich membranes. Membrane was incubated (2 hours) with increasing concentrations of colchicine (25 nM – 1 mM) and [3H]-BRL-43694 at the Kd = 3.5 nM. Total (▼), specific (■) and non-specific (▲) binding. Non-specific binding was measured with MDL-7222 (3-tropanyl-3, 5-dichlorobenzoate), and specific binding was calculated by subtracting non-specific from total binding. No displacement of the radioligand was observed.

Figure 3. Interaction of colchicine with the human 5-HT_{3A}R. A: Colchicine enhances currents evoked by 0.5 μM 5-HT in oocytes expressing the human 5-HT_{3A}R. Serotonin, 0.5 μM was applied for 30 s to obtain a baseline current. Colchicine (300 μM) was co-applied with 5-HT, 0.5 μM, for 30 s. A potentiation of ~75 % of the baseline current was observed in this receptor. Washout of colchicine-induced potentiation was observed with the next application of 5-HT five min later. B: A concentration-response curve for colchicine (10-1000 μM) was generated in oocytes expressing human 5-HT_{3A}Rs (n=4-5). An EC_{50} for colchicine of 226.6 $\pm$ 25.1 μM and a Hill coefficient of 2.38 $\pm$ 0.64 were determined. C: The potentiating actions of colchicine at the human 5-HT_{3A}R is 5-HT-concentration dependent and microtubule independent. Colchicine, 300 μM, was co-applied with 5-HT, 0.5, 1, 3, or 10 μM for 30 s (n=3-4). The effect of colchicine was

expressed as a percent of the baseline current produced by the respective concentration of 5-HT alone.

Figure 4. Colchicine action at the human 5-HT3ARs. A: [3H]-BRL-43694 binding to HWTA 5-

HT3A receptor rich membranes. Membranes were incubated for 2 hours with increasing concentrations of [3H]-BRL-43694 (0.1 nM – 23 nM). Total ( ), specific ( ) and non-specific ( ) binding. Nonspecific binding was measured with MDL-7222 (3-tropanyl-3, 5-dichlorobenzoate), and specific binding was calculated by subtracting non-specific from total binding. Scatchard plot of the binding data shown. The Kd (2.58 ± 0.5 nM) was calculated as the negative reciprocal of the slope of three 3-5 separate experiments. B: Colchicine displacement of [^{3}H]-BRL-43694 binding to HWTA 5-HT_{3A} receptor rich membranes. Membrane was incubated (2 hours) with increasing concentrations of colchicine (25 nM – 1 mM) and [3H]-BRL-43694 at the Kd = 2.58 nM. Total (▼), specific (■) and non-specific (▲) binding. Non-specific binding was measured with MDL-7222 (3-tropanyl-3, 5-dichlorobenzoate), and specific binding was calculated by subtracting non-specific from total binding. No displacement of the radioligand was observed.

Figure 5. Amino acid domains in the N-termini are involved in species-selective colchicine actions on the mouse and human 5-HT_{3A}Rs. Responses of the wild-type or chimeric receptors to colchicine (300 μM) in the presence of 0.5 μM 5-HT were

measured. The schematic representations of the chimeric receptors tested are shown at the bottom of the diagrams. Oocytes expressing wild-type or chimeric receptors were perfused with 5-HT in the absence or presence of colchicine (300 μM). The bar graphs represent percent change by induced by colchicine (300 μM), n=4-21. One-way ANOVA demonstrated a significant effect of mutation ($F_{(5,39)} = 244.94$, $p < 0.0001$). Student-Newman-Keul's post-hoc test revealed that the colchicine-induced modulation in M181H239M, H176M244H, M244H, and MWT receptors was significantly different than that in the HWT receptor ($p < 0.001$).

Figure 6. The distal one-third of the N-termini of the mouse 5-HT_{3A}R confers colchicine's inhibitory effects. A: A colchicine concentration response curve in the H176M244H receptor was generated and compared with that obtained for the MWT receptor. Serotonin mediated currents were measured in the absence and presence of colchicine (1-500 μM) (n=3-9). A colchicine IC_{50} of 45.72 ± 2.28 μM, and a Hill coefficient of 1.12 ± 0.07 were obtained for the H176M244H receptor, which is similar to that obtained in the MWT receptor. B: Representative tracings of currents produced in a single oocyte expressing H176M244H 5-HT_{3A}Rs. Serotonin, 0.5 μM was applied for 30 s to obtain a baseline current. Serotonin, 0.5 μM, was applied in the presence of colchicine (300 μM) for 30 s. An inhibition of ~93 % of the 0.5 μM 5-HT induced baseline current was observed for the receptor. Washout of colchicine inhibition was observed with the next application of 5-HT five min later.

Figure 7. The distal one-third of the N-termini of the human 5-HT_{3A}Rs confers colchicine's stimulatory effects. A: The actions of colchicine, 1-500 μM, were compared in the MWT and M181H239M receptors. In both constructs, 1 μM 5-HT was used; this concentration is ~ an EC_{50} for both. Replacement of the distal one-third of the N-terminus of the mouse receptor with that of the human receptor is sufficient to remove inhibitory effects of colchicine (1-500 μM). An IC_{50} of 96.5 ± 6 μM, and a Hill slope of 1.4 ± 0.12 were obtained for the MWT receptor. B: A colchicine concentration response curve in the M181H239M receptor was generated and compared with that obtained for the HWT receptor. Serotonin mediated currents were measured in the absence and presence of colchicine (1-1000 μM) (n=4-21). A colchicine EC_{50} of 296.4 ± 97.4 μM, and a Hill coefficient of 1.09 ± 0.59 were obtained for the M181H239M receptor. C: Colchicine enhances currents evoked by 0.5 μM 5-HT in oocytes expressing the M181H239M 5-HT_{3A}R. Serotonin, 0.5 μM was applied for 30 s to obtain a baseline current. Colchicine (300 μM) was co-applied with 5-HT, 0.5 μM, for 30 s, and potentiation of 5-HT-mediated currents was observed. Washout of colchicine-induced potentiation was observed with the next application of 5-HT five min later.

Table 1. Effect of temperature on colchicine modulatory actions on human and mouse 5-HT_{3A}Rs

5-HT_{3A}R	MWT				HWT			
Colchicine	50 µM		200 µM		300 µM		1000 µM	
Temperature	22°C	4°C/2hrs	22°C	4°C/2hrs	22°C	4°C/2hrs	22°C	4°C/2hrs
% Change	42.9 ± 5.0	43.4 ± 3.0	80.4 ± 6.0	81.5 ± 2.5	79.3 ± 8.7	90.3 ± 4.3	-39.0 ± 7.9	-34.3 ± 5.0

Table 2. Colchicine effects on 5-HT potency at both MWTA and HWTA receptors.

$5\text{-}HT_{3A}$ Construct	MWTA	HWTA
[^{3}H]-BRL-43694 Kd (nM)	3.53 ± 0.3	2.58 ± 0.6
Colchicine Ki (nM)	N/A	N/A
5-HT Ki (nM)	311 ± 0.5	1530 ± 230
5-HT + 300 µM Colchicine Ki (nM)	406 ± 0.37 [a]	738 ± 0.64 [c]
5-HT + 1000 µM Colchicine Ki (nM)	1250 ± 150 [b]	2940 ± 0.15[d]

[a]$p < 0.05$ and [b]$p < 0.01$ compared to 5-HT Ki for MWTA; [c]$p < 0.05$ and [d]$p < 0.01$ compared to 5-HT Ki for HWTA, Student's t-test.

Table 3. Serotonin Concentration Response Curve Values for Human and Mouse 5-HT_{3A}Rs

5-HT_{3A}-R	MWT	M244H	M181H239M	H176M244H	H239M	HWT
5-HT EC_{50} (μM)	0.92±0.06	1.22±0.05	1.21±0.03	1.65±0.34	3.9±0.2	1.39±0.06
Hill Number	2.8	2.1	3.2	1.8	2.6	2.7

Figure 1

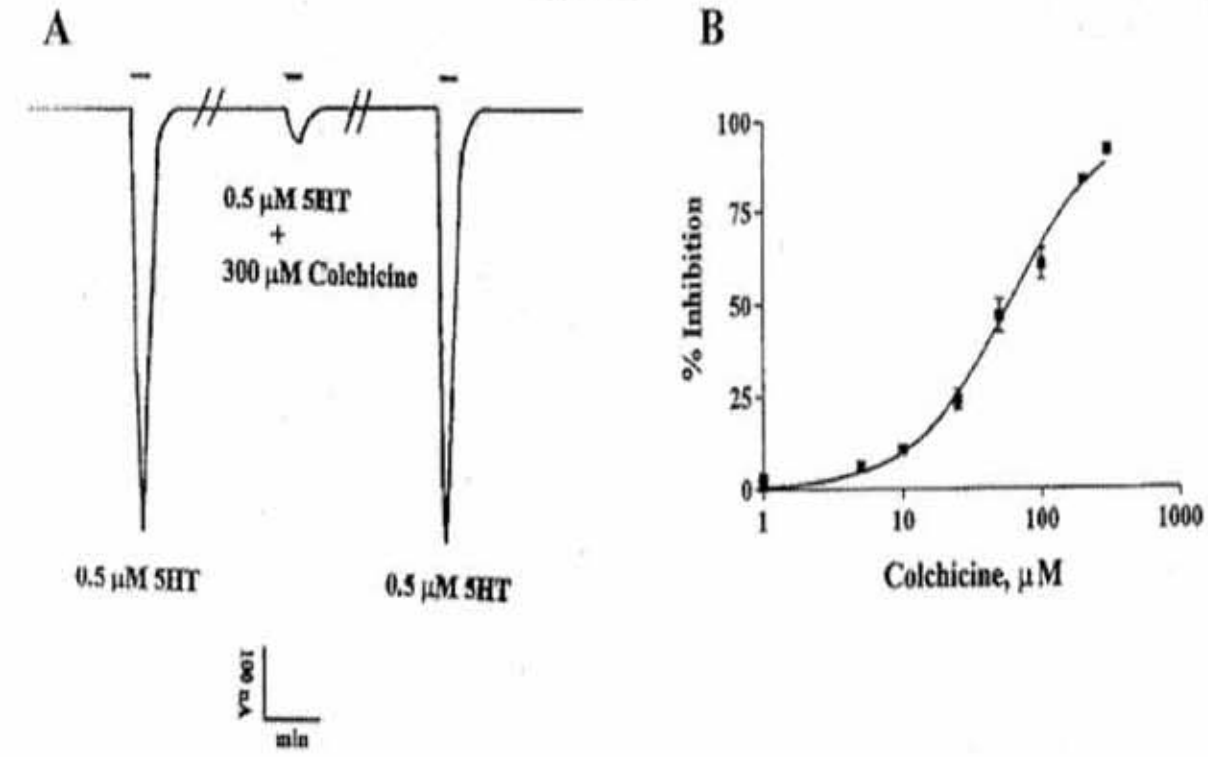
A
0.5 μM 5HT
+
300 μM Colchicine
0.5 μM 5HT
0.5 μM 5HT
B
% Inhibition
100
75
50
25
0
1
10
100
1000
Colchicine, μM

Figure 2

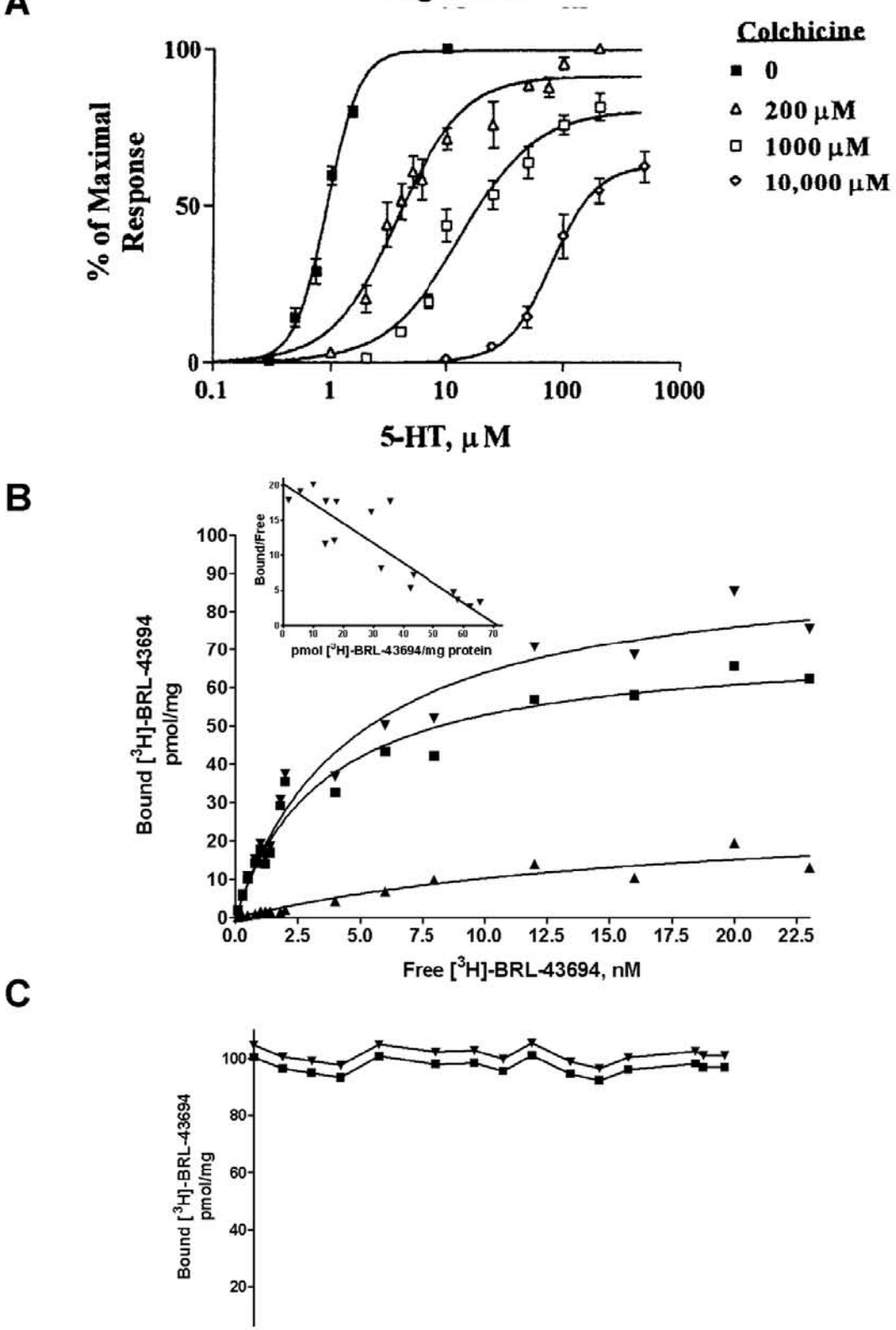
A
% of Maximal Response
100
50
0
0.1
1
10
100
1000
5-HT, μM
Colchicine
0
200 μM
1000 μM
10,000 μM
B
Bound [3H]-BRL-43694 pmol/mg
Free [3H]-BRL-43694, nM
Bound/Free
pmol [3H]-BRL-43694/mg protein
C
Bound [3H]-BRL-43694 pmol/mg

Figure 3

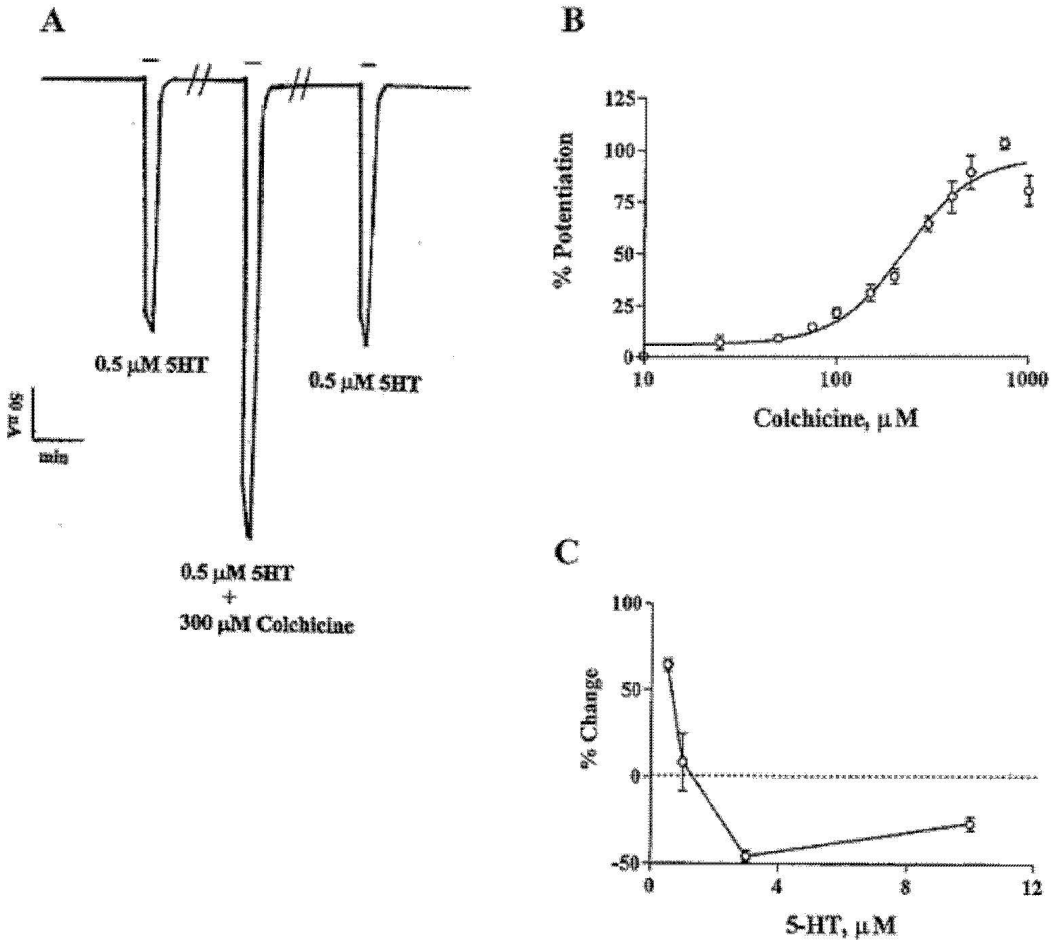
A
0.5 μM 5HT
0.5 μM 5HT
0.5 μM 5HT
+
300 μM Colchicine
50 nA
min
B
% Potentiation
125
100
75
50
25
0
10
100
1000
Colchicine, μM
C
% Change
100
50
0
-50
0
4
8
12
5-HT, μM

Figure 4

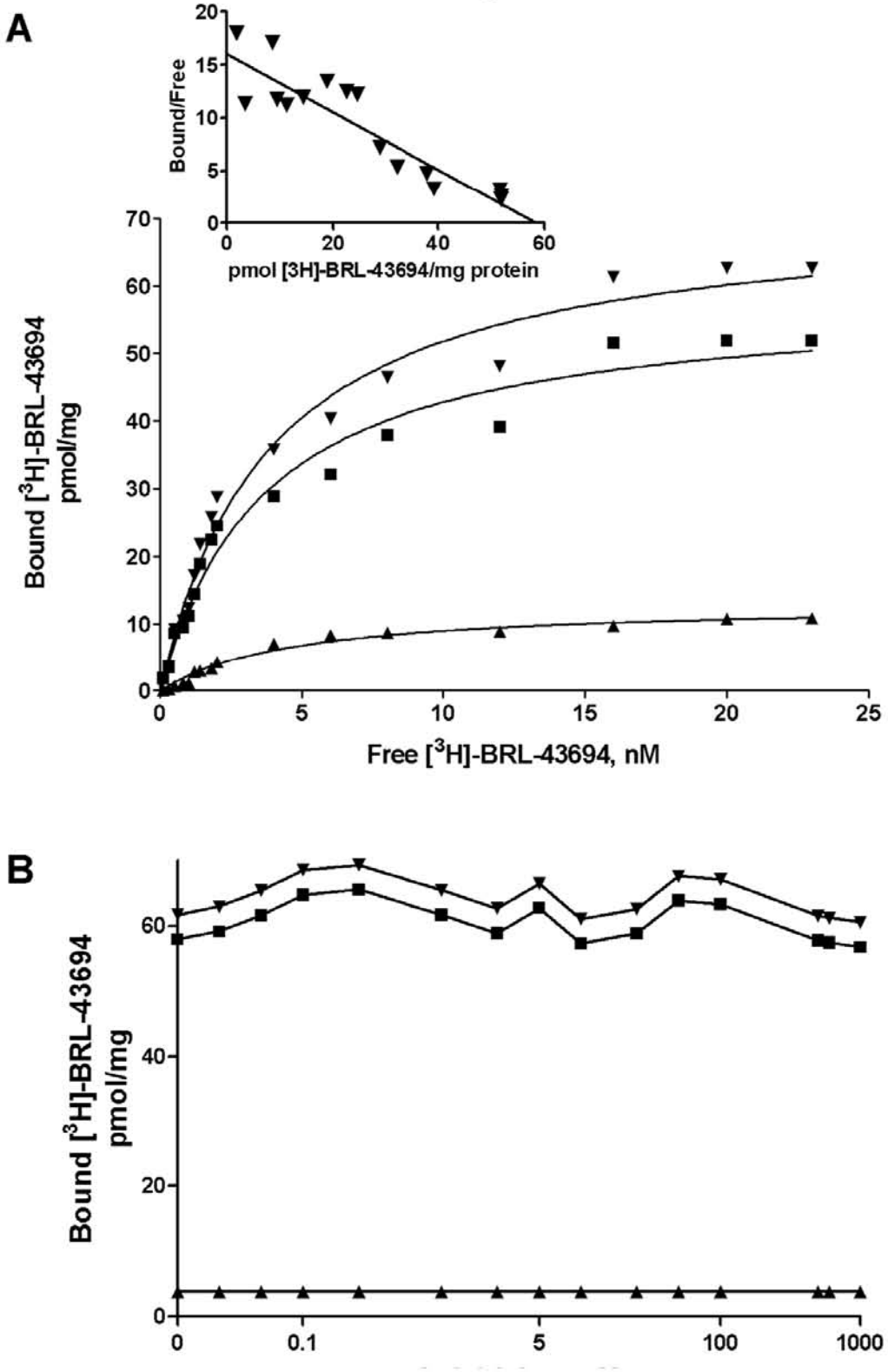
A
Bound/Free
pmol [3H]-BRL-43694/mg protein
Bound [3H]-BRL-43694 pmol/mg
Free [3H]-BRL-43694, nM
B
Bound [3H]-BRL-43694 pmol/mg

Figure 5

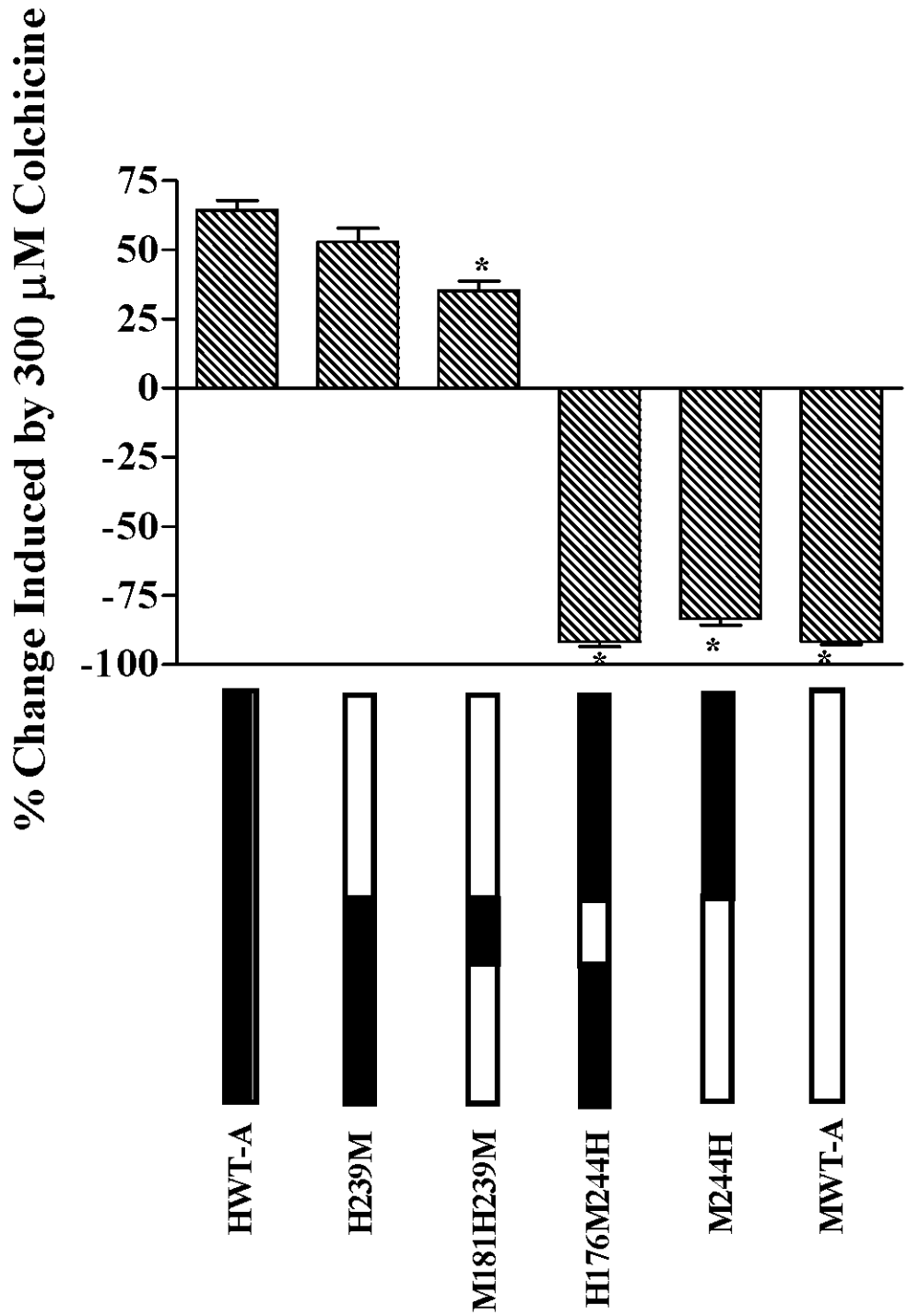
% Change Induced by 300 μM Colchicine
75
50
25
0
-25
-50
-75
-100
*
*
*
*
HWT-A
H239M
M181H239M
H176M244H
M244H
MWT-A

Figure 6

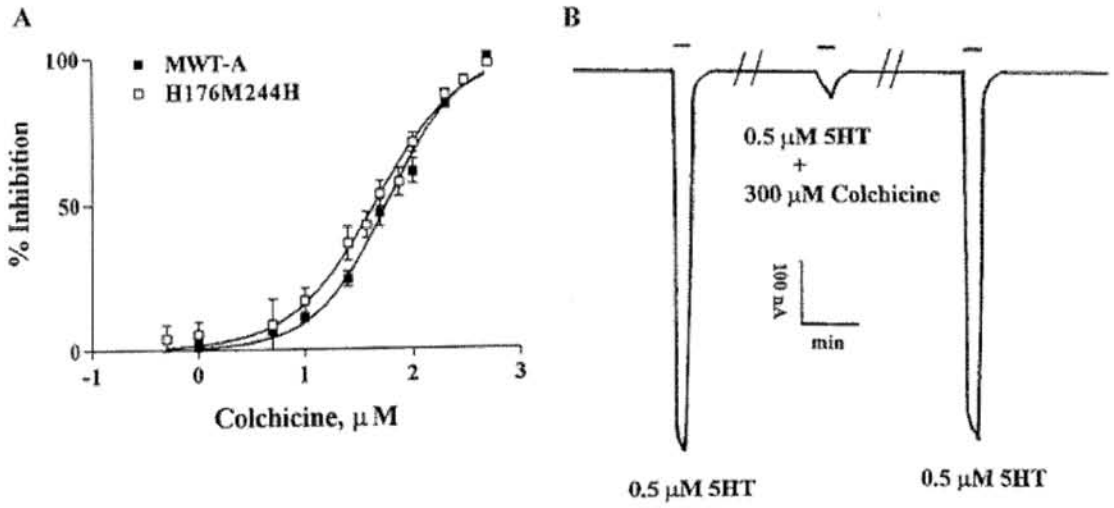
A
100
50
0
% Inhibition
MWT-A
H176M244H
-1
0
1
2
3
Colchicine, μM
B
0.5 μM 5HT
+
300 μM Colchicine
100 nA
min
0.5 μM 5HT
0.5 μM 5HT

Figure 7

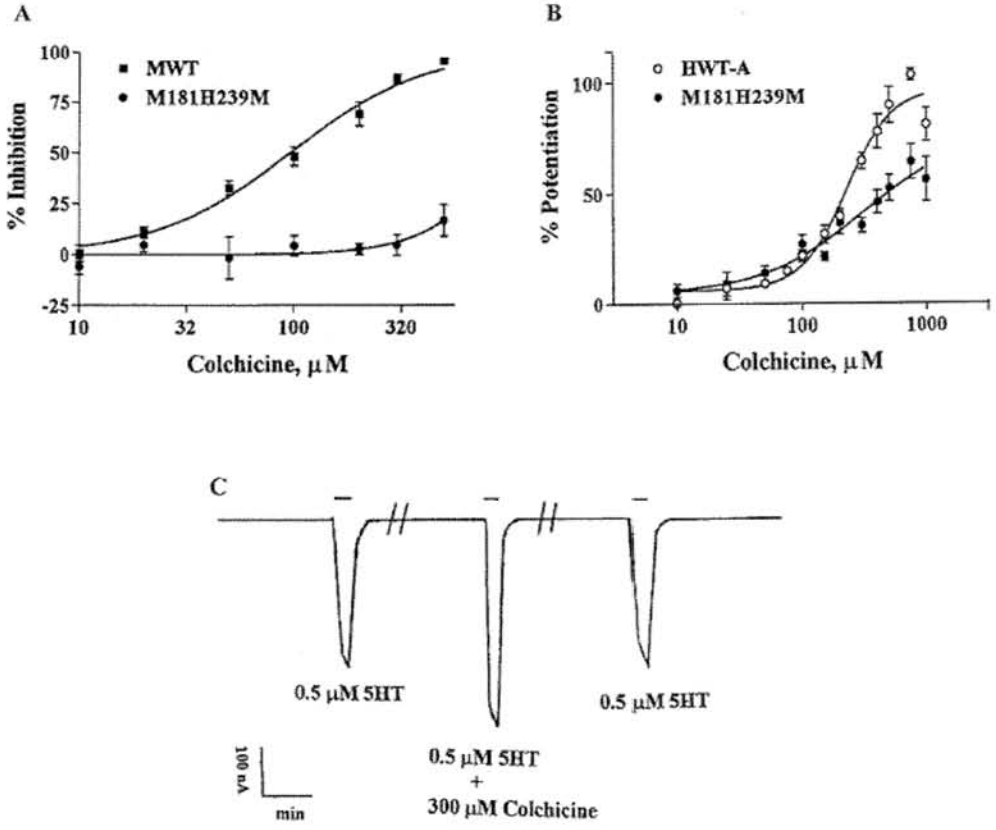
A
MWT
M181H239M
% Inhibition
100
75
50
25
0
-25
10
32
100
320
Colchicine, μM
B
HWT-A
M181H239M
% Potentiation
100
50
0
10
100
1000
Colchicine, μM
C
0.5 μM 5HT
0.5 μM 5HT
0.5 μM 5HT
+
300 μM Colchicine
100 nA
min

A.N. DE OLIVEIRA-PIERCE, PHD

12405 Quincy Lane, Dallas, TX 75230 | 469.576.8663 | aoliveir@hsc.unt.edu

EDUCATION

University of North Texas Health Science Center, Ft. Worth, TX
Ph.D. in Biomedical Sciences **2005-2009**
Primary Areas of Research: Neuroscience and Pharmacology
Secondary Areas of Research: Molecular Biology and Physiology
Dissertation Topic: Structure and Function of the $5HT_3$ Receptor - Ligand-gated Ion channels

Neve Yerushalayim, Jerusalem, Israel
Seminary **1999**
Areas of Concentration: Jewish Philosophy and Jewish Law

University of North Texas, Denton, TX
Graduate Studies **1996-1998**
Area of Concentration: Clinical Psychology

University of North Texas, Denton, TX
B.S. in Kinesiology **1992-1995**
Minor: Sociology

AWARDS

MORE Scholar, National Institutes of Health **2007-2009**
Dean's Honor List, University of North Texas **1992-1995**

RESEARCH, PROFESSIONAL PRESENTATIONS

"Discriminative stimulus effects and receptor binding of dimethyltryptamine."
Poster presented at Behavior, Biology, and Chemistry: Translational Research in Addiction Conference, San Antonio, TX **2009**

"The Role of Loops C and F Residues in Ligand Recognition in the 5-hydroxytryptamine$_{3A}$ Receptor."
Poster presented at the Society for Neuroscience Conference, Washington, DC **2008**

"The Role of Loops C and F in Interspecies Differential Pharmacology of the 5-HT$_{3A}$ Receptor."
Poster presented at the Experimental Biology Conference, San Diego, CA **2008**

"The Role of Critical Amino Acid Residues in Mouse and Human 5-HT$_{3A}$ Receptors in Conferring Differential Pharmacological Sensitivities to 2-OHMBA."
Poster presented at the Research Appreciation Day, Ft. Worth, TX **2006**

University of North Texas Health Science Center, TX
Graduate Research Assistant/PhD Candidate **2006-2007**
Supervisor: Tina Machu, Ph.D.
Research Area: Structure and function of the 5-HT_3 receptor.

"Health Belief Model: Applicability to Women of Mexican Descent"
Poster presented at the American Psychological Association Convention, Boston, MA 1999

University of North Texas, TX
Research Assistant **1998-1999**
Supervisor: Kenneth Sewell, Ph.D.
Research Area: Mental Illness, Schizophrenia and Self-perception, Affect Cognition and Neurophysiology.

University of North Texas, TX
Research Assistant **1995-1996**
Supervisor: Rick Smith, Ph.D.
Research Area: Self-injurious behavior and mental retardation.

PUBLICATIONS

de Oliveira-Pierce, A. N., Lote, R., Zhang, R., White, M. M., and Machu, T. K. (2009) Loop C is the Major Determinant of Differential *d*-Tubocurarine Affinity in Human 5-Hydroxytryptamine$_{3A}$ Receptors. *J. Biol. Chem.* [submitted].

de Oliveira-Pierce, A. N., Zhang, R., and Machu, T. K. (2009) Colchicine: A Novel Positive Allosteric Modulator of the Human 5-Hydroxytryptamine3A Receptor. *J. Pharmacol. Exp. Ther.* **329:** 838-847.

de Oliveira-Pierce, A. N., and Machu, T. K. The Role of Loops C and F in Interspecies Differential Pharmacology of the 5-HT3A Receptor [abstract]. In: Experimental Biology Conference; 2008 Apr 5-9; San Diego, CA. *FASEB J.* **22**: lb624.

SELECTED RESEARCH LABORATORY TECHNIQUES
Site-directed Mutagenesis
  PCR/Primer Design
DNA/RNA Extraction and Purification
Electrophysiology
  Two-electrode Voltage Clamp
Saturation/Competition Radioligand Binding
Gel Electrophoresis
Microinjection
Amphibian Oocyte Removal Surgery (*Xenopus laevis*)

LANGUAGES
English, Spanish, Portuguese – speak, read and write fluently
Hebrew – speak, read and write at conversational level

TEACHING EXPERIENCE
Mesorah, High School for Girls
Hebrew Substitute Teacher **2004**
Taught beginner Hebrew classes and administered exams.

Language Consultant – English, Spanish, Portuguese, and Hebrew **1997-2004**
Provided professional language translation, instruction and live interpretation.

OTHER EMPLOYMENT/VOLUNTEER EXPERIENCE
Dallas Metrocare Services, TX
Quality Mental Health Professional **2004-2006**
Provided counseling and skills training to children 3-18 yrs old suffering from psychosis.

Collin County Rape Crisis Center, TX
Volunteer Counselor **1997**
Provided immediate/first-response support to rape victims in the Collin County area.

Baylor Tom Landry Sports Medicine Research Center, TX
Fitness Consultant **1996**
Developed and administered training routines for female geriatric clients.

The Texas Club
Assistant Athletic Director **1995-1996**
Organized basketball and squash tournaments, supervised workout facilities. Other tasks included payroll and manager on duty responsibilities.

Cooper Aerobic Institute, TX
Wellness Specialist **1995**
Taught aerobic classes and developed fitness and nutritional programs.

United Parcel Service
On-site Lead Supervisor **1994-1995**
Supervised 10+ employees in the accounts receivable department.

MEMBERSHIPS
American Chemical Society
American Mensa
American Society for Pharmacology and Experimental Pharmaceutics (ASPET)
Sigma Xi, The Scientific Research Society
Society for Neuroscience (SfN)